

**CORTICAL PROCESSES UNDERLYING
ATTENTIONAL MODULATIONS OF
DYNAMIC VISION**

A DISSERTATION SUBMITTED TO
THE GRADUATE SCHOOL OF ENGINEERING AND SCIENCE
OF BILKENT UNIVERSITY
IN PARTIAL FULFILLMENT OF THE REQUIREMENTS FOR
THE DEGREE OF
DOCTOR OF PHILOSOPHY
IN
NEUROSCIENCE

By
Esra Nur Çatak
September 2022

Cortical Processes Underlying Attentional Modulations of Dynamic
Vision

By Esra Nur Çatak

September 2022

We certify that we have read this dissertation and that in our opinion it is fully adequate, in scope and in quality, as a dissertation for the degree of Doctor of Philosophy.

Hacı Hulusi Kafalıgönül(Advisor)

Tolga Çukur

Yusuf Ziya İder

Didem Kadıhasanoğlu

Murat Perit Çakır

Approved for the Graduate School of Engineering and Science:

Orhan Arıkan
Director of the Graduate School

ABSTRACT

CORTICAL PROCESSES UNDERLYING ATTENTIONAL MODULATIONS OF DYNAMIC VISION

Esra Nur Çatak

Ph.D. in Neuroscience

Advisor: Hacı Hulusi Kafalgönül

September 2022

Visual attention is one of the most fundamental cognitive functions guiding and influencing a various number of processes. However, how different neural mechanisms are modulated by selective attention to process information is still subject to debate. Utilizing electroencephalography (EEG), the current thesis focused on understanding the time course of visual information processing and its neural underpinnings with paradigms that operate in different attentional modes, such as visual masking, attentional load, and transparent motion design. First, we aimed to understand the role of spatial attention in information processing and its possible interactions with metacontrast masking mechanisms. The behavioral results revealed an interaction effect that suggests differential effects of spatial attention on metacontrast masking. The following EEG analyses revealed significant activation due to masking and attentional load on early negative components located over occipital and parieto-occipital scalp sites, followed by a late positive component centered over centro-parietal electrodes. These findings suggest that the effect of spatial attention may have distinct characteristics at different stages of sensory and perceptual processing regarding its relationship with metacontrast masking. Secondly, by employing a novel variant of transparent motion design with color and motion swapping, we aimed to isolate the object-based cueing effect from a possible feature-based explanation in both psychophysical measures and neural activities. Our results demonstrate that the behavioral effects of attentional cueing survived feature swaps, providing evidence for an object-based attention mechanism. We also observed event-related potential correlates of these object-based selection effects in the late N1 component range, over occipital and parieto-occipital scalp sites, significantly associated with the variation in behavioral performance. Our findings provide the first evidence of the role of the N1 component in object-based attention in this transparent-motion design under conditions that rule out possible feature-based explanations. Taken together, the

present results highlight the substantial effects of selective attention on the processing of visual information after the initial entry of information into the visual system and before the completion of its processing.

Keywords: EEG, attention, attentional load, object-based attention, masking, metacontrast, visibility, temporal dynamics, transparent-motion.

ÖZET

DİNAMİK GÖRMENİN DİKKAT MODÜLASYONLARININ TEMELİNDEKİ KORTİKAL SÜREÇLER

Esra Nur Çatak

Nöro bilim, Doktora

Tez Danışmanı: Hacı Hulusi Kafalgönül

Eylül 2022

Görsel dikkat, çok sayıda süreci yönlendiren ve etkileyen temel bilişsel işlevlerden biridir. Bununla birlikte, seçici dikkatin bilgiyi işlemek için kullandığı sinirsel mekanizmalar hala tartışma konusudur. Elektroensefalografi (EEG) tekniğinin kullanıldığı tez araştırmasında, görsel maskeleyme, dikkat yükü ve saydam-hareket dizaynı gibi farklı dikkat modları aktive eden paradigmlar kullanılarak görsel bilgi işlemenin zaman süreci ve sinirsel temelleri aydınlatılmaya odaklanılmıştır. İlk olarak, bilgi işlemede uzamsal dikkatin rolünü ve metakontrast maskeleyme mekanizmalarıyla olası etkileşimlerini gözlemlemek ve anlamayı amaçladık. Davranışsal sonuçlar, uzamsal dikkatin metakontrast maskeleyme üzerindeki farklı etkilerini öneren bir etkileşim etkisini ortaya çıkarmıştır. Takip eden EEG analizleri, maskeleyme ve dikkat yükünden kaynaklanan, oksipital ve paryeto-oksipital bölgeler üzerinde yer alan erken negatif bileşenlere ile merkezi-paryetal elektrotlar üzerinde oluşan geç bir pozitif bileşene işaret etmektedir. Bu bulgular, uzamsal dikkatin etkisinin, metakontrast maskeleyme ile ilişkisine ilişkin olarak, algısal işlemenin farklı aşamalarında farklı özelliklere sahip olabileceğini düşündürmektedir. İkinci olarak, renk ve hareket yönü takası koşullarına sahip yeni bir saydam hareket tasarımının bir varyantı kullanarak, hem psikofiziksel hem de nöral faaliyetlerde nesne tabanlı ipucu etkisini olası bir nitelik tabanlı açıklamadan ayırmayı amaçladık. Sonuçlarımız, ipucu ile yönlendirilen dikkatin davranışsal etkilerinin, nitelik takaslarından etkilenmeyerek, nesne tabanlı bir dikkat mekanizmasından kaynaklandığını göstermektedir. Ayrıca, EEG analizleri sonucunda oksipital ve parieto-oksipital bölgeleri üzerinde gözlemlenen geç N1 bileşen aralığında, bu nesne tabanlı seçim etkilerinin davranışsal performanstaki varyasyonla da önemli ölçüde ilişkili olduğu kaydedilmiştir. Bulgularımız, olası nitelik tabanlı açıklamaları hariç tutan koşullar altında nesne tabanlı dikkatte

N1 komponentinin rolünü ortaya koyan ilk önemli veriyi sağlamaktadır. Birlikte ele alındığında, mevcut sonuçlar, görsel sisteme ilk bilgi girişinden sonra ve işlenmesinin tamamlanmasından önce, seçici dikkatin görsel bilginin işlenmesi üzerindeki önemli etkilerini vurgulamaktadır.

Anahtar sözcükler: EEG, dikkat, dikkat yükü, nesne tabanlı dikkat, maskeleye, metakontrast, görünürlük, zamansal dinamikler, şeffaf-hareket.

Acknowledgement

This work would not have been possible without the support of many people.

I would like to start by thanking my thesis advisor Dr. Hulusi Kafalgönül for his continuous support, patience, and guidance throughout my Ph.D. journey. I have benefited greatly from his knowledge and meticulous editing. I am extremely grateful that he took me on as a student and continued to have faith in me over the years. I would also want to thank Dr. Gene Stoner for accepting me into his “elite team” and letting me experience his way of critical thinking.

I also would like to express my gratitude to the past and present members of my thesis committee, Dr. Tolga Çukur, Dr. Aslıhan Örs Gevrekçi, Dr. Cengiz Acartürk, Dr. Didem Kadıhasanoğlu, Dr. Yusuf Ziya İder and Dr. Murat Perit Çakır for their valuable time and feedback.

I am grateful to have the opportunity to work and grow side by side with the members of our research lab; Sibel Akyüz, Afife Konyalı, İrem Hergüner, Şeyma Koç Yılmaz, Efsun Kavaklıoğlu, Gaye Başaran and Alaz Aydın. I owe special thanks to Mert Özkan and Utku Kaya for their intellectual and technical contributions to this work as well as Ceyda Tekalp for her support in data collection. Finally, I want to thank Merve Kımıkıoğlu for being a comforting presence and the best neighbor both in the office and at home.

I don't think I could manage to come this far without Ayşenur Karaduman Ütkür in my life. She was an invaluable friend for over a decade of my life and is still the first person to call when I am happy or sad. I also want to thank Gökçen Bulut for the generous support and insight she brought.

Most importantly, I am forever grateful for my family's unconditional and unequivocal love. They were my safety net and pillar of support throughout my academic life.

Finally, I would like to acknowledge the financial support provided by the Scientific and Technological Research Council of Turkey (TUBITAK 1001 Grant: 119K368, BİDEB 2221 Program, 2211-E BİDEB National Graduate Scholarship Program) as well as the Turkish Academy of Sciences (TUBA-GEBİP Award).

Contents

1	Introduction	1
1.1	Human Visual System	2
1.2	Visual Masking	8
1.2.1	Metacontrast masking	10
1.2.2	Common onset masking	17
1.3	Attention	20
1.3.1	Theories and models of attention	20
1.3.2	Spatial attention	22
1.3.3	Feature-based attention	25
1.3.4	Object-based attention	27
1.4	Specific Aims	32
1.4.1	Study 1: Electrophysiological Investigation of Attentional Modulation on Metacontrast Masking	33
1.4.2	Study 2: Behavioral and ERP evidence that Object-based Attention Utilizes Fine-grained Spatial Mechanisms	35
2	Electrophysiological Investigation of Attentional Modulation on Metacontrast Masking	38
2.1	Introduction	38
2.2	Methods	39
2.2.1	Participants	39
2.2.2	Apparatus	40
2.2.3	Behavioral pilot data collection	40
2.2.4	Stimuli and procedure	41
2.2.5	Performance testing	43

2.2.6	EEG data acquisition and preprocessing	44
2.2.7	ERP analyses	45
2.3	Results	46
2.3.1	Behavioral Results	46
2.3.2	ERP results	47
2.4	Discussion	54
2.4.1	Summary	54
2.4.2	Do masking and spatial attention interact?	55
2.4.3	Neural correlates of visual awareness and attention	58
2.5	Conclusions	61
3	Behavioral and ERP Evidence that Object-based Attention Utilizes Fine-grained Spatial Mechanisms	62
3.1	Introduction	62
3.2	Methods	64
3.2.1	Participants	64
3.2.2	Apparatus	65
3.2.3	Training and performance testing	65
3.2.4	Stimuli and procedure	67
3.2.5	EEG data acquisition and preprocessing	70
3.2.6	ERP analyses	71
3.3	Results	73
3.3.1	Behavioral results	73
3.3.2	EEG results	76
3.4	Discussion	83
3.4.1	Summary	83
3.4.2	Object-based versus motion-competition explanations	84
3.4.3	Behavioral findings	84
3.4.4	Role of color	85
3.4.5	Spatial attention	86
3.4.6	ERP findings	87
3.5	Conclusions	88
4	General Discussion and Future Directions	89

4.1	Contributions to the models of attention	90
4.2	Neural correlates of spatial and object-based attention	95
4.3	Potential Implications for Applied Research	96
4.4	Future Directions	99
4.4.1	How would paracontrast masking interact with attention?	99
4.4.2	What is the neuronal basis of object-based attention? . . .	100

List of Figures

1.1	Simplified illustration of the connections in the retina. Cell types are marked with following letters: R, rod; C, cone; H, horizontal cell; FMB, flat midget bipolar; IMB, invaginating midget bipolar; IDB, invaginating diffuse bipolar; RB, rod bipolar; A, amacrine cell; P, parasol cell (M cell); MG, midget ganglion cell (P cell). Adapted from [1].	3
1.2	Hierarchical organization of parallel processing streams in the macaque monkey. Boxes represent visual areas, sections within the area, and subcortical centers; solid lines represent major connections between structures; and icons below represent characteristic neurophysiological properties. Subcortical streams in the retina and lateral geniculate nucleus (LGN) include the Magnocellular, Koniocellular, and Parvocellular streams (grey, yellow, and pink, respectively). Adapted from [2].	6
1.3	The response latency profiles of each visual area located at different levels of processing. The percentile of active neurons is depicted as a function of time from stimulus onset. Retrieved from [3]. . .	7
1.4	Conventional pairs of mask and target stimuli for different masking forms. Examples of (a) paracontrast/metacontrast masking, (b) masking by noise and (c) masking by structure are illustrated. Retrieved from [4].	9

1.5 A typical representation of (a) the monotonic/type A and (b) the U-shaped/type B for paracontrast (forward) and metacontrast (backward) masking functions. The horizontal axis represents the stimulus onset asynchrony (SOA) and the vertical axis corresponds to target visibility. Retrieved from [4]. 11

1.6 Schematic representation of the RECOD model. Filled and open triangles depict inhibitory and excitatory connections, respectively. The bottom ellipses represent the M and P retinal ganglion cells. M pathway represents the transient channel with fast and short-lasting activity. P pathway represents the slow and long-lasting activity. Retrieved from [5]. 12

1.7 Representations of model predictions for metacontrast (top panel) and paracontrast masking (lower panel). Retrieved from [5]. 14

1.8 (Left) Averaged ERP waveforms for aware and unaware conditions in response to visual stimuli over occipital sites. (Right) Difference ERP waveform between the unaware and aware trials, indicating that awareness correlates with a negative increase in amplitude around 200 ms after the onset of the stimulus (VAN), followed by a positive increase in activation in P300 time range (LP). Retrieved from [6]. 17

1.9 (a) Illustration of the display sequence of a common-onset masking experiment with a four-dot mask. The observer is required to indicate the orientation of the gap in a broken ring that is cued by surrounding four dots. The other rings serve as distractors. (b) Results of a typical common-onset masking paradigm with various set-size conditions. Retrieved from [7]. 18

1.10 Delayed-onset design. (A) One rotating dot field appears followed by the second “delayed” dot field. Two superimposed dot fields rotate in opposite directions around the fixation point, allowing the perception of two transparent surfaces. Following the rotation, either the delayed (cued) or non-delayed (uncued) dot field translates briefly. After the translation, both dot fields continue to rotate. (B) Feature-based illustration of timeline. The two dot fields are differentiated by line style (dashed or solid) and with dot field colors indicated by the line colors. The vertical line placement indicates the different motion directions: clockwise rotation (CW), counter-clockwise rotation (CCW), and translation. The onset differences in this design result in “cued” translations that occur in the presence of the older rotation direction and “uncued” translations that occur in the presence of the newer rotation direction. 29

2.1 Behavioral results from the pilot data (n = 23). The percent correct values for baseline (dashed lines) and mask (solid lines) conditions separately as a function of SOA with blue and red lines corresponding to set-size two and six conditions, respectively. . . . 42

2.2 Schematic representation of stimulation and timeline on each trial. Each trial started with a variable fixation period (500-1000 ms) followed by either 2 or 6 target bars that presented on the screen for 20 ms. After a period of SOA (30, 60 or 150 ms) where only the fixation point was left on the screen either a mask over the target bar location or a cue near the target bar appeared for 20 ms. Participants were instructed to press left or right arrow indicating orientation of the target (tilted in leftwards or rightwards) in a time window of 1000 ms. 43

2.3 Behavioral results (n = 19). (A)The percent correct values for baseline (dashed lines) and mask (solid lines) conditions seperately as a function of SOA with blue and red lines corresponding to set-size two and six conditions, respectively. (B) The percent correct difference between mask and baseline for each SOA and set-size conditions. The blue and red lines similarly illustrate the two and six target conditions. 47

2.4 The voltage topographical maps displaying overall differential activation (baseline-mask) in selected time ranges (90-210 ms, 240-310 ms and 350-580 ms). The averaged differece for each SOA (columns) and set-size (rows) condition are displayed seperately. 49

2.5 The averaged activities and derived waveforms from the parieto-occipital scalp sites. Each SOA and set-size condition is displayed in a separate plot. The locations of exemplar electrodes that were used in analyses are shown on a head model (i.e., PO3, PO8, PO7, PO4, POz, Oz, O1, O2). In each plot, evoked activities for mask (blue lines), baseline (red lines) conditions and the difference waveforms (green lines) are displayed. The ERPs were time-locked to the onset of the target display. The identified time windows where follow up analyses were conducted are highlighted by grey rectangles. The vertical dashed lines indicate the appearance of the mask or cue according to the SOA condition. 50

2.6 The averaged activities and derived waveforms from the centro-parietal scalp sites. Each SOA and set-size condition is displayed in a separate plot. The locations of exemplar electrodes that were used in analyses are shown on a head model (i.e., CPz, PO3, POz, PO4, P3, Pz, Cz, CP1, CP2, CP3, CP4, P1, P4, P2, C1, C2). In each plot, evoked activities for mask (blue lines), baseline (red lines) conditions and the difference waveforms (green lines) are displayed. The ERPs were time-locked to the onset of the target display. The identified time window where follow up analyses were conducted is highlighted by a grey rectangle. The vertical dashed lines indicate the appearance of the mask or cue according to the SOA condition. 51

2.7 Average values used in ERP analyses (n = 19). The averaged differential amplitude between baseline and mask conditions displayed in the time ranges 90-210 ms (top), 240-310 ms (middle) and 350-580 ms (bottom) for each SOA. The blue and red lines correspond to two and six target conditions, respectively. The locations of exemplar electrodes that were used in analyses are shown on head models. 53

- 3.1 Schematic representation of stimuli. (A) Each trial started with a variable fixation period, followed by the appearance of the first dot field rotating around the fixation point for 750 ms. A second (delayed) dot field appeared and both fields rotated in opposite directions around the fixation point for 300 ms. (B) Following this period of dual rotation, one dot field translated in one of the eight directions for 133 ms. At the translation onset, the non-translating dot field either continued to rotate in its original direction (no-swap) or reversed rotation direction (motion-swap). The colors of the two dot fields were similarly swapped at the onset of translation on half of the trials (color-swap). The resulting six different conditions are illustrated separately. (C) After the translation, the translating dot field either resumed its original rotation direction or assumed the other dot field's previous rotation direction, and both surfaces kept rotating for 500 ms in their newly assigned directions. The subject's response window started 100 ms after the translation onset and ended 1 second after stimulus offset. The stimulus shown in (A) is an example of the cued no-swap condition. 69
- 3.2 Behavioral results (n=15). The percentage of correct responses for each condition with blue and orange bars corresponding to cued and uncued conditions, respectively. Dots represent the data from individual participants. The dashed line indicates chance performance level (i.e., 12.5%). Error bars \pm SEM. 75

- 3.3 Voltage topographical maps of the averaged waveforms within the identified time window (238-326 ms). The voltage topographical maps of cued and uncued conditions are shown in separate rows. The averaged activities of each swap condition, combined waveforms across swap conditions, and the difference between them ($cued_{comb} - uncued_{comb}$) are displayed on the maps in separate columns. The result of the cluster-based base permutation test comparing the combined waveforms ($cued_{comb}$ vs. $uncued_{comb}$) is indicated in the last column. The electrodes that were part of the significant spatiotemporal cluster for at least 70 ms (i.e., more than 75% of the time-range) were chosen as exemplar electrodes and are marked by red-filled circles on the right-most topographical map (i.e., Oz, O1, O2, POz, PO3, PO4, PO7, PO8, P1, P3, P4, P5, P6, P7, P8, CP3, CP5, CP6, C5, TP8, TP7). 77
- 3.4 Voltage topographical maps of the averaged waveforms within the identified time window (134-224 ms). The voltage topographical maps of cued and uncued conditions are shown in separate rows. The averaged activities of each swap condition, combined waveforms across swap conditions, and the difference between them ($cued_{comb} - uncued_{comb}$) are displayed on the maps in separate columns. The result of the cluster-based base permutation test comparing the combined waveforms ($cued_{comb} - uncued_{comb}$) is indicated in the last column. The electrodes, which were part of the spatiotemporal cluster for at least 20 ms are marked by red-filled circles on the rightmost topographical map (i.e., Oz, O1, O2, POz, PO3, PO4, PO7, Pz, P1, P2, P4, P3, P5, CPz, CP1, CP2, CP3, Cz, C1). 78

- 3.5 Averaged activities and derived waveforms from the exemplar scalp sites (n=15). The exemplar electrodes that were used in analyses are shown on a head model (i.e., Oz, O1, O2, POz, PO3, PO4, PO7, PO8, P1, P3, P4, P5, P6, P7, P8, CP3, CP5, CP6, C5, TP8, TP7). (A) The averaged ERPs for each swap condition are displayed in separate plots, the blue and orange curves correspond to evoked activities for cued and uncued conditions, respectively. The ERPs were time-locked to the onset of the translation and displayed in the range from the start of each trial to 400 ms after translation. The 100 ms time window before the onset of the first dot field was used as the baseline period. The identified time window based on the cluster-based permutation test is marked by a dashed rectangle. (B) The averaged combined waveform for the cued (blue) and uncued (orange) conditions after translation. The difference waveform ($cued_{comb} - uncued_{comb}$) is indicated by the gray curve, and the shaded area corresponds to the standard error (+SEM) across participants. (C) Bar plots displaying the averaged amplitudes within the identified time window (238-326 ms) for each condition. The blue and orange bars correspond to cued and uncued conditions, respectively. The dots represent the data from individual participants. Error bars \pm SEM. 80
- 3.6 Averaged potentials in the time-range of the identified cluster (238-326 ms) with the performance values for each condition (2 cued/uncued x 3 feature swaps). The locations of exemplar electrodes used in our analyses are shown in Figure 3.5. Filled and open symbols correspond to the cued and uncued conditions, respectively. Each swap condition is represented by different symbols. Vertical and horizontal error bars correspond to the variance across observers (+SEM). The black solid line indicates the best linear fit and dotted lines denote the 95% confidence intervals on the linear fit. 81

List of Tables

3.1	The results of the post-hoc paired t-tests comparing swap conditions for each cueing condition. The descriptive statistics (mean, SEM) are based on the difference between the compared conditions. The values for each cueing condition are grouped in separate rows. Only the significant differences (Bonferroni-corrected $p < 0.05$) are listed in the table and highlighted in bold. The follow-up tests did not reveal any other significant comparisons across swap conditions.	74
3.2	The results of post-hoc paired samples t-tests for the cueing effect (cued vs. uncued) for each swap condition. The descriptive statistics (mean, SEM) are based on the difference between cued and uncued conditions. Significant p values (Bonferroni-corrected $p < 0.05$) are highlighted in bold.	76

3.3 The results of Bayesian repeated-measures ANOVA on the N1 amplitude, latency, and half-peak latency values. The Model Comparisons column displays the Null model, followed by the four alternative hypotheses models. The “Cueing” and “Swaps” rows displays the probabilities based on the alternative hypothesis that one of the main factors alone is responsible for the variability in the data. The “Cueing + Swaps” model is based on the alternative hypothesis that the changes the data depends on both Cueing and Swaps factors together, and the “Cueing + Swaps + Cueing * Swaps” model displays the probabilities for the alternative hypothesis that the change is due to both main factors and the interaction. P(M) indicates the prior probabilities of each model which was set to be equal at the beginning. P(M|data) shows the updated posterior probabilities after the data was provided as input. BF_M shows the change in prior model odds due to data. BF_{10} indicates the Bayes factors for each model. The percent error in the last column is based on the accuracy of the Bayes factor calculations. 82

Chapter 1

Introduction

Since humans and many other species are mobile visual explorers, vision is a naturally dynamic process due to frequent shifts of gaze to investigate the world full of moving objects and complex scenery. Given the average number of fixations per second, in a very small time period behaviorally relevant information as well as highly dense representations must be built and modified continuously by the visual system. After the retinal input, there are several processing pathways, each with several stages of processing that are required before a behavioral response or visual awareness is generated. Thus, even the manifest steady-state properties of visual experience during a fixation period rely on highly dynamic underlying neural processes that must be actively updated several times per second.

The current thesis focuses on understanding the time course, possible pathways, and stages of visual processing and selection required for perception using refined paradigms such as visual masking and transparent motion design that operate in different attentional modes with a steady-state setting. In the following sections, a general background on the human visual system, followed by visual masking mechanisms and models, information on visual attention models as well as studies on different modes of attention are presented. Afterward, two conducted studies within the scope of this thesis are introduced in separate chapters.

1.1 Human Visual System

Studying the visual system offers an important perspective of the brain functions at various levels including the complex physical and biochemical mechanisms that culminate into different physiological and psychological states. In the face of the immense amount of information the eye is presented with, the visual system has progressed to solve many challenging problems to ensure efficiency and robustness in a dynamic stimulation profile.

Through vision, animals access the physical world to identify food, members of their own and other species and judge the distances or speed of moving objects. Therefore, for many animals, a high proportion of the brain is dedicated to vision, compared to the rest of the sensory functions, to sort and interpret the overwhelming amount of visual information from the environment.

The visual processing starts when the light from an object reaches the cornea. Through the lens behind the cornea, an inverted image is focused onto the retina triggering a flow of neural impulses. In the retina two major types of photoreceptors transform the light into neurotransmitters [8, 9]. The first type is the cones which are color selective photoreceptors via the photo-pigments each one contains. These photo-pigments are sensitive to various wavelengths of light that result in the ability to distinguish primary colors. The cones are densely packed at the center of the retina, the fovea, where the fine details of the directly observed objects are perceived. Inversely, while there are fewer cones in the rest of the retina, resulting in blurrier and less vividly colored peripheral vision, the proportion of the rods increases in the periphery [10]. Rods are the second type of photoreceptor that contain photo-pigments that have sensitivity to low levels of light making them important for night vision (Figure 1.1). The signals from these photoreceptors in the form of neuro-chemicals are then, processed by a collection of midway neurons, such as bipolar cells, horizontal cells, and amacrine cells [1]. Finally, these signals reach the ganglion cell layer where the axons of the neurons that form this layer leave the retina creating the optic nerve (Figure 1.1).

Bipolar cells that send input to retinal ganglion cells are divided into two general categories, labeled on- and off-bipolar neurons according to their response patterns to light stimuli. Specifically, while on-bipolar cells react to light by depolarization, off-bipolar cells react by hyperpolarization. According to the bipolar cell type that provides their input, ganglion neurons also have on and off response patterns following light stimulation [11]. Retinal ganglion neurons typically have center-surround receptive fields. A neuron's receptive field marks the part of the visual field that can increase or decrease the activity of the cell.

Specifically, a retinal ganglion cell with an on-center off-surround receptive field generates a strong response to a light stimulus that falls at the center of its receptive field, however, as the area of the stimulus increases and spreads beyond the boundary of the on-center area onto the off-surround region, the response of the cell starts to decline. The opposite response setting can be observed for the cells with an off-center on-surround receptive field.

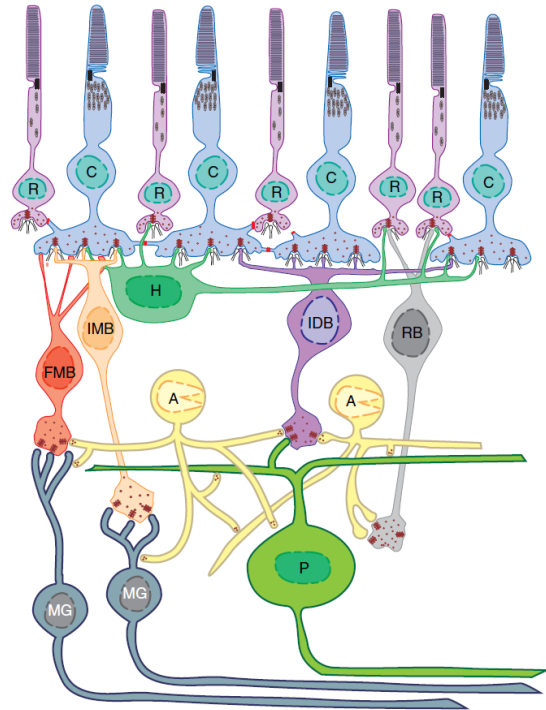


Figure 1.1: Simplified illustration of the connections in the retina. Cell types are marked with following letters: R, rod; C, cone; H, horizontal cell; FMB, flat midget bipolar; IMB, invaginating midget bipolar; IDB, invaginating diffuse bipolar; RB, rod bipolar; A, amacrine cell; P, parasol cell (M cell); MG, midget ganglion cell (P cell). Adapted from [1].

Starting with the bipolar cells onward the distinct response to light indicates that ocular neurons operate best in terms of contrast rather than absolute light levels. Lateral inhibition is a fundamental concept regarding contrast that entails the inhibition of a neuron's response with inputs from a neighboring neuron [12]. The purpose of lateral inhibition is for neurons to become sensitized to spatial variation in the environment rather than uniformity [13, 14]. This is achieved by suppressing a neuron's response to spatially uniform stimuli through inhibition by neighboring neurons and securing a stronger response in case of spatial variation through the lack of inhibition from surrounding neighboring neurons. This scenario consequently ensures that sudden changes in the spatial stimuli such as edges, features, and shapes are prioritized while preserving metabolic energy since only a small amount of neurons with receptive fields correspond to the spatial change need to be active to represent the visual stimulus [14]. Another advantage of lateral inhibition is to ensure that the neural response pattern to the visual scene is not affected by the changes in the absolute brightness levels. Since relative brightness is the focal point in identifying a visual scene, the representation of the stimuli stays the same in dim or bright illumination conditions.

Retinal ganglion cells that project to the lateral geniculate nucleus (LGN) have several different categories with diverse cellular morphology leading to different visual response patterns. The first and most frequently found classes of ganglion cells in the retina are P cells, named after the projection site in the LGN which are the parvocellular layers. The second class of ganglion cells which project to the magnocellular layers of the LGN is also named M cells. Apart from their different projection patterns, the P and M cells also have distinct cell morphologies. P cells (also known as midget ganglion cells) have small dendritic fields, while M cells (also known as parasol cells) have much larger dendritic fields (Figure 1.2). Another distinguishing factor between these two classes of cells is the response patterns. While P cells have smaller receptive fields, are sensitive to color stimulation, and are a lot less sensitive to low contrast stimuli, M cells have larger receptive fields and they are less sensitive to color while being very tuned to low contrast stimuli. Furthermore, P cells have more sustained response profile to a prolonged visual stimulus, whereas M cells tend to react more transiently. The

LGN neurons project outputs to the first cortical region, the primary visual cortex, commonly labeled as V1. The primary visual cortex is also often referred to as the striate cortex due to tissue characteristics. Similar to the structure of LGN, V1 also has a layered nature and while magnocellular layers of LGN send signals to $4C\alpha$ and 4B layers, parvocellular layers project to $4C\beta$ layers (Figure 1.2).

This segregated information processing later leads to the dorsal and ventral pathways that continue beyond the primary cortex. One of the most important visual features of V1 neurons is that they are differentially sensitive to orientation information. Some V1 neurons fire preferentially to vertical lines while others prefer tilted ones and so forth [15, 16]. Along with orientation, V1 neurons are also sensitive to the direction of motion, color or color differences, and binocular disparities [17, 18, 19]. V1 sends feedforward signals to higher visual areas through parallel pathways that can be broadly divided into two; the dorsal pathway directed to the parietal lobe and the ventral pathway directed to the temporal lobe. The separation of these two pathways is established through anatomical connections between the areas that belong to these pathways as well as the differential response properties of these areas [20].

The dorsal pathway starts with the signals from V1 traveling to the thick stripes of V2 and then toward the extrastriate areas MT (medial temporal, or referred to as M5) and MST (medial superior temporal) before major projections further into the parietal lobe. Area MT is crucial for motion perception since most neurons in this area respond selectively to a specific range of motion directions only while staying unresponsive for the remaining directions [21, 22]. Not to mention, a number of these neurons can combine different motion directions into patterns and determine the overall directions of the stimuli [23]. The dorsal pathway is also important for controlling object-directed action. More specifically, this pathway directs actions by transforming the visual inputs into suitable motor outputs [24]. While areas MT and MST are significant for the perception of visual motion and depth, further into the dorsal pathway, the parietal lobe contains specialized areas for guiding eye movements or other motor actions such as object-directed actions.

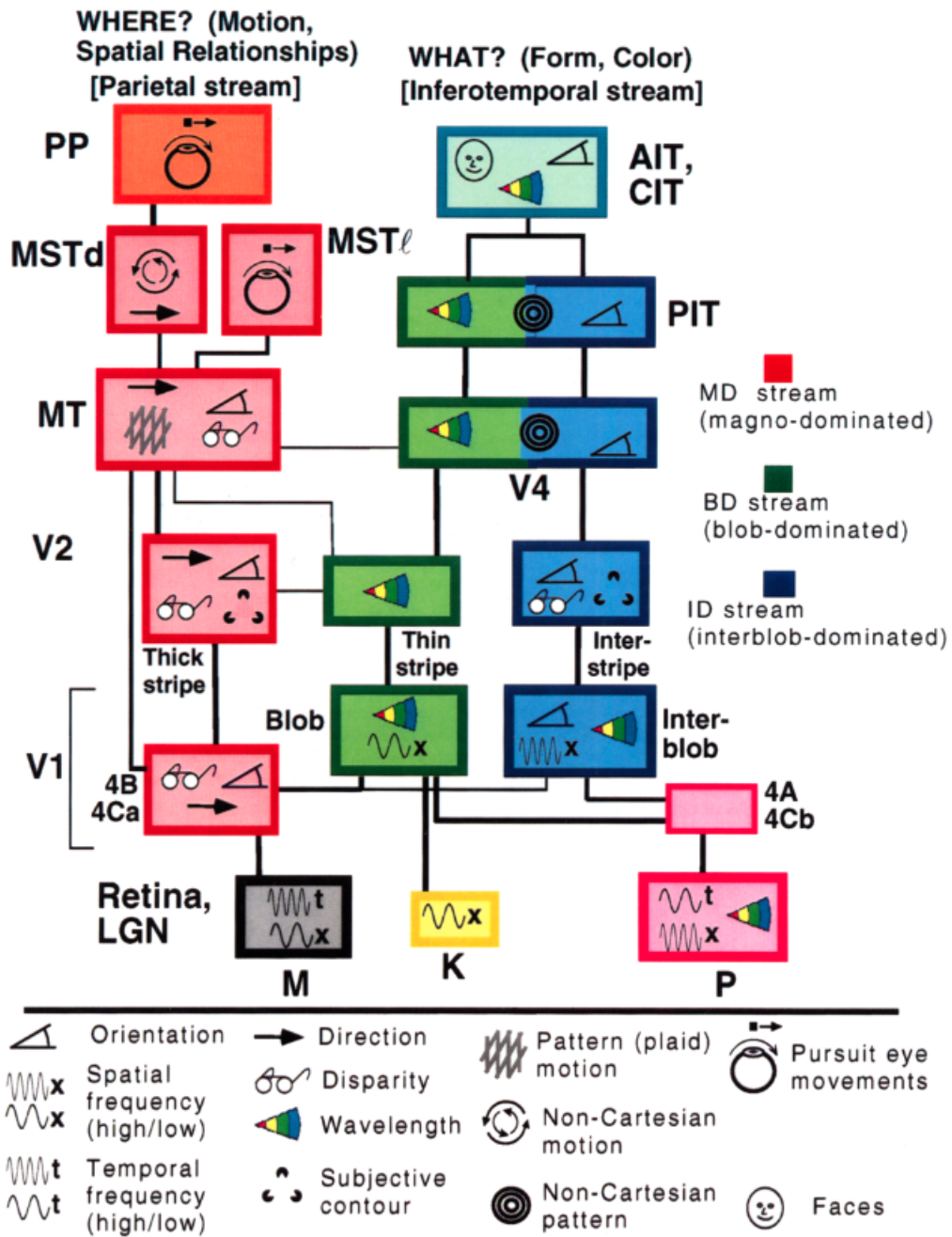


Figure 1.2: Hierarchical organization of parallel processing streams in the macaque monkey. Boxes represent visual areas, sections within the area, and subcortical centers; solid lines represent major connections between structures; and icons below represent characteristic neurophysiological properties. Subcortical streams in the retina and lateral geniculate nucleus (LGN) include the Magnocellular, Koniocellular, and Parvocellular streams (grey, yellow, and pink, respectively). Adapted from [2].

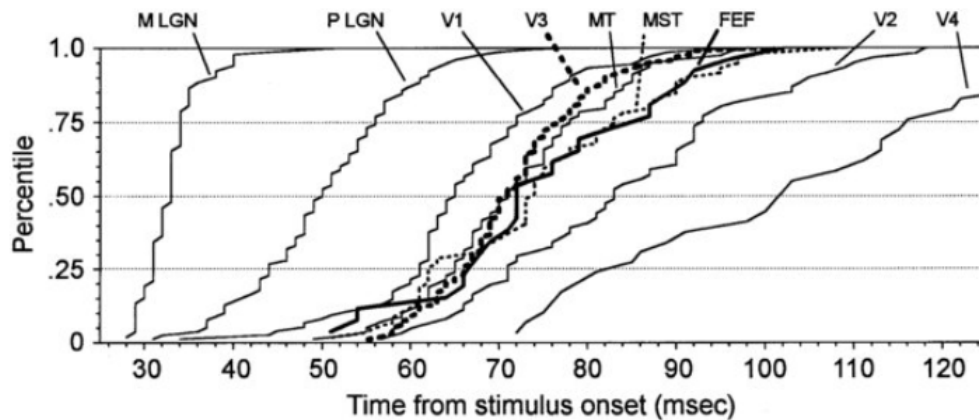


Figure 1.3: The response latency profiles of each visual area located at different levels of processing. The percentile of active neurons is depicted as a function of time from stimulus onset. Retrieved from [3].

The ventral pathway, on the other hand, is important for identifying objects as well as processing their constant features such as color and shape. Through this pathway, signals from V1 travel to thin and pale stripes of V2 and then move onto extrastriate areas V3, and V4 before being forwarded towards the temporal lobe. Within the ventral pathway, the area V4 is known to be especially important for color perception as well as for perceiving complex features and their combinations [25, 26]. Area V4 then sends signals to higher visual areas such as the ventral temporal cortex which is important for object recognition [20].

Notably, the difference in functional properties of distinct neural pathways leads to variation in the information processing speed as well (Figure 1.3). Mounting evidence indicates that the neuron populations that generate these two pathways have distinct response latencies (e.g.,[3]). The response latency patterns for the cortical structures along the dorsal pathway which are responsible for motion perception are shorter compared to those along the ventral pathway which mainly underlies object identification and recognition. These differences in temporal dynamics have important implications for understanding visual dynamics and explaining well-known phenomenon such as visual masking.

While the dividing and grouping of these areas as dorsal and ventral pathways

are very practical to understand the information processing and flow within these pathways, the interaction between these pathways at different levels of processing exist and these interactions are crucial for a coherent percept in a dynamic environment [27, 28]. Even though there is still an ongoing debate on the exact role of each of these interactions, it is well accepted that both feed-forward and feedback connections play a crucial role in perception [29]. Furthermore, the projections from each pathway interact and bind in common regions in the prefrontal cortex to have conscious visual experience [30, 31].

1.2 Visual Masking

Visual masking is a powerful experimental paradigm used widely in vision research for investigating the differences between the preconscious and conscious visual processing as well as neural correlates of conscious perception, spatiotemporal parameters of visual discrimination, and many more. Since the beginning of the 20th-century, visual masking has been extensively studied by itself as an interesting phenomenon and used as an effective technique to study dynamic visual processes [32, 33, 4].

In essence, masking refers to a reduction in the visibility of a stimulus (the target) that is caused by the presentation of another stimulus (the mask) close to the target in space and time [34, 4]. As a result of masking, the target stimulus appears to have low visibility (i.e., reduction in perceived brightness/contrast), and contrast or might be fully invisible to the observer. In terms of information processing, a visual mask can suppress and almost erase the contents of sensory memory, which is believed to be the first stage of memory where a massive amount of information about the environment is encoded only for a very brief period [35]. Empirical, as well as computational evidence, indicates that visual masking mechanisms play an important role in establishing the clarity of our vision for moving objects by suppressing the contents of sensory memory [36, 37]. Secondly, visual masking plays an important functional role in controlling which

information from the sensory memory will be available for transfer to visual short-term memory (VSTM) which is described as a long-lasting but low-capacity store with resistance to masking effects [38, 39, 40, 41].

In initial studies, a basic type of mask consisted of an increase or decrease of an evenly distributed light. These types of masking by light have been used to investigate primarily retinal processes such as rapid light and dark adaptation [42, 43, 44], however, in the following decades, research interests mostly shifted focus to post-retinal, cortical levels of visual masking. At these further levels, where masking depends on the assumption that during the required time a stimulus needs to reach conscious awareness, the information provided by the stimulus is actively processed in various levels of visual pathways and that the responses to the mask and target should interact at identifiable levels of this process [45]. To achieve this, the stimuli must include spatial patterns with defined contours attained by the difference in luminance compared to the background [4]. The approach has been known as pattern masking. This masking type can be separated into different sub classes depending on the spatiotemporal characteristics of the stimuli used.

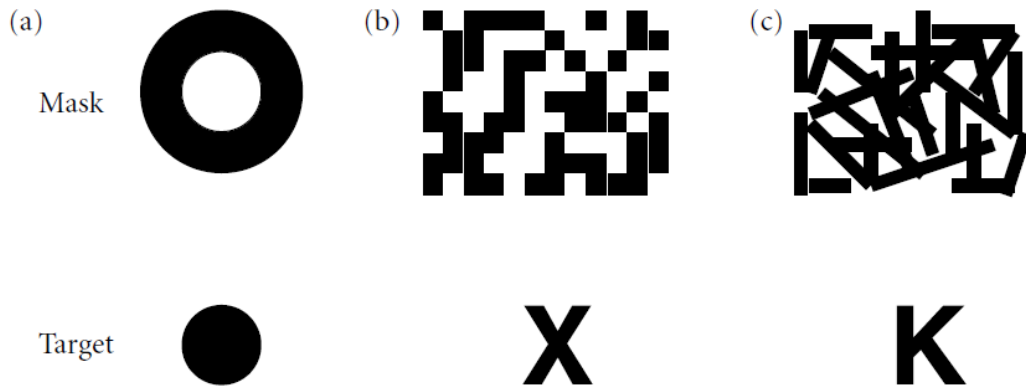


Figure 1.4: Conventional pairs of mask and target stimuli for different masking forms. Examples of (a) paracontrast/metacontrast masking, (b) masking by noise and (c) masking by structure are illustrated. Retrieved from [4].

First, the level of overlap between target and mask is an important factor for differentiation in spatial properties. When the target is completely covered by a mask consisting of randomly scattered dots, it is called masking by noise. If the

mask is made of shapes that are structurally related to the target's contours, it is referred to as masking by structure (Figure 1.4). However, when the mask and target are not overlapping but very close in position by sharing similar contours, depending on their timing, the masking effect is called paracontrast or metacontrast masking. Second, the outcome of masking depends heavily on the temporal dynamics between target and mask. Specifically, the time interval between the onsets of the target and mask stimuli, known as stimulus onset asynchrony (SOA), can greatly affect the masking magnitude. When the mask precedes the target, it is labelled forward (paracontrast) masking whereas if the target is followed by the mask, it is labelled backward (metacontrast) masking. Further, if the onsets of target and mask are the same but the mask offset exceeds the target, it is called common-onset visual masking.

The concept of masking function is essential to understanding the concept of visual masking. A masking function demonstrates the relationship between the target visibility and the target-mask temporal asynchrony (Figure 1.5). Visibility is measured by task performance as the indication of the masking effect. Both accuracy and response time can be used as a measure of performance. As shown in Figure 1.5, the negative SOA values indicate paracontrast masking, while the positive values show metacontrast. For metacontrast masking, typical masking functions are type A (monotonic) where the masking effect is expected to be the strongest when the SOA is minimum and type B (u-shaped /non-monotonic) where the masking effect is assumed to be strongest in intermediate SOA values between 30-80 ms. The morphology of masking function can be influenced by several variables such as stimulus parameters including luminance, duration, contrast polarity, orientation, intensity, and location as well as target-mask spatial separation and criterion content [4, 46, 47, 48].

1.2.1 Metacontrast masking

The metacontrast (backward) masking phenomenon is informative as it is very intriguing due to the counterintuitive nature of the following mask interrupting

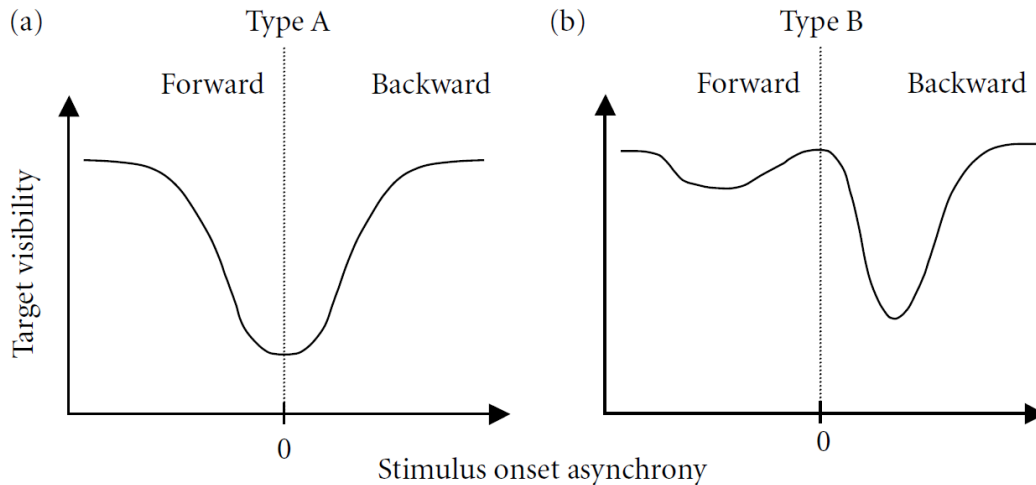


Figure 1.5: A typical representation of (a) the monotonic/type A and (b) the U-shaped/type B for paracontrast (forward) and metacontrast (backward) masking functions. The horizontal axis represents the stimulus onset asynchrony (SOA) and the vertical axis corresponds to target visibility. Retrieved from [4].

the visibility of the already presented target [34, 4]. Various models developed to understand backward visual masking may also be relevant to our understanding of a variety of spatiotemporal phenomena, such as motion perception, visual persistence, reaction time (RT), and discrimination of temporal sequencing and various levels of information processing in the visual system [34, 49, 4, 5] as well as visual awareness [50, 51, 52, 53].

Currently, many theories attempting to explain the underlying mechanisms of masking can be found ranging from spatio-temporal integration of mask-target signals to attentional shifts, or temporal delay of target evoked thalamocortical mechanisms to lateral inhibition of feedforward processing between target and mask [54]. Among these theories, the ones focus on the distinct temporal response properties of magnocellular and parvocellular pathways have been influential in explaining the main characteristics of visual masking. An early and important model built upon these temporal differences and incorporated into visual masking studies is the sustained-transient dual-channel model [55]. The model assumes that the sustained channels (P-pathway) are responsible for relatively slow processing of features such as color, edges, and brightness while transient channels

(M-pathway) are involved in fast pattern processing and spatial location information of a stimulus. Accordingly, metacontrast masking is theorized to be due to the inter-channel inhibition of activity generated by the target-activated sustained channels by the mask-activated transient channels (see below for further explanation). Even in earlier unrevised form, the dual-channel theory accounts for a large portion of masking data, as well as for a wide range of findings obtained from related areas of research [56].

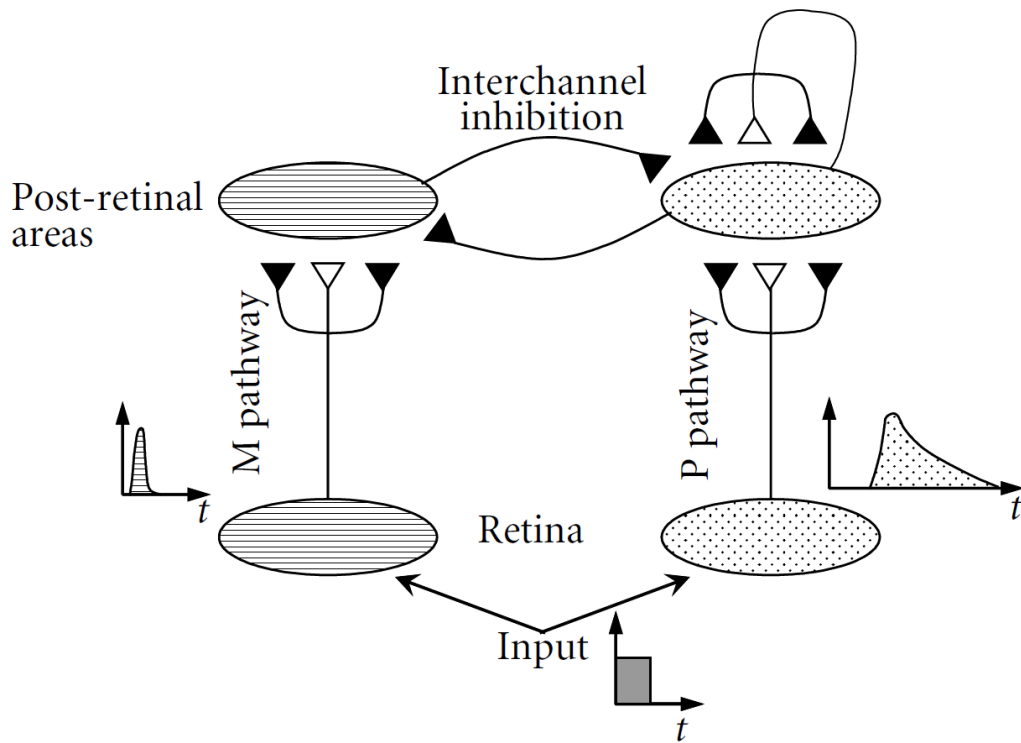


Figure 1.6: Schematic representation of the RECOD model. Filled and open triangles depict inhibitory and excitatory connections, respectively. The bottom ellipses represent the M and P retinal ganglion cells. M pathway represents the transient channel with fast and short-lasting activity. P pathway represents the slow and long-lasting activity. Retrieved from [5].

Building on the dual-channel approach, the retino-cortical dynamics (RECOD) model emphasizes the non-linear reentrant processes while addressing how the visual system solves the unstable state that arises from possible delays in the feedback activity [4]. The initial design of RECOD model includes two bottom layers

representing the retinal ganglion cell populations with distinct morphologies (Figure 1.6). Typical responses of the neurons that form these two populations to a pulse (representing a brief visual stimulation) input are depicted in small activity to time graphs in Figure 1.6. Open and filled synaptic symbols in Figure 1.6, depict excitatory and inhibitory connections, respectively. These magnocellular and parvocellular pathways mirror the properties of transient and sustained channels, respectively [57, 58]. Therefore, these pathways are considered to be neural correlates for these afferent transient and sustained streams in the model. These retinal ganglion cells project to separate layers of LGN represented by the top layers as lumped networks and develop into two parallel afferent pathways (the magnocellular on the left and the parvocellular on the right) as shown in Figure 1.6. The primary cortical targets of the magnocellular stream represent the areas in the dorsal pathway. In contrast, the primary cortical targets of the parvocellular stream represent the areas in the ventral pathway (see the upper ellipses in Figure 1.6).

The model proposes that the parvocellular and magnocellular neurons mutually inhibit one another as shown by the arrows between the upper layers. This mutual inhibition is referred to as inter-channel inhibition while inhibitory interactions within each channel in turn are called intra-channel inhibition [4]. The recurrent connections shown between the upper layers that involve the visual areas responsible for processing motion and brightness represent the comprehensive feedback loop observed between cortical areas as well as the feedback loop from the cortex back to LGN [59]. The model further indicates that these feedback loops operate in three phases. Firstly, a feed-forward dominant phase occurs where the afferent signals move onto higher cortical areas, followed by a feedback dominant phase where feedback (re-entrant) signals influence the information processing, and finally, a reset phase follows allowing the restart of the feed-forward dominant phase when there is a change in the visual inputs.

In metacontrast masking paradigms, the preceding target stimulus produces an initial transient activation which is followed by a slower sustained activation in the afferent pathways. The target visibility is assumed to be correlated with the activation in post-retinal areas that receives information from the sustained

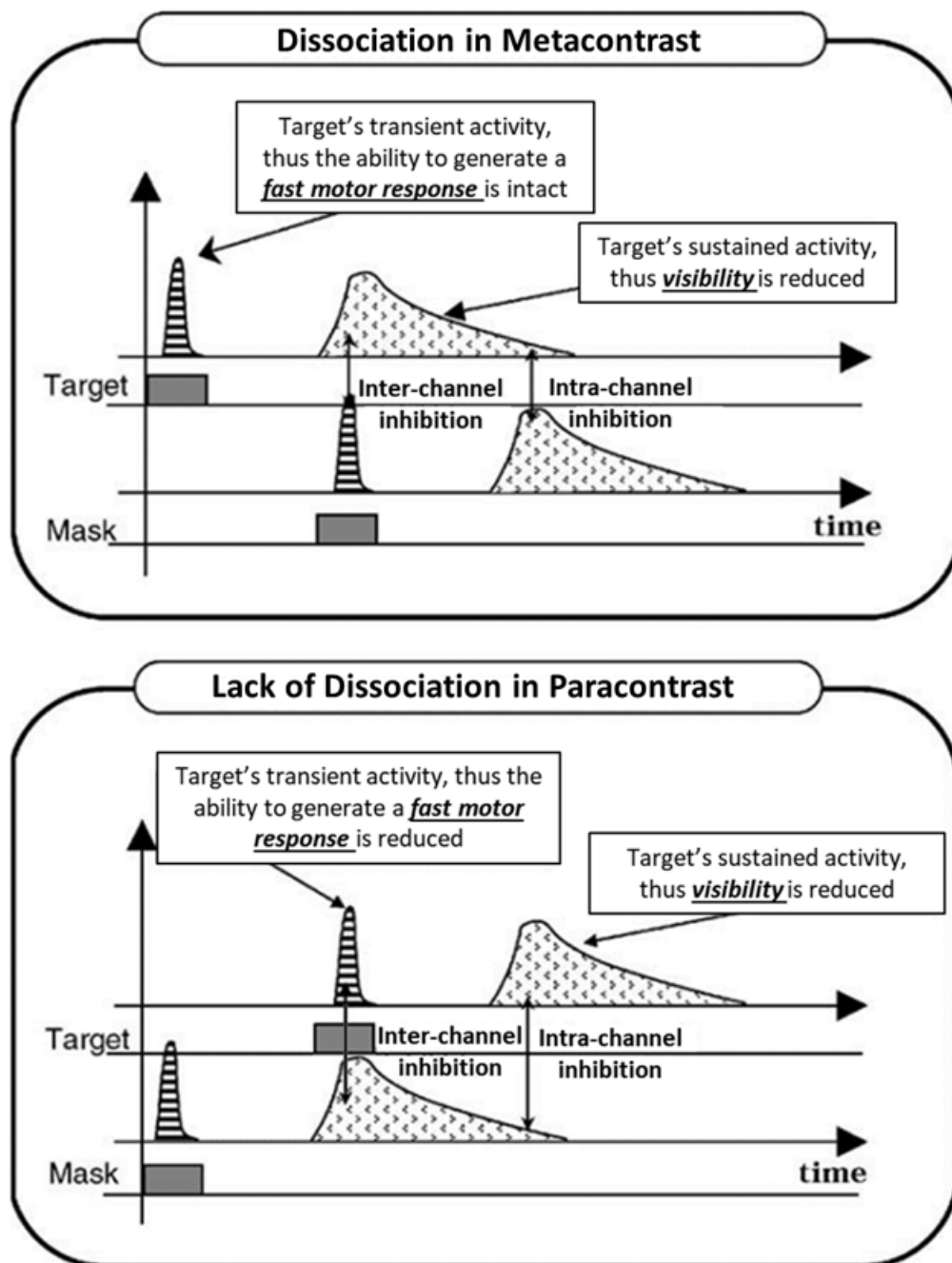


Figure 1.7: Representations of model predictions for metacontrast (top panel) and paracontrast masking (lower panel). Retrieved from [5].

(parvocellular) pathway. Both sustained and transient pathways carry spatial location information about the target stimulus. However, when the observers are required to respond as fast as they can, due to the nature of the transient signals with shorter latency [60, 3], the target localization will be achieved largely by the transient activation. Following the target presentation, a mask is displayed secondly which generates a similar activation pattern to the target. A delay corresponding to the stimulus onset asynchrony (SOA) separates the activities produced by the target and mask. The amount of temporal overlap between the target’s sustained and mask’s both transient and sustained activation is a deciding factor for the suppression over the sustained activation of the target due to both the intra-channel and inter-channel inhibition. As a result, the visibility of the target is predicted to decrease. On the other hand, the transient activation of the target remains mainly unsuppressed therefore the location information of the target is predicted to remain intact [5]. In the case of paracontrast masking where the mask is presented first, the model predicts that both the transient and sustained activities generated by the target would be inhibited by the sustained activation due to the mask, resulting in a decrease in the visibility of the target ([5]; Figure 1.7).

1.2.1.1 Neural correlates of metacontrast masking

Various brain imaging methods have been used to identify the underlying neural mechanisms of visual masking. Due to its temporal sensitivity, EEG (Electroencephalography) is one of the most commonly used techniques to directly identify the time course of neural processing with millisecond precision during cognitive tasks.

Early studies on ERP (event-related potentials) correlates of backward masking revealed reduced amplitude of P2 due to the masking effect [61], while early components such as C1 remained unchanged [62]. Metacontrast masking is commonly used to understand the underlying neural processes underlying visual awareness [63, 64, 65, 66, 67]. These studies typically reported enhanced visual awareness negativity (VAN) related to visual awareness which is manipulated by

SOA, in posterior temporal and occipital recording sites peaking around 200–250 ms after the stimulus onset, often starting shortly after 100 ms. This negative activation is usually followed by a late positive differential activation (LP), typically in the P3 time range, in parietal and central areas. (Figure 1.8). It should be noted that VAN is operationally defined as the negative difference between ERPs that are generated by the stimuli in aware and unaware conditions. Therefore, the measurement of VAN requires always at least two stimulus conditions [6].

Using a pseudo-mask that has minimal masking effect and an effective mask, Railo and Koivisto [68] found that ERPs were more negative for the pseudo-mask (aware) condition compared to the effective mask condition (unaware) at the intermediate SOAs of the U-shaped masking function. This negativity (VAN) was found to be focused on lateral posterior sites between 300 and 400 ms and was followed by a positive difference (LP) after 400 ms. Even though the typical VAN timing is roughly around 200 ms, its onset and peak latency may change based on the experimental design and paradigm. For instance, some studies reported reasonably delayed VAN onset and peak latencies due to low-contrast stimulation [6, 69] and visibility [68].

The late positivity (LP) component is considered as the second component associated with awareness and it is commonly found as the third positive peak (P300) after target onset in the ERP waveform. Some previous ERP studies reported the LP component alone as a correlate of visual awareness (e.g., [70, 71, 72]). However, it was also argued that while these studies were able to observe LP activation due to its larger size, they might not be sensitive enough to detect the smaller VAN activation.

While infrequently observed, the earliest ERP correlate of visual awareness that is observed in response to reduced contrast stimuli [69] or change detection [73] is an early positive increase of P1 (100-130 ms). However, the P1 component is also known to be reactive to selective attention [74]. Thus, the enhanced P1 might only reflect the amplified stimulus signal that was able to cross over the consciousness threshold due to receiving an attentional boost.

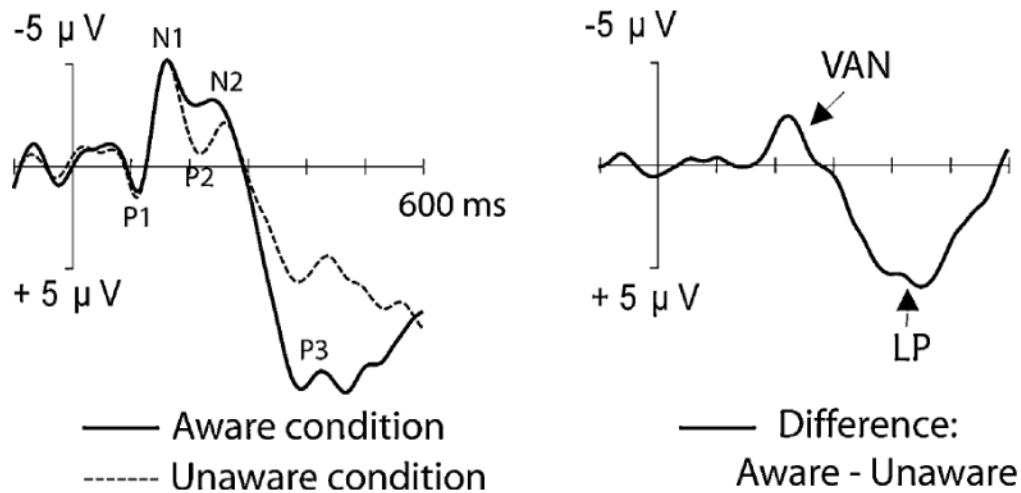


Figure 1.8: (Left) Averaged ERP waveforms for aware and unaware conditions in response to visual stimuli over occipital sites. (Right) Difference ERP waveform between the unaware and aware trials, indicating that awareness correlates with a negative increase in amplitude around 200 ms after the onset of the stimulus (VAN), followed by a positive increase in activation in P300 time range (LP). Retrieved from [6].

1.2.2 Common onset masking

Common-onset masking (also referred to as object substitution masking) occurs when a form-wise inefficient mask (such as four dots surrounding a target) and target are simultaneously presented among other spatially distributed distractors to prevent the observer from identifying the location of the target in advance. In a typical common-onset masking paradigm, the mask acts as a cue for the target stimulus among other competing stimuli while also initiating the masking effect on the target (Figure 1.9A).

Typically, target and mask share the same onset, but the offset of the mask is delayed relative to the target offset. It has been observed that in such a design, traditionally ineffective masks have strong effects when attention is not focused on the target before its presentation ([75, 7]; Figure 1.9B). The common-onset paradigm has become one of the common design to investigate the relationship between perception and attention in the context of re-entrant processes involved in vision and awareness [76, 75, 7].

The effect of common-onset masking is explained by the interaction between selective attention and the re-entrant signals that monitor consistency between the higher-level pattern representation and low-level feature signals [76, 75, 7]. When attention is not well focused because of the distractors, more reentrant cycles are needed for forming a representation and this process takes longer compared to a single target presentation. During this extra time, target signals are replaced by mask signals at the entry-level, leading to a mismatch. Thus, the target representation is substituted by the mask representation.

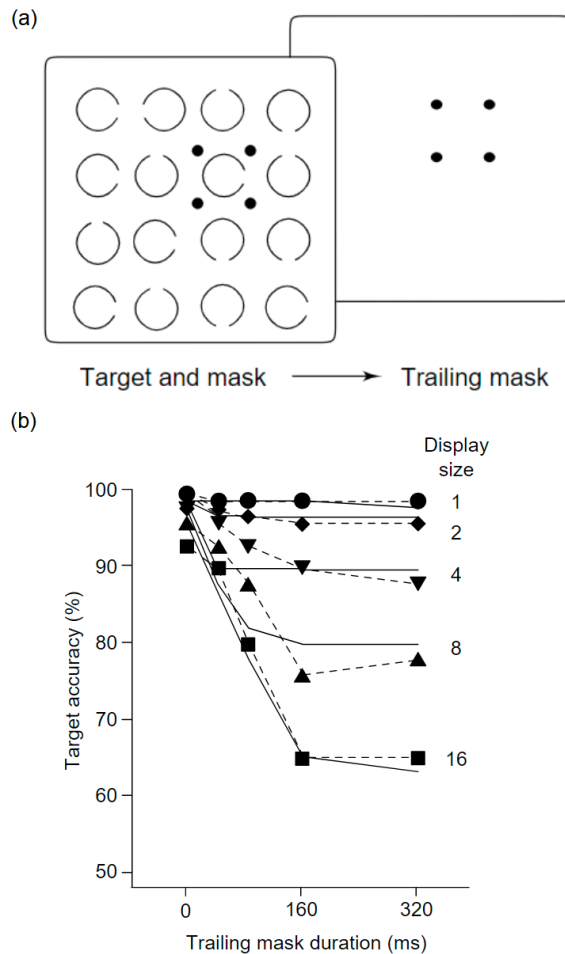


Figure 1.9: (a) Illustration of the display sequence of a common-onset masking experiment with a four-dot mask. The observer is required to indicate the orientation of the gap in a broken ring that is cued by surrounding four dots. The other rings serve as distractors. (b) Results of a typical common-onset masking paradigm with various set-size conditions. Retrieved from [7].

The effect of common-onset masking relies on the premise that attention cannot be focused quickly enough on the target location, therefore there is an interaction between the set size of possible targets and the duration of the mask following the target. However, mounting evidence points to the possibility that this interaction occurs only when there is ceiling and floor effect in behavioral performance values (e.g., accuracy scores) [77].

With regards to the metacontrast masking paradigm, Agaoglu et al. [78] similarly designed an experiment where the stimulus parameters for each observer were adjusted to avoid these possible saturation or floor effects. They found evidence against interactions between the metacontrast masking effect and attentional mechanisms. These findings rather fitted best with a regression model indicating that masking strength (a function of SOA) and attentional load (a function of set size) independently influence the response errors of observers.

1.2.2.1 Neural correlates of common onset masking

Neurophysiological studies on common-onset masking were especially focused on revealing the stage of information processing where the masking effect operates. Recent ERP studies found markers for selective attention (N2pc) as well as visual working memory consolidation in the form of sustained posterior contralateral negativity (SPCN) [79, 80]. These results suggested that being unable to perceive the target due to the delayed-offset masking effect can be a result of failing to encode the target in visual short-term memory. Consistent with these results, evidence from an fMRI experiment demonstrated that successfully masked targets could not form any neural representations in the lateral occipital cortex [81]. Furthermore, Woodman [82] reported that the error-related negativity that is typically observed for incorrect trials, was absent in the delayed-offset condition, possibly suggesting that the effect of common-onset masking prevents the formation of a target representation that would be necessary for error detection.

1.3 Attention

The visual system is sophisticated and complex. On the other hand, it has also limited capacity for the vast amount of available information provided by the natural environment. Therefore, it is inevitable that visual processing is very selective by allocating perceptual or cognitive resources to the preferred stimulus at the expense of ignoring others. The distribution of resources to the relevant portion of the visual input, while ignoring irrelevant perceivable information, is referred as selective attention [83, 84, 85].

1.3.1 Theories and models of attention

At a given time, only a specific amount of information can be retained and used to control behavior and selecting the relevant information to be used means filtering out competing information. This idea of competition led to the development of a theory of attention named the biased competition theory which attempts to explain the processes leading to visual attention and its neural correlates [85]. The biased competition theory assumes that multiple stimuli in the visual field activate groups of neurons that participate in competitive interactions. Attending to a stimulus at a particular location or with a particular feature, results in biased competition in favor of neurons that are preferentially active in response to that particular feature or location. The attentional effect, therefore, is produced by the feedback signals originating from outside the visual cortex that is sent back to extrastriate areas, in which they bias the competition by increasing the activation of the neurons associated with the attended stimulus, thereby suppressing the activity of cells representing the distracting stimuli [84, 85]. Early recording studies on monkeys provide evidence that supports the biased competition theory at extrastriate areas. Moran and Desimone [86] illustrated that the tuning of visual neurons in the cortex was modified by the instructions given to the monkeys to attend to the location of the target stimulus. They used stimuli that would be effective to elicit a response from the neuron such as a vertical white bar and also the stimuli that would be ineffective like a horizontal black bar. In other

words, they made sure that the effective stimulus made the neuron fire whereas the ineffective stimulus did not. They presented these two stimuli simultaneously within the neuron's receptive field, and when spatial attention was directed to the effective stimulus, the pair of stimuli elicited a strong response. However, when the attention was directed to the ineffective stimulus, even though the effective stimulus was still in its original location, the identical pair produced a weaker activation. Similar studies by Luck, Chelazzi, Hillyard and Desimone [87] and Reynolds, Chelazzi and Desimone [88] revealed similar findings on area V4 and showed similar attentional modulation effects in areas V1 and V2 as well [89]. Another influential model on visual attention is the attentional contrast-gain hypothesis which suggested that stronger responses due to an increase in attention could be achieved by increasing the effective luminance contrast of the attended stimuli (e.g., [85, 90, 91]). The attentional contrast-gain hypothesis was motivated by the fact that relative stimulus contrast impacts stimulus competition within the receptive field. The model suggests that the underlying mechanisms of attention take advantage of the predisposition of a visual neuron to respond to the highest contrast preferentially, within its receptive field [92]. By increasing the active contrast of the selected stimulus relative to ignored stimuli within the receptive field, attention can ensure that a visual neuron responds primarily to the attended stimulus. An ERP study investigating the modulation of contrast appearance due to exogenous attention revealed the perceived contrast of the stimulus at the attended location increased simultaneously with amplification of early neural response (around 100-140 ms) in the ventral, occipito-temporal visual cortex contralateral to the target [93]. Moreover, the increased amplitude of the neural response correlated positively with the perceived contrast of the previously cued stimulus. These findings provide support for the contrast gain model [88, 91] that adopts the notion that attending to a stimulus increases perceived contrast by enhancing early sensory processing in the visual cortex, thus increasing the effective contrast of the stimulus. An important concern about contrast-gain model is that it does not address the problem of saturation due to high contrast stimulation. Visual neurons have a limited range in the contrast domain, therefore if the contrast of the stimuli is high, a further increase in contrast, does

not increase the neuron’s spike rate at the same level. Therefore, due to this saturation, while attention should be effective for low to medium contrast stimuli, it should be ineffective for high contrast stimuli. Although this prediction was supported by some studies (e.g., [91, 94]) others showed that attention effects on neuronal spike rates were relatively independent of stimulus contrast or in some cases even stronger for higher-contrast stimuli (e.g., [95, 96]). The normalization model of attention [97], resolves this apparent discrepancy by integrating divisive normalization. The model predicts that the effectiveness of selective attention for different levels of contrast depends on stimulus size relative to the receptive field as well as the size of the spatial focus of attention. A strong attention effect is expected for low to medium levels of contrast when the stimulus is small and the focus of attention is large, and for high-contrast levels when the stimulus is large and the focus of attention is narrow. These predictions resolve previously discrepant results in the literature regarding how neuronal effects of attention depend on stimulus contrast (see [97] for a review). The normalization model also accounts for feature-based attention (e.g., attending to a specific orientation or motion direction) by combining neural tuning and attentional focus in a feature dimension.

1.3.2 Spatial attention

Spatial attention allows the information available within a prioritized area of the visual field to be selectively processed. Metaphors such as a spotlight have been used to explain spatial attention in early studies. According to these accounts, visual attention selects any stimuli that fall within a selected region, so that the information from these stimuli can be subjected to thorough processing and identification while the area outside the attentional spotlight will be processed much less thoroughly. In other words, an observer is typically faster and more accurate at detecting a target that appears in an expected location compared to an unexpected location [98]. Similarly, a zoom-lens metaphor has been suggested with the addition that this focus of attention can narrow or widen in distribution with an inverse relationship between the size of the attentional focus and the

efficiency of processing [99].

However, accumulating evidence indicates that a simple comparison and direct representation of metaphors for attentional focus is limited to explain many different situations in daily life. Instead, the data collected from many other studies using different methods suggest that visual attention shows a gradient profile with enhanced sensory processing at the attended location and it is gradually decreasing while the distance from the focus increases. Behavioral evidence shows that the speed or accuracy of stimulus detection continuously decreases with distance from the center of attention [100, 101, 102]. Consistent with these results, observations based on ERP recordings demonstrated a similar graded decrease in the attention-related amplitude enhancement of early sensory components (P135, N190) with increasing distance to the focus of attention [103]. Similarly, it was reported that sensory ERP components (N1, Nd1, Nd2) elicited by items presented at unexpected locations were gradually diminished with distance to the expected target location [104].

Many experimental reports also suggest a more complex profile or topology supported by behavioral data indicating a performance decrement in the immediate surround of the attentional focus falling even below the performance values recorded at locations at a greater distance away from the focus [105, 106, 107, 108, 109]. This suggests that spatial attention operates in a more complex profile than a simple gradient, instead, a central enhancement could be surrounded by an area where a comparable reduction is observed. Visual search experiments mostly provide evidence for the center-surround type of profile where detection performance at the target location was high as expected but it was also better at the distractor locations far from the target as compared to the locations closer to the target [105]. Similarly, behavioral results based on target discrimination, item-matching as well as distractor interference indicate a performance difference between the vicinity of the target, where there is a decline in the performance, and locations further away, where the performance restores back [110, 111, 106, 107]. Overall, such behavioral results from various experimental paradigms point to a center-surround form of attentional focus which was later supported by neuroimaging evidence from humans [112, 113, 114]. In

one such study, functional magnetic resonance imaging (fMRI) results revealed neural suppression in regions of the striate visual cortex that retinotopically correspond to the surrounding attended locations [114]. Systematic evidence for such a center-surround profile has also been provided in a number of experiments using visual search paradigms with magnetoencephalographic (MEG) recordings [115, 116, 117, 113].

Finally, research further suggests that whether the spatial focus operates with a simple gradient design or uses a more complex center-surround profile depends on the task requirements. Specifically, the center-surround profile is adopted when there is a need for higher spatial resolution or detailed item localization for target discrimination. Whereas, a simple gradient profile is used when the task depends on feature discrimination without detailed spatial resolution. This change in spatial focus profile according to task requirements is suggested to be a result of recurrent top-down selection since the initial feedforward sweep of processing is assumed to be too coarse for differentiating the task-relevant needs [118].

1.3.2.1 Neural mechanisms of spatial attention

The temporal precision of EEG has been useful in probing the time course of neural processing of spatial attention. Directing attention to the location of a stimulus typically results in an enhancement of the amplitude of the early P1 (latency of 90–130 ms) as well as N1 (130–200 ms) ERP components over posterior scalp sites contralateral to the attended visual field (see [119, 120, 121] for reviews). This increase in amplitude suggests that spatial attention selectively amplifies the flow of sensory information in the hierarchical processing [122, 123]. Through this amplification mechanism, stimuli from attended locations are assumed to have an improved signal-to-noise ratio facilitating the extraction of relevant information from attended areas. The pattern of enhanced P1 and N1 amplitude is believed to be common for the spatial focusing of attention across a variety of task situations such as speeded reaction times and improved detectability in trial-by-trial cueing tasks [120, 124, 125], as well as increased accuracy in

visual search tasks [126]. In contrast, an earlier ERP component C1 (50-90 ms) has been the subject of an ongoing debate regarding its sensitivity to spatial attention (see [127, 128]). While earlier studies found C1 component to be invariant to spatial attention [119, 129, 130], more recent studies reported early activation that falls into C1 range [131, 132].

ERP recording combined with other neuroimaging techniques such as PET [133, 134, 135, 136] and fMRI [137, 138, 139, 140, 141] also found increased activity in many extrastriate cortical areas connected to the observed ERP amplitude changes, confirming the idea that the frontal and parietal areas part of the attentional network are involved in producing attentional effects, and subsequently, there is modulation of activation strength in visual occipital areas [138, 142].

Furthermore, several studies reported a difference between the attentional effects of P1 and N1 components which indicates that they might reflect different aspects of early spatial selection [143, 144, 124, 145]. While the P1 effect might be an indicator for facilitation for selectively processing of endogenously attended stimuli, the N1 effect might indicate a transient distribution of attention activated by the stimulus appearance. This differentiation can also be observed as a similar P1 and N1 dissociation found in previous ERP studies [143, 144, 124, 146]. Moreover, evidence also points to a link between N1 and attention switch to a task-relevant location [144, 147]. Taken together, this evidence suggests that while P1 could be an indicator of a predetermined bias and a consequently sustained gating of input at the attended location, N1 might be related to a shift of attention elicited by potentially relevant events.

1.3.3 Feature-based attention

In daily life, we have no prior information about the location of a potential target, but rather need to rely on featural information for its detection. Independent of spatial attention, it is also possible to selectively attend to particular features throughout the visual field. Feature-based attention directs limited processing

resources on the task-relevant sensory inputs in the form of features such as particular orientations, colors, or directions of motion, regardless of their locations by enhancing the features within a dimension at the expense of unattended or behaviorally irrelevant features. Many psychophysical studies have demonstrated that feature-based attention improves detection or otherwise enhances behavioral performance across the visual field [148, 149, 150, 151, 152]. While there is ample evidence indicating feature-based attention operates within the spatial locus of attention (e.g., [153, 154]), there are also psychophysical and neurophysiological studies revealing that the effects of feature-based attention are deployed simultaneously throughout the visual field, independent of the locus of spatial attention modulating visual processing even in locations that are irrelevant to the observer’s current task [155, 156, 157, 158, 159, 160, 161, 162].

Visual search is a popular paradigm that has been used to study the ability to detect, discriminate or localize a target among distractors. In a ‘feature search’ where the observer is instructed to detect a specific feature of a target amongst distractors, it would be useful for the observer to grant priority in processing relevant features, or to enhance their representation. Indeed, it has been proposed that an early stage of the search process is to select the subset of stimuli that contain at least one of the target’s features [163, 164, 165]. Support for this proposal comes from studies in which cueing relevant features (either size or color) aided performance in visual search tasks, under some conditions, by prioritizing the processing of those stimuli and guiding spatial attention to these features compared to others [166, 167].

1.3.3.1 Neural mechanisms of feature-based attention

The effects of feature-based attention are typically characterized by a broad negative deflection over posterior electrode sites, the selection negativity (SN), which begins 140–180 ms after stimulus onset and persists for 200 ms or more. A smaller selection positivity (SP) occurring in the same interval as the SN but with a topographical distribution over anterior scalp regions, is also often observed (for

reviews see [168, 121]). A slight variation of onset latency and scalp distribution of SN and SP have been reported for several different non-spatial features such as orientation, color, spatial frequency, the direction of motion, and shape [121, 139, 169].

Based on guided search theories, feature selection would be expected to precede the indices of location selection during visual search. During visual search tasks, where the location of the target changes from trial to trial, feature-based attention might guide spatial attention to potential target objects [170, 171]. Using a visual search task, Hopf et al. [172] investigated the spatiotemporal correlates of feature-based and location-based selection at the same time. They found an enhanced response to distractor stimuli that contain the target feature, observed in the ERPs contralateral to the side of stimulus presentation. Importantly, this feature-selective modulation emerged as early as 140 ms after the onset of the stimuli, while the N2pc component indicating the focusing of attention on the location of the target did not arise until 170 ms post-stimulus. These results demonstrate that the processing of task-relevant features precedes the selection of the target location in visual search, indicating that feature-based selection can guide spatial attention to the location of the target object, further adding to the notion that feature selection is temporally flexible and adapts according to the specific task requirements.

1.3.4 Object-based attention

Object-based selective processing, conversely, is based on the observation that when one feature of an object is selectively attended to, the processing of other features of the same object can also benefit the effects (e.g., [173, 174, 175, 176, 177, 178, 179, 180, 181, 182, 183, 184, 185, 186, 187]).

In a well-known study [174], two overlapping objects, a box and a line, each with two varying feature dimensions were presented. The observers performed better at reporting two features of the same object than two features that belong to different objects. Since the two objects overlap in space, the modulation of

accuracy cannot be attributed to spatial factors, rather, it should be attributed to the switching of attention from one object to the other. Valdes-Sosa et al. [185] introduced a transparent-motion design as a more refined tool to examine object-based attention without the potential influence of feature-based or spatial attention. There have been numerous follow-up studies that have used variants of this design to investigate behavioral and/or neuronal correlates of object-based attention. Although there have been some design differences all of these studies used stimuli composed of two superimposed counter-rotating, differently colored dot fields. One of the two dot fields is “cued”, either endogenously (e.g., fixation point color indicating the color of field to be attended) or exogenously (e.g., by a delayed-onset of one dot field, see below). The rotations of the dot fields are interrupted by brief translations (one or two translations, depending upon the design), and subjects are asked to report the direction of those translations. These translations consist of a subset of the dots moving coherently in typically one of eight directions. To discourage tracking of individual dots, the remaining dots of the translating dot field translate in randomly chosen directions. Numerous studies using this basic design have repeatedly found that subjects judge translations of the cued dot field more accurately than translations of the uncued dot field [184, 185, 176, 177, 178, 188, 180, 181, 182, 189]. In these experiments, spatial attention is ruled out by the spatial intermixing of the moving dots, and feature-based (i.e., based on motion direction) selection is ruled out since the direction of the translation is unpredictable. Finally, by removing the color differences between the two dot fields, Mitchell et al. [178] revealed that the performance bias is not color based. These findings have thus been taken as evidence of object-based (sometimes referred to as surface-based) attention whereby attention is cued to one of the rotating dot fields, and an attentional benefit extends to a new unpredictable feature (i.e., the translation) of that object.

While simpler than the original design of Valdes-Sosa and colleagues (i.e., fewer translations and responses per trial, and no endogenous attentional cue), Reynolds et al. [181] provided evidence that this delayed-onset design (Figure 1.10A) captures the essence of the original design. In the delayed-onset design, subjects obtain stable fixation followed by the appearance of the first rotating

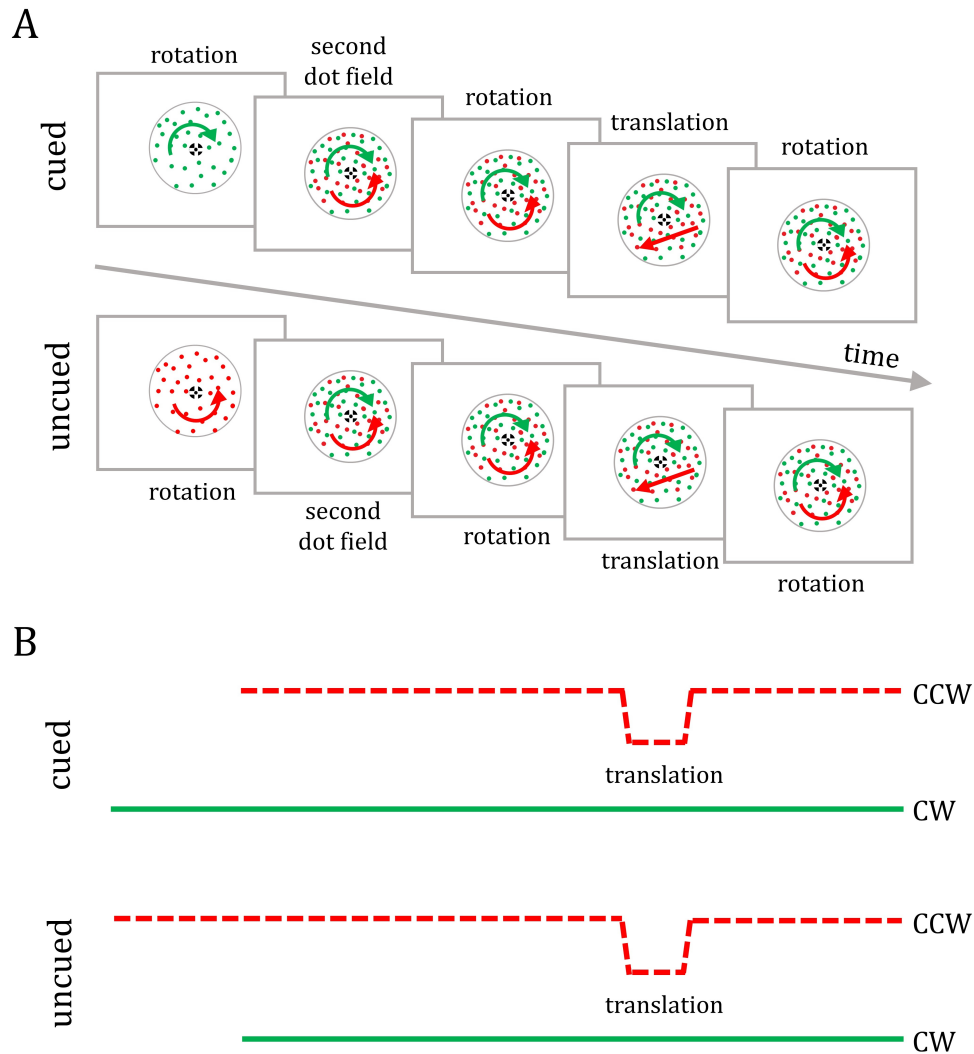


Figure 1.10: Delayed-onset design. (A) One rotating dot field appears followed by the second “delayed” dot field. Two superimposed dot fields rotate in opposite directions around the fixation point, allowing the perception of two transparent surfaces. Following the rotation, either the delayed (cued) or non-delayed (uncued) dot field translates briefly. After the translation, both dot fields continue to rotate. (B) Feature-based illustration of timeline. The two dot fields are differentiated by line style (dashed or solid) and with dot field colors indicated by the line colors. The vertical line placement indicates the different motion directions: clockwise rotation (CW), counter-clockwise rotation (CCW), and translation. The onset differences in this design result in “cued” translations that occur in the presence of the older rotation direction and “uncued” translations that occur in the presence of the newer rotation direction.

dot field. After a delay, a second (delayed) dot field appears that is rotating in the opposite direction. Following a period of dual rotation, one of the two dot fields (either the first or the delayed dot field) translates briefly (as described above), and then both dot fields resume rotation for a brief period of time. Subjects report the direction of the translation at the end of the trial. Reynolds et al. [181] found that the translations of the delayed dot field were judged more accurately than translations of the dot field that appeared first. As stimulus onsets appear to act as exogenous cues that briefly attract attention [190, 191], Reynolds et al. [181] postulated that the onset of the delayed dot field acted as an exogenous cue that captures attention and yields an object-based processing benefit if the delayed dot field translates a few hundred milliseconds later. Their results were interpreted as providing further evidence of object-based selection in transparent-motion stimuli whereby the successive motions (i.e., the rotation followed by the translation) of a cued object are preferentially processed relative to motions of an uncued object. Taken together these numerous studies appear to provide abundant psychophysical (and also neuronal) evidence of object-based attention, whereby attention embraces all the features of a cued object (e.g., a specific color and rotation direction) including new features such as a brief translation. Given that Mitchell et al. [178] found that the cueing effect survived the removal of color differences, Stoner and Blanc [189] observed that for this object-based account to be valid, a processing advantage would seemingly have to first be granted to the rotation direction of the cued object and that this advantage would then have to extend to the translation in an object-specific manner. The object-based account thus requires a mechanism that somehow links or “binds” successive motions (i.e., rotations and translations) with each other in an object-specific manner. Stoner and Blanc [189] questioned the necessity of the object-based explanation and offered an alternative motion-competition explanation. Unlike the object-based account, the motion-competition model posits that the key determinant of behavioral performance is not whether the cued or uncued object (i.e., dot field) translates but whether the translation “competes” with the rotation direction that was presented first or second regardless of which set of dots undergo those motions (Figure 1.10B). To distinguish between the motion-competition and object-based models, Stoner and Blanc [189] introduced motion

(rotation direction) swaps between the two dot fields at the onset of the brief translation. These motion swaps reverse the relationship between cueing and which rotation direction (delayed or undelayed) competes with the translation. As a consequence, the motion-competition model, contrary to the object-based account, predicts that this manipulation should reverse the performance asymmetry seen in the standard paradigm without motion swaps. Specifically, if the rotation direction is swapped at the onset of the translations, then translations of the cued (delayed) dot field should be harder to judge than translations of the uncued dot field. Stoner and Blanc [189] found, however, that the performance advantage did not reverse with these motion direction swaps. They also found that color-swaps similarly did not reverse the performance advantage. Stoner and Blanc’s [189] findings thus supported the object-based account and ruled out the established competition and normalization models (e.g., [192, 97]) as an explanation for their results. Moreover, their finding that the cueing effect was dot-field specific implicated mechanisms that could distinguish between the spatially intermixed and moving dots of the two dot fields.

1.3.4.1 Neuronal correlates of object-based attention

Unlike feature and spatial attention, the neuronal mechanisms underlying object-based attention are not readily explained by current models. However, in addition to providing behavioral evidence of object-based attention, variants of the original transparent-motion design have been adapted to study single-unit correlates in the non-human primate [193] and neural mechanisms using functional magnetic resonance imaging (fMRI) [194, 195]. Of particular interest here is the use of these designs to study the neural substrates of object-based attention via EEG [176, 196, 177, 180, 184, 197]. In the first such study, Valdes-Sosa et al. [184] found that when attention was endogenously cued to one dot field, the amplitude of both P1 (134–203 ms) and N1 (244–293 ms) components elicited by an uncued translation was reduced (see also [196]). Both of these components have been generally associated with extrastriate areas [i.e., beyond the level of the primary visual cortex (V1)]. This early experiment used a blocked design in which

subjects continuously attended to either green- or red-colored dot fields within a block of stimuli. Follow-up studies have used trial-by-trial cueing and have consistently found N1 modulation but (except for [176]; see below) have not found significant modulation of earlier components [177, 180, 197]. The source of N1 modulation in these studies was found to be consistent with the involvement of area MT+ (human middle temporal complex) and area V4 and hence associated with the changes in mid-level visual processing [197]. Using a design introduced by Reynolds et al. [181], Khoe et al. [176] found modulation of the N1, but, surprisingly, also found modulation of the C1 component. The C1 component is believed to reflect activities in the striate cortex [198, 199]. Specifically, they reported that the posterior C1 (75-110 ms) and N1 (160-210 ms) components elicited by the translations of the cued dot field were larger compared to those elicited by the translations of the uncued dot field. A subsequent fMRI study, using a design similar to that of Reynolds et al. [181], found enhanced activation in areas V1, V2, V3, V3A, and MT+ for translations of a cued dot field compared to translations of the uncued dot field [194]. Overall, these studies consistently implicate mid-level cortical areas in the performance biases seen in these stimulus designs with some studies also suggesting earlier cortical areas, including area V1.

1.4 Specific Aims

Vision is a complex, dynamic process that allows humans to efficiently deal with massive amounts of information in the visual scene by selecting relevant information and filtering out irrelevant information by recruiting distinct processing pathways. From an operational perspective, attention is a matter of organizing or prioritizing different neural stages while processing information, and consequently, studying attentional processes allows the observation of neural mechanisms of vision in various neural stages. In the present thesis, we employed the EEG methodology to explore attentional selection due to its temporal resolution in conjunction with refined experimental paradigms that cover different complementary modes of attention. Using metacontrast masking combined with the manipulation of attentional load in the visual field, we aimed to understand

the role of spatial attention in information processing and possible interactions with masking mechanisms. This approach allowed us to understand the role of spatial attention in visual dynamics by using a simple but informative masking paradigm. Moreover, we also investigated the role of feature- and object-based attention in relatively complex visual scenes including dynamic moving objects. Particularly, by employing a novel variant of transparent motion design, we aimed to isolate the object-based effect from a possible feature-based explanation in both psychophysical measures and neural activities.

1.4.1 Study 1: Electrophysiological Investigation of Attentional Modulation on Metacontrast Masking

It has been established that both selective attention and metacontrast masking control the information processing at the sensory level. At the same time, previous studies suggest that the mechanisms underlying their effects are distinct, although both processes influence similar levels of information flow, from sensory information to consciousness. There is still an ongoing debate on whether selective attention and masking effects are completely independent processes. In this respect, determining whether masking and selective attention interact has important implications for theories of attention and visual masking.

Attention typically influences low-level visual processes to enhance visual awareness. There is evidence that pre-cueing attention to the location of the target-mask pair causes a release from metacontrast masking [200, 201] while increased attentional demand by presenting distractor stimuli results in a stronger metacontrast effect [202]. However, selective attention has overall facilitative and inhibitory effects in almost all aspects of vision regardless of criterion contents [98, 203]. Initial models of masking did not incorporate the effects of attention, assuming that attention and masking are independent processes (e.g., [204, 55, 205, 206, 207]). In other words, depending on the locus of attention or attentional load, selective attention can be incorporated into these models largely as an add-on process rather than dismissing the role of attention.

Conversely, the interaction between attention and masking is an essential element of the object substitution theory of common-onset masking. Specifically, the common-onset masking effect depends on the involvement of selective attention in target perception, and whether attentional load allowed enough time for higher-level processing in the visual system to send reentrant signals back to the early sensory levels [76, 75, 7]. These reports of interactions have not been limited to the common-onset masking paradigm but included metacontrast masking studies as well [208, 209, 210]. Yet, recent evidence shows that previous studies may have suffered from ceiling or floor effects that induced an artefactual appearance of interactions [77, 211, 212] pointing to an overall modulatory role of spatial attention. Finally, Agaoglu et al. [78] further investigated the existence of an interaction between metacontrast masking and attention while avoiding saturation/ceiling and floor artifacts by adjusting stimulus parameters for each participant and found no evidence of such interaction.

Neurophysiological studies of common-onset masking particularly question the level of information processing hierarchy where the masking effect takes place, therefore require precision to register and analyze the correlates of processing. An ERP study using a standard stimulation setup of common-onset masking found a significant relationship between the amplitude of the P2 component and behavioral response accuracy [213]. On the other hand, these results were reported using analyses that lacked comparison between ERPs of correctly reported versus incorrectly reported trials with identical stimulation conditions. Therefore, direct interpretation of the results was highly speculative due to this problematic design approach (see also [214] for more details). Although more comprehensive analyses approach were in the following ERP studies of masking [215, 216], they also suffer from the same methodological problem. These methodological problems were better addressed by some of the masking studies [217, 218, 79]. However, further evidence is needed to understand the neural underpinnings of the effect of attention over the masking process for common-onset masking as well as metacontrast masking using a controlled experimental design and appropriate ERP analyses.

Based on previous research, the first study of the current thesis were focused

on investigating whether metacontrast masking and attention interact by using an experimental design similar to Agaoglu et al. [78], in which saturation and floor effects are avoided. We specifically aimed to examine the effects of spatial attention on metacontrast masking using electroencephalography with an orientation discrimination task under different masking conditions achieved by different SOAs while manipulating spatial attention by changing the set size in the visual field.

1.4.2 Study 2: Behavioral and ERP evidence that Object-based Attention Utilizes Fine-grained Spatial Mechanisms

Numerous studies appear to provide abundant psychophysical and neuronal evidence of object-based attention, whereby attention embraces all the features of a cued object (e.g., a specific color and rotation direction) including new features such as a brief translation. Stoner and Blanc [189] questioned the necessity of the object-based explanation and offered an alternative motion-competition explanation. The motion-competition explanation by Stoner and Blanc [189] begins with the same assumption as the object-based account: the delayed-onset grants the rotation direction of the delayed dot field a momentary processing advantage (yielding larger neuronal responses) relative to the rotation direction of the dot field that appears first. The motion-competition explanation diverges from the object-based account in not assuming that this advantage is somehow extended to the translation in an object-specific manner. Instead, the motion-competition account simply assumes that this processing advantage persists during the translation. It follows that translations of the cued (i.e., delayed) dot field would occur in the presence of rotation direction responses that are larger than the ones that occur in the presence of translations of the uncued dot field. This assumption leads to the motion-competition explanation of how cueing impacts neuronal and behavioral responses in these experiments. To appreciate this explanation, first, note that a key feature of the competitive stimulus interactions observed in area MT and elsewhere (and in the models that capture those interactions) is that

competing stimuli that elicit larger responses also elicit greater inhibition. This fact coupled with the assumption of a response asymmetry to the rotations of the cued vs. uncued dot fields thus leads to the prediction that responses to translations of the cued (delayed) dot field would be less inhibited (and hence larger) than responses to translations of the uncued dot field. Indeed, using simulations, Stoner and Blanc [189] showed that a model based on competitive stimulus interactions could account for the neuronal (and, by extension, the behavioral) effects observed with the various transparent-motion paradigms reviewed above. Their motion-competition model parsimoniously accounts for these findings without the need to invoke object-specific attentional enhancement. This alternative explanation casts doubt on the object-based interpretation of the numerous studies that had used variants of the Valdes-Sosa et al. [185] design. As these studies seemingly constituted some of the best evidence of object-based attention [181], the analyses of Stoner and Blanc [189] suggested that the case for object-based attention was less overwhelming than had been thought.

Unlike the object-based account, the motion-competition model posits that the key determinant of behavioral performance is not whether the cued or uncued object (i.e., dot field) translates but whether the translation “competes” with the rotation direction that was presented first or second regardless of which set of dots undergo those motions. To distinguish between the motion-competition and object-based models, Stoner and Blanc [189] introduced motion (rotation direction) swaps between the two dot fields at the onset of the brief translation. These motion swaps reverse the relationship between cueing and which rotation direction (delayed or undelayed) competes with the translation. As a consequence, the motion-competition model, contrary to the object-based account, predicts that this manipulation should reverse the performance asymmetry seen in the standard paradigm without motion swaps. Specifically, if the rotation direction is swapped at the onset of the translations, then translations of the cued (delayed) dot field should be harder to judge than translations of the uncued dot field. Stoner and Blanc [189] found, however, that the performance advantage did not reverse with these motion direction swaps. They also found that color swaps similarly did not reverse the performance advantage. Stoner and Blanc’s

[189] findings thus supported the object-based account and ruled out the established competition and normalization models (e.g., [192, 97] as an explanation for their results. Moreover, their finding that the cueing effect was dot-field specific implicated mechanisms that could distinguish between the spatially intermixed and moving dots of the two dot fields. Stoner and Blanc's [189] study is the only study of the numerous studies cited above that provided evidence of object-based selection that cannot potentially be explained by previously identified competitive/normalization mechanisms. In the second study of the current thesis, we wanted to confirm these findings indicating that the behavioral effect of cueing survives feature swaps. Secondly, since ERPs have not been previously collected with the delayed-onset design, it is conceivable that the ERP correlates observed using other variants of that paradigm are specific to the details of those designs (e.g., the presence of two translations per trial rather than one translation per trial as in the delayed-onset design). Indeed, different studies using slightly different designs have found somewhat different ERP results. However, we aimed to confirm that the N1 modulation found in previous studies was not specific to those designs and would also be found with the delayed-onset design. This would support the conclusion by Reynolds et al. [181] that the delayed-onset design captured the key features of the more complicated designs. Third, and most importantly, the ERP correlates observed in previous experiments are all subject to a motion-competition interpretation. Hence, it is unclear whether the previously identified ERPs associated with cueing are truly related to object-based attention. Thus, the identification of ERPs associated with cueing that survived the feature-swaps could be recognized as supporting object-based attention rather than reflecting competitive interactions between direction-selective neurons. Lastly, based on their findings, Stoner and Blanc [189] hypothesized that area V1 is involved in the object-based they identified. We were, therefore, interested in determining whether we might find further evidence of V1's involvement, such as seen by Khoe et al. [176] and Ciaramitaro et al. [194]. Any such ERP modulation tentatively associated with V1 would need to survive feature swaps to be identified as supporting object-based cueing.

Chapter 2

Electrophysiological Investigation of Attentional Modulation on Metacontrast Masking

2.1 Introduction

The relationship between visual masking and attention has been extensively studied since both mechanisms control sensory and perceptual processing. Even though the proposed mechanisms underlying these effects are thought to be distinct, both processes influence similar levels of information flow, starting from sensory processing up to consciousness. Therefore, the relationship between the mechanisms of masking and attention remains to be further investigated with neurophysiological techniques. In the current chapter, we studied the effects of spatial attention on metacontrast masking using EEG. We employed an orientation discrimination task under different masking conditions in which saturation and floor effects are controlled and manipulated spatial attention by changing the target set-size. We hypothesized that increasing attentional load would result in an overall decrease in behavioral accuracy scores regardless of the metacontrast masking effect induced by different SOAs, suggesting these two mechanisms work

independently. We also expected to observe a higher difference in amplitude between high and low visibility SOA conditions, spatiotemporally emulating the components for visual awareness negativity (VAN) and late positivity (LP). Reflecting on the expected behavioral results, we hypothesized that the attentional load to be an add-on effect that further increases the amplitude difference regardless of the metacontrast masking conditions.

The behavioral results revealed a main effect of both set-size and metacontrast masking with a two-way interaction that suggests differential effects of spatial attention on metacontrast masking. On the other hand, the EEG analyses revealed significant effects for masking and attentional load on early negative components (P1/N1 range: 90-210 ms and VAN range: 240-310 ms) located over occipital and parieto-occipital scalp sites. The effects of set-size and masking were also found to be dominant in the late positivity range (LP, 350-580 ms) centered over centro-parietal electrodes. Overall, these findings indicate that spatial attention takes place at different stages of sensory and perceptual processing. Regarding the relationship between attention and metacontrast masking, they further suggest that the effect of spatial attention may also have distinct characteristics at different stages.

2.2 Methods

2.2.1 Participants

Nineteen adult human volunteers (12 females and 7 males, age range 18 - 34 years) completed all experimental procedures and sessions. All participants had normal or corrected-to-normal visual acuity and no history of neurological disorders. All participants were informed about experimental procedures before participation and signed a consent form. The inclusion/exclusion criteria were established prior to data analyses. All procedures were carried out under the Declaration of Helsinki (World Medical Association, 2013) and approved by the local Ethics

Committee of Bilkent University.

2.2.2 Apparatus

Visual stimuli were generated with Matlab 7.12 (The MathWorks, Natick, MA) using the PsychToolbox 3.0 [219, 220]. A 20-inch CRT monitor (Mitsubishi Diamond Pro 2070sb) with 1280×1024 pixel resolution and 100 Hz refresh rate was used to display the stimulus. The distance between the display and the observer was 57 cm. All procedures were carried out in a dimly lit room. A photometer (SpectroCAL, Cambridge Research Systems, Rochester, Kent, UK) was used for the calibration of the display. Using a digital oscilloscope (Rigol DS 10204B, GmbH, Puchheim, Germany) connected to a photodiode which detected visual stimulus onsets and offsets, we synchronized the triggers that mark the stimulus onset times in EEG recordings with the onset times of each stimulus shown on the screen during a trial. Observers responded via a standard keyboard after each trial.

2.2.3 Behavioral pilot data collection

The visual stimuli and the experimental design were adapted from Agaoglu et al. [78]. In their design, they adjusted luminance values for each participant to avoid ceiling and floor effects. Specifically, the mask and target luminance was arranged for each observer to optimize the masking effect. However, in an experimental design for EEG data collection, personalizing these values could contribute to the variations across subjects as well as an overly extended experimental session. Consequently, one of the reasons we designed a behavioral pre-study was to find the optimal luminance settings that separate the masking conditions efficiently. Ten participants participated in the extended version of the following experimental procedure where we kept the mask luminance constant and tested three different target luminance conditions (54, 61.6, and 68 cd/m^2) over six SOA conditions (30, 60, 80, 100, 120, 150 ms) along with the

main research conditions. The concluding target luminance to be used in the rest of the experimental sessions was 68 cd/m^2 which was determined by considering the average performance values obtained during this pilot data collection. Other basic parameters of target, mask, and timeline of events for mask and baseline (cue) conditions are provided in the following section 2.2.4. Another reason for collecting pilot data was to evaluate masking functions and to identify critical SOA conditions. Since there is a time constraint during EEG data collection, we aimed to keep the number of SOA conditions minimum while representing the critical SOA conditions of the masking function. Using the previously identified luminance value, we collected pilot data from 23 participants to determine the three critical SOA values to be used during EEG data collection. According to the average performance values (Figure 2.1); for the SOA value of 60 ms, there was strong inhibition in both set-size conditions and at 150 ms SOA value the target visibility was high (i.e., no masking) in both set-size conditions. We also included an earlier SOA with similarly higher target visibility to represent the essential points of the U-shaped masking function. Therefore, these SOA values (30, 60, and 150 ms) were used in the main EEG experiment.

2.2.4 Stimuli and procedure

Each trial started with a fixation screen with a red $1^\circ \times 1^\circ$ fixation square (35 cd/m^2) at the center of a gray screen (92.2 cd/m^2). After a variable duration between 500 ms and 1 sec, several oriented bars (1° long, 0.1° wide) with centers equidistant from the fixation point were presented briefly for 20 ms (Figure 2.2). Each of these bars (68 cd/m^2) was tilted to a random angle and presented with their centers on an imaginary circle with a radius of 4° around the fixation square. Participants saw either six bars; three on each side of the fixation point with equal distance to each other, or two bars in a semi-random manner so that the bars always appeared bilaterally.

After an SOA (30, 60, or 150 ms), a mask as a non-overlapping ring over one of the bars with 1.1° inner and 1.5° outer diameters (2.3 cd/m^2) was presented.

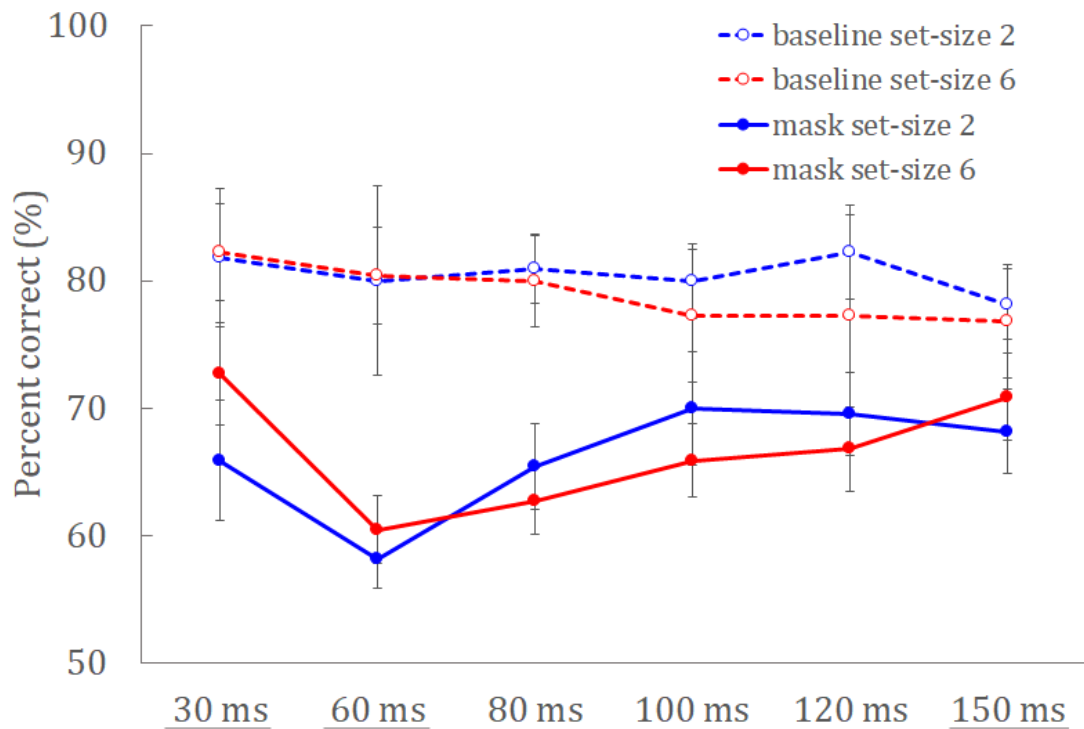


Figure 2.1: Behavioral results from the pilot data ($n = 23$). The percent correct values for baseline (dashed lines) and mask (solid lines) conditions separately as a function of SOA with blue and red lines corresponding to set-size two and six conditions, respectively.

The following mask also marked the target bar. In other words, only one mask stimulus was presented and its location cued which oriented bar is the target. The remaining bars served as distractors. Alternatively, a cue in the form of a $1^\circ \times 1^\circ$ square (2.3 cd/m^2) near the target bar indicated the target location to have a baseline condition with a minimum masking effect. The duration of the mask and the cue was 20 ms (two frames). After the stimulus offset, the observers used the keyboard to report the orientation of the target bar; whether it was leaning toward the right or left. Each condition was repeated 126 times in one EEG session. Accordingly, there were a total of 1512 trials ($12 \text{ conditions} \times 126 \text{ trials per condition}$) in each experimental session.

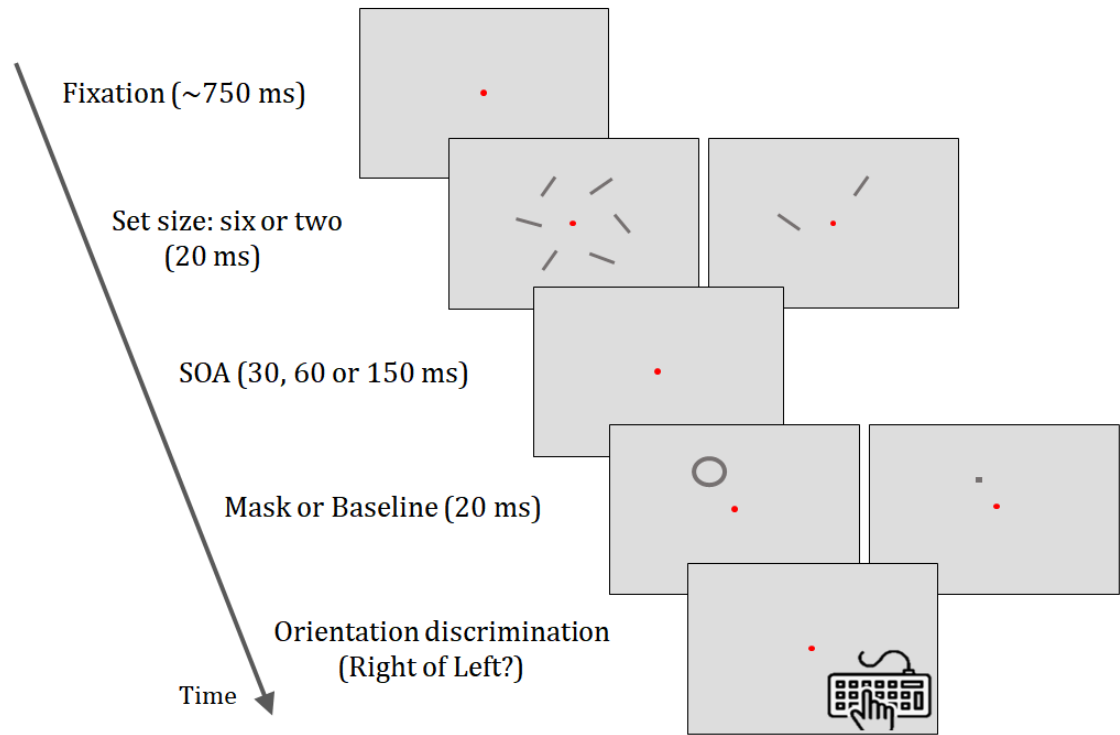


Figure 2.2: Schematic representation of stimulation and timeline on each trial. Each trial started with a variable fixation period (500-1000 ms) followed by either 2 or 6 target bars that presented on the screen for 20 ms. After a period of SOA (30, 60 or 150 ms) where only the fixation point was left on the screen either a mask over the target bar location or a cue near the target bar appeared for 20 ms. Participants were instructed to press left or right arrow indicating orientation of the target (tilted in leftwards or rightwards) in a time window of 1000 ms.

2.2.5 Performance testing

Prior to the main EEG session, each participant went through a behavioral session for performance testing. As mentioned above (section 2.2.3), we introduced a pre-testing session with selected luminance values since we could not personalize the stimuli parameters for each subject to avoid any floor or ceiling effects. Our inclusion criteria for the participants were as follows: First, the maximum performance with masking must be lower than the baseline performance (the ceiling). Second, the minimum performance with masking must be significantly

higher than the chance level which was 50% for accuracy (the floor). Participants completed 21 trials per condition over a full range of SOA conditions (30, 60, 80, 100, 120, and 150 ms) with two set-size (two and six) and two masking (baseline and mask) conditions, totaling up to 504 trials. The data from participants that failed to reach criterion performance or could not complete a full number of experimental sessions were not included in the further analyses.

2.2.6 EEG data acquisition and preprocessing

A 64-channel MR-compatible system (Brain Products GmbH, Gilching, Germany) was used to record high-density EEG activities. Before each experimental session, we carefully placed the EEG cap on a participant’s head. The placement of scalp electrodes was based on the extended 10-20 system. Two electrodes were used as reference (FCz) and ground (AFz). We used q-tips and a syringe with a blunt tip to apply conductive paste (ABRALYT 2000 FMS, Herrsching-Breitbrunn, Germany) to reduce the impedance of each electrode below 10 k Ω . The impedance levels were monitored during the sessions for reliable recording. EEG signals were sampled at 5 kHz and band-pass filtered between 0.016 and 250 Hz. We stored the EEG data, event markers, and behavioral responses using the Vision Recorder Software (Brain Products GmbH, Gilching, Germany) for offline analyses. Brain Vision Analyzer 2.0 software (Brain Products GmbH, Germany) was used to carry out the preprocessing procedures. First, EEG signals were down-sampled to 500 Hz and filtered using a zero-phase Butterworth band-pass filter (0.5-100 Hz, 24 dB/octave) and a 50 Hz notch filter (50 Hz +/-2.5 Hz, 16th order). The cardio-ballistic artifacts were removed using the recorded signal from the electrocardiogram electrode [221]. Next, the data were segmented into epochs from 200 ms before the onset of the target stimulus to 1 sec after the offset of the stimulus. To remove common EEG artifacts (e.g., eye blinks, muscle artifacts, any residual heartbeat components), the data was further submitted to independent component analysis (ICA) using the Infomax algorithm. A baseline correction was also applied using the 200 ms time window before the onset of the stimulus. Last, artifact-contaminated trials (i.e., epochs)

and momentarily bad channels were identified and removed through a combination of automated screening and manually by eye. In the automatic screening, any trial with oscillations over 50 $\mu\text{V}/\text{ms}$, voltage changes more than 200 μV in 200 ms, or a change less than 0.5 μV in 100 ms was rejected. The excluded trials during the EEG preprocessing stage were also not used in the analysis of the behavioral data. Finally, we removed four participants that lost more than an average of 20% of the trials from each condition. After applying these preprocessing steps, on average 91% of trials (SEM = 0.98%) were preserved for further ERP analyses.

2.2.7 ERP analyses

After the initial preprocessing, using Matlab software toolboxes (e.g., Fieldtrip), we averaged the EEG signals from each electrode across all valid trials to compute ERPs time-locked to the onset of the target. For further smoothing, these averaged ERPs were filtered with a low-pass filter (6th order zero-phase Butterworth IIR filter with 40 Hz cut-off frequency). In experimental designs focusing on neural correlates of visual masking, the basic idea is to contrast the neural responses to high target visibility conditions with those to low visibility conditions [222, 6]. In these designs the stimuli for different conditions are kept as physically identical as possible to ensure the only difference is the perceived experience of the participants, therefore the difference in neural responses (e.g., in ERPs) between these conditions can be inferred as due to the masking effects on perceived visibility. Therefore, to determine masking-specific activity as well as to avoid the potential confounds originating from the stimulation differences, we subtracted the averaged ERPs of the masking trials from those of baseline trials for each SOA and set-size condition. We used these difference ERPs (baseline-masking) as well as the corresponding behavioral performance difference (baseline-masking) for further statistical analyses. Based on previous studies [223, 6] and inspection of present grand-averaged ERPs and voltage topographical maps, we computed the mean amplitudes for the two common time-range and scalp location information referring to VAN and LP/P3 components. We, then, performed two-way

repeated-measures ANOVA analyses with SOA and set-size as factors on the averaged activity values within these time ranges and electrode locations. During these analyses, when Mauchly’s test indicated that the assumption of sphericity had been violated, the Greenhouse–Geisser correction was applied. The corresponding epsilon (ϵ) values (i.e., sphericity estimates) are supplied when the ANOVA results are presented.

2.3 Results

2.3.1 Behavioral Results

In Figure 2.3, the accuracy values for each set-size are plotted across different SOA conditions. We computed the difference between the mask and corresponding cue/baseline and these difference performance values are shown in Figure 2.3B. A two-way repeated-measures ANOVA with set-size (two vs six) and SOA (30, 60, 150 ms) as factors on these difference values indicated significant main effects of set-size ($F_{1,18} = 399.9$, $p < 0.001$, $\eta_p^2 = 0.957$) and SOA ($F_{2,36} = 3980.8$, $p < 0.001$, $\eta_p^2 = 0.995$) and a two-way interaction ($F_{1,47,26.4} = 193.1$, $p < 0.001$, $\eta_p^2 = 0.915$, $\epsilon = 0.73$)¹. Post hoc pairwise comparisons (Bonferroni corrected) revealed that the effect of set-size was only significant in SOA levels of 60 ms ($t_{19} = -8.829$, $p < 0.001$, Cohen’s $d = -2.026$) and 150 ms ($t_{19} = -38.128$, $p < 0.001$, Cohen’s $d = -8.747$), but it was absent only for 30 ms SOA condition ($t_{19} = -0.329$, $p = 0.746$, Cohen’s $d = -0.076$). While there was an overall significant decline in visual suppression strength as the SOA length increased, the decline was more prominent for the set-size two condition (Figure 2.3). More specifically, the differential performance was significantly lower in set-size two condition compared to set-size six, indicating a higher suppression of visibility in both 150 ms (set-size two: $M = -4.23$, $SEM = 0.21$; set-size six: $M = 6.66$, $SEM = 0.26$) and 60 ms (set-size two: $M = 19.18$, $SEM = 0.21$; set-size six: $M = 22.43$, $SEM = 0.37$) conditions.

¹Mauchly’s test indicated that the assumption of sphericity had been violated for main effect of swapping, therefore degrees of freedom were corrected using Greenhouse-Geisser estimates of sphericity.

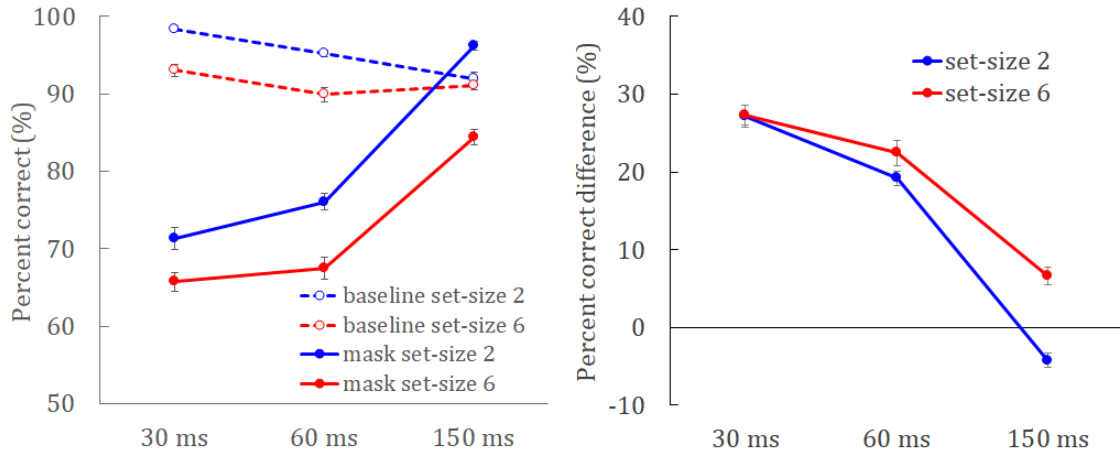


Figure 2.3: Behavioral results ($n = 19$). (A) The percent correct values for baseline (dashed lines) and mask (solid lines) conditions separately as a function of SOA with blue and red lines corresponding to set-size two and six conditions, respectively. (B) The percent correct difference between mask and baseline for each SOA and set-size conditions. The blue and red lines similarly illustrate the two and six target conditions.

When the SOA was 30 ms, however, a strong and similar masking effect can be observed for both set-sizes (set-size two: $M = 27.13$, $SEM = 0.32$; set-size six: $M = 27.30$, $SEM = 0.30$).

2.3.2 ERP results

Following behavioral analyses, we investigated the ERP waveforms locked to the target onset. First, the waveforms for both baseline and mask conditions revealed a positive early evoked peak around the P1 range (90-150) followed by a larger negative component that peaked around the late N1 component range (150-250). These activations were mainly over occipital and parieto-occipital scalp sites. Following this, we also observed that both mask and baseline conditions elicited a P300 component that was distributed in centro-parietal electrodes (Figure 2.5 and Figure 2.6).

Secondly, to determine masking-specific activity, we subtracted the averaged ERPs of the masking trials from those of baseline trials for each SOA and set-size

condition. The topographical maps of the difference waveforms within the early time windows mainly displayed a stronger activation over occipital and parietal electrodes with some differences due to SOA conditions followed by a later positive difference that can be observed over central and parietal electrodes (Figure 2.4). The resulting difference in ERPs revealed two separate negative peaks around the time range of the P1/N1 complex (90-210) and in the late VAN range (240-310) which can be seen in Figure 2.5. The topographical maps also revealed a steadily increasing later component in the 350-580 ms (LP) range, especially for 30 ms and 60 ms SOA conditions (Figure 2.4). The averaged potentials over these electrodes are shown in Figure 2.6.

To evaluate these ERP modulations, we performed a two-way repeated-measures ANOVA with set-size (two vs six) and SOA (30, 60, 150 ms) as factors. The analyses on a negative component (P1/N1 range, 90-210 ms) located over occipital and parieto-occipital scalp sites revealed significant main effects of SOA ($F_{2,36} = 15.276$, $p < 0.001$, $\eta_p^2 = 0.459$) and set-size ($F_{1,18} = 18.036$, $p < 0.001$, $\eta_p^2 = 0.501$), without any interaction effect ($F_{2,36} = 1.668$, $p = 0.203$, $\eta_p^2 = 0.085$). Follow-up Bonferroni corrected post hoc comparisons revealed that the negative differential activation was significantly smaller in 150 ms condition (M= 0.27, SEM= 0.13) compared to the 30 ms (M= -0.85, SEM= 0.22; 30 vs 150 ms: $t_{19} = -3.958$, $p = 0.003$, Cohen's d = -0.908) and 60 ms (M= -0.82, SEM= 0.15; 60 ms vs 150 ms: $t_{19} = -5.254$, $p < 0.001$, Cohen's d = -1.205) conditions, while the remaining comparison was not significant (30 ms vs 60 ms: $t_{19} = -0.138$, $p = 0.892$, Cohen's d= -0.032; Figure 2.7).

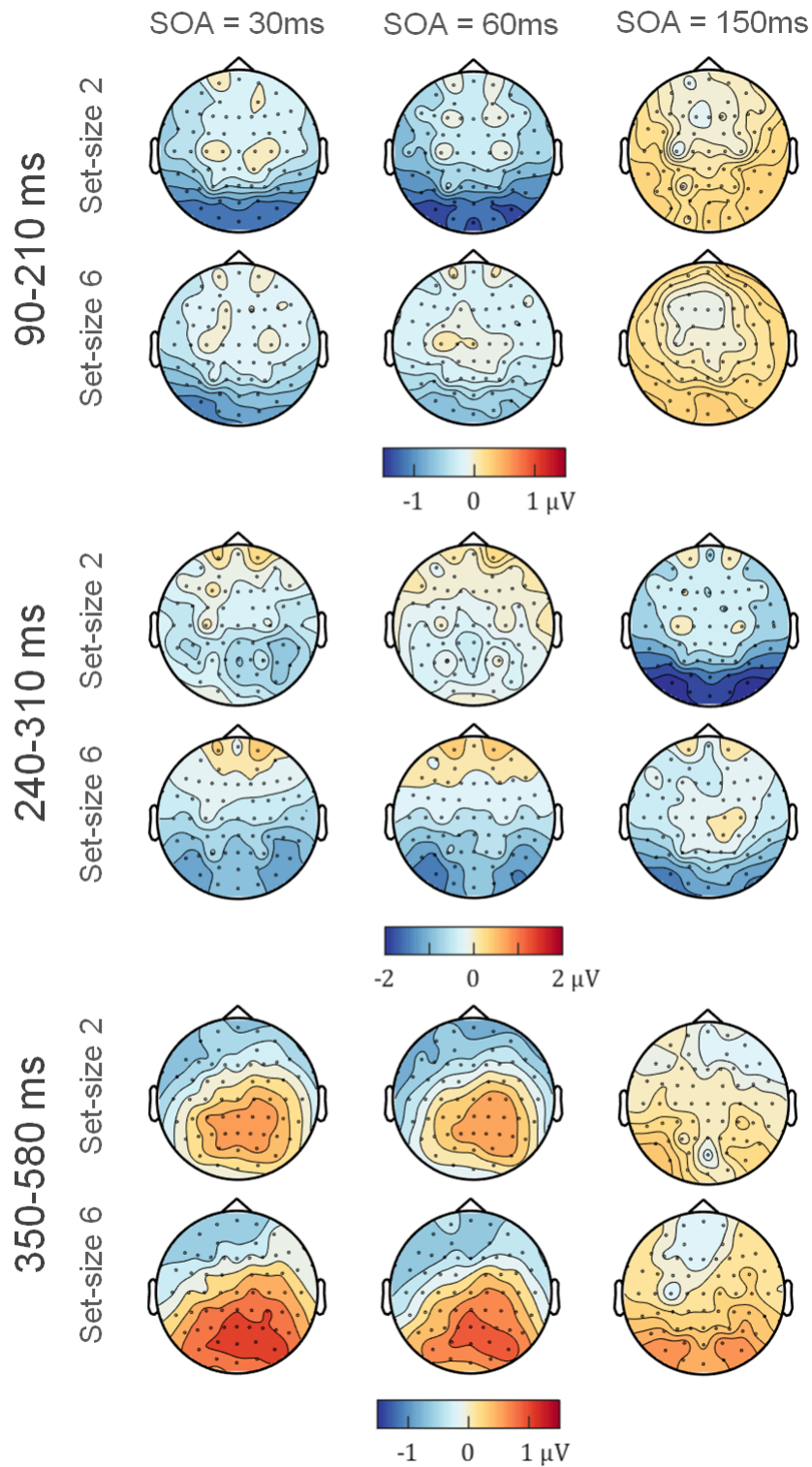


Figure 2.4: The voltage topographical maps displaying overall differential activation (baseline-mask) in selected time ranges (90-210 ms, 240-310 ms and 350-580 ms). The averaged difference for each SOA (columns) and set-size (rows) condition are displayed separately.

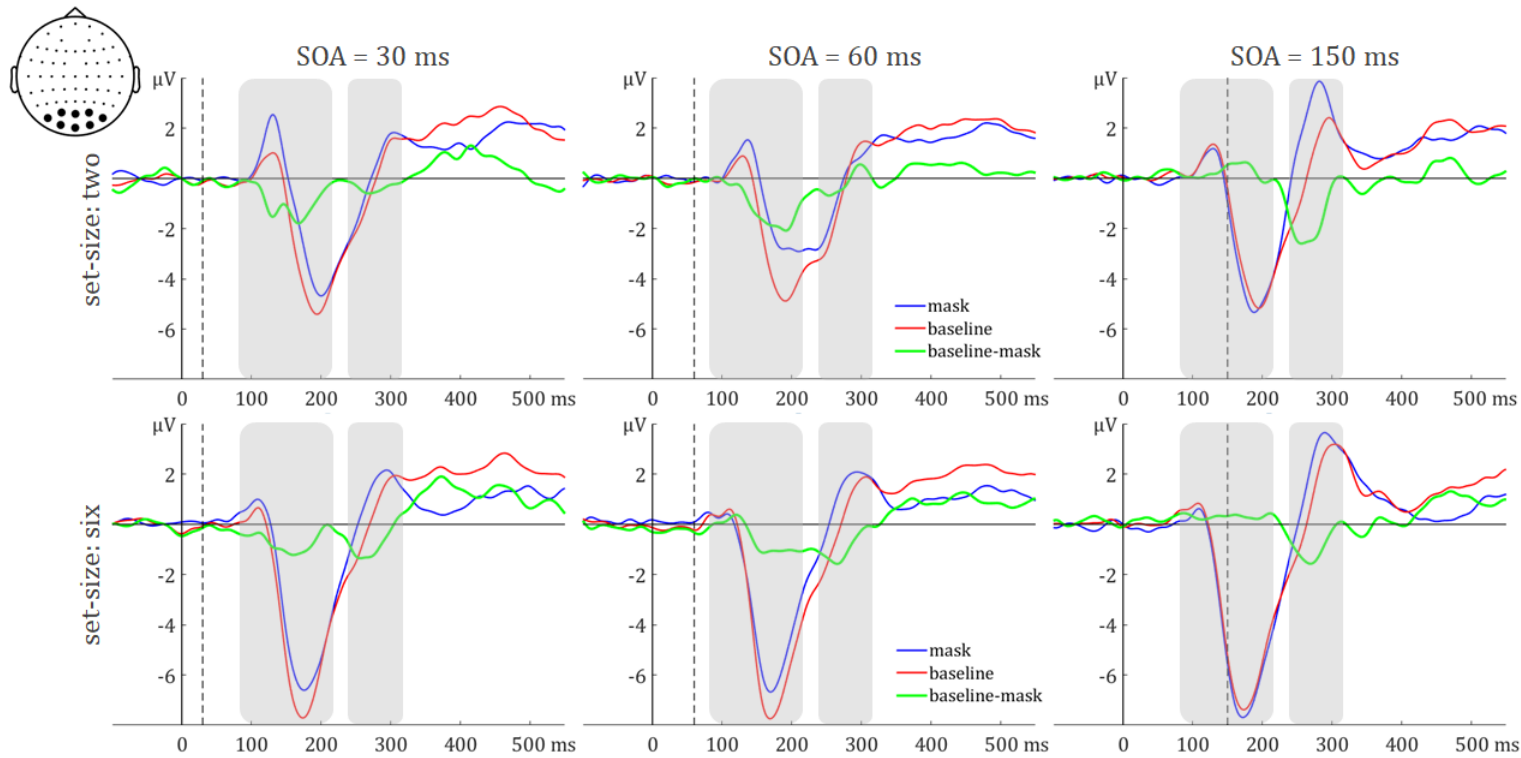


Figure 2.5: The averaged activities and derived waveforms from the parieto-occipital scalp sites. Each SOA and set-size condition is displayed in a separate plot. The locations of exemplar electrodes that were used in analyses are shown on a head model (i.e., PO3, PO8, PO7, PO4, POz, Oz, O1, O2). In each plot, evoked activities for mask (blue lines), baseline (red lines) conditions and the difference waveforms (green lines) are displayed. The ERPs were time-locked to the onset of the target display. The identified time windows where follow up analyses were conducted are highlighted by grey rectangles. The vertical dashed lines indicate the appearance of the mask or cue according to the SOA condition.

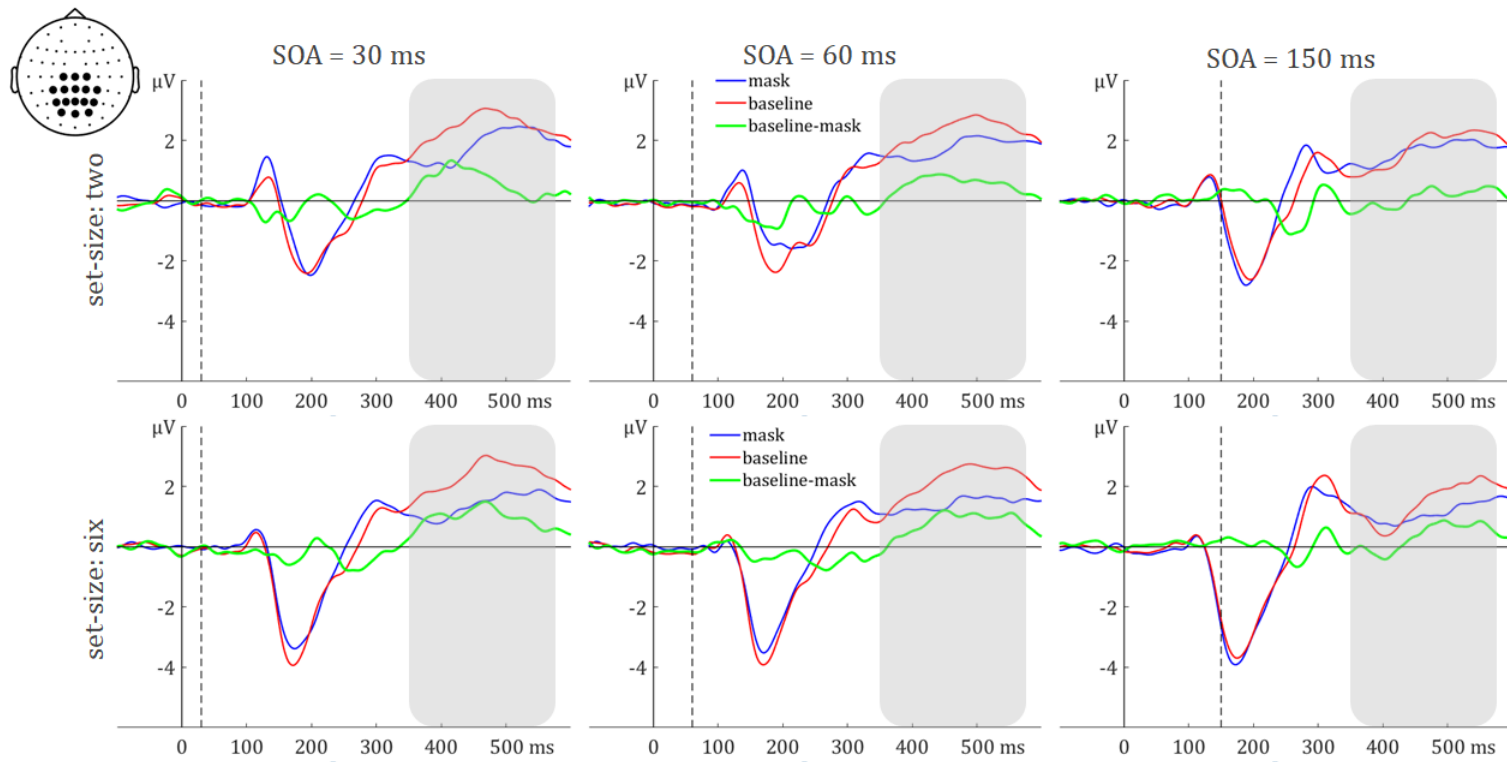


Figure 2.6: The averaged activities and derived waveforms from the centro-parietal scalp sites. Each SOA and set-size condition is displayed in a separate plot. The locations of exemplar electrodes that were used in analyses are shown on a head model (i.e., CPz, PO3, POz, PO4, P3, Pz, Cz, CP1, CP2, CP3, CP4, P1, P4, P2, C1, C2). In each plot, evoked activities for mask (blue lines), baseline (red lines) conditions and the difference waveforms (green lines) are displayed. The ERPs were time-locked to the onset of the target display. The identified time window where follow up analyses were conducted is highlighted by a grey rectangle. The vertical dashed lines indicate the appearance of the mask or cue according to the SOA condition.

Similarly, the ANOVA analyses were applied on a second negative component (late VAN range, 240-310 ms) that was observed over occipital and parieto-occipital scalp sites. The ANOVA test revealed a significant main effect of SOA ($F_{2,36} = 5.990$, $p = 0.006$, $\eta_p^2 = 0.250$) while main effect of set-size was not significant ($F_{1,18} = 0.758$, $p = 0.396$, $\eta_p^2 = 0.040$). More importantly, a significant interaction was observed between SOA and set-size ($F_{2,36} = 7.930$, $p = 0.001$, $\eta_p^2 = 0.306$). Follow-up post hoc comparison on the interaction effect revealed that only in the set-size two condition, the average activation was significantly different for 150 ms condition compared to both 30 ms ($t_{19} = 3.370$, $p = 0.010$, Cohen's $d = 0.773$) and 60 ms conditions ($t_{19} = 3.957$, $p = 0.003$, Cohen's $d = 0.908$). The mean values indicated that when the set-size was two, in both 30 ms ($M = -0.38$, $SEM = 0.27$) and 60 ms ($M = -0.16$, $SEM = 0.25$) conditions, the negativity was smaller compared to 150 ms condition ($M = -1.72$, $SEM = 0.40$).

Finally, the ANOVA analyses on the late positivity range (LP, 350-580 ms) centered over centro-parietal electrodes, did not reveal any two-way interaction ($F_{2,36} = 0.139$, $p = 0.871$, $\eta_p^2 = 0.008$), but both the main effects of set-size ($F_{1,18} = 13.333$, $p = 0.002$, $\eta_p^2 = 0.426$) and SOA ($F_{1,54,27.74} = 5.547$, $p = 0.015$, $\eta_p^2 = 0.236$, $\epsilon = 0.77$)² were present (Figure 2.7). The main effect of set-size points to a significantly larger positive activation in set-size six condition ($M = 0.71$, $SEM = 0.19$) compared to set-size two condition ($M = 0.43$, $SEM = 0.16$; Figure 2.7). Furthermore, Bonferroni corrected post hoc comparisons on main effect of SOA revealed that the positive activation is significantly higher for 30 ms of SOA ($M = 0.79$, $SEM = 0.22$) condition compared to the 150 ms ($M = 0.23$, $SEM = 0.13$; 30 ms vs 150 ms: $t_{19} = 2.691$, $p = 0.045$, Cohen's $d = 0.617$). There was no significant difference between 30 ms and 60 ms of SOA ($M = 0.69$, $SEM = 0.23$; 30 ms vs 60 ms: $t_{19} = 0.843$, $p = 0.424$, Cohen's $d = 0.193$) or between 60 ms vs 150 ms ($t_{19} = 2.345$, $p = 0.092$, Cohen's $d = 0.538$).

²Mauchly's test indicated that the assumption of sphericity had been violated for main effect of swapping, therefore degrees of freedom were corrected using Greenhouse-Geisser estimates of sphericity.

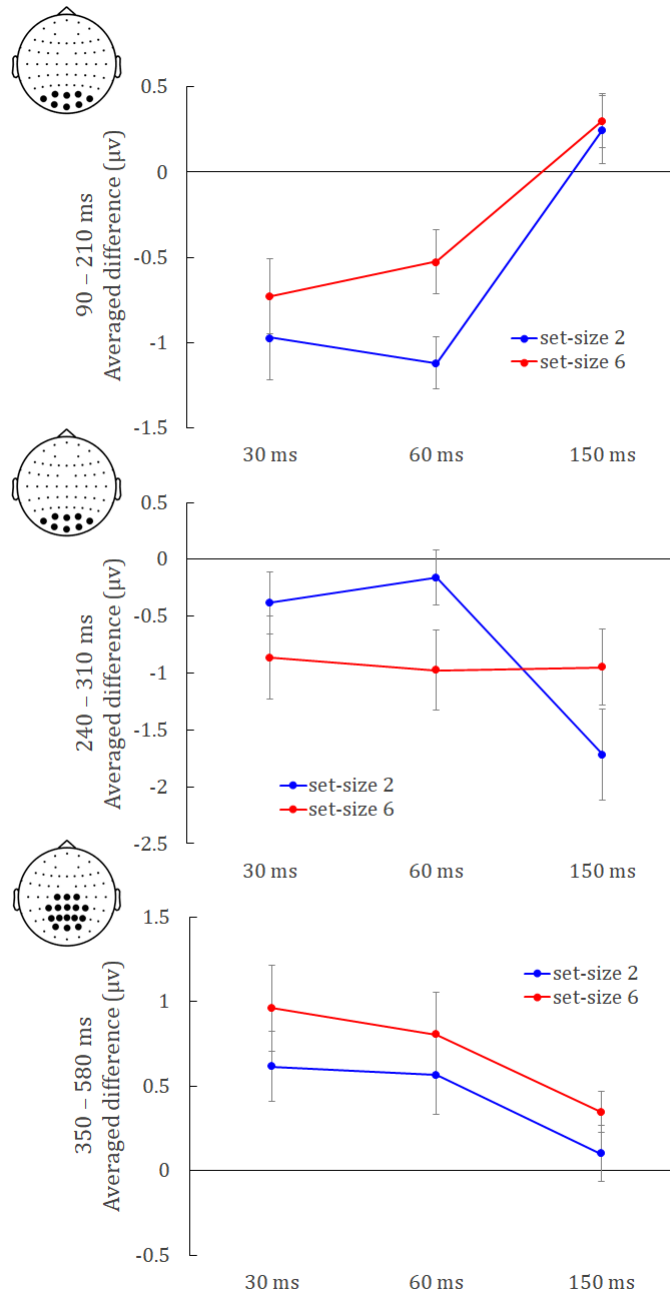


Figure 2.7: Average values used in ERP analyses ($n = 19$). The averaged differential amplitude between baseline and mask conditions displayed in the time ranges 90-210 ms (top), 240-310 ms (middle) and 350-580 ms (bottom) for each SOA. The blue and red lines correspond to two and six target conditions, respectively. The locations of exemplar electrodes that were used in analyses are shown on head models.

2.4 Discussion

2.4.1 Summary

We investigated the effects of metacontrast masking and spatial attention on behavioral performance and neural activities recorded from the scalp surface. Behavioral results indicated that visual suppression of the target due to metacontrast masking diminished as the SOA value was increased. Conversely, as the masking effect declined, the performance differences between conditions with different attentional loads increased. More specifically, when the attentional load was low (set-size two), the visibility of the target was higher compared to the high attentional load condition (set-size six) in late SOA conditions (150 ms) where the masking effect was very low. However, this difference was absent at small SOAs in which the masking effect was the most influential (Figure 2.3).

Our ERP analyses revealed that attentional load (i.e., set-size) and SOA variation modulate the early activation that corresponds to P1/N1 complex range over occipital and parieto-occipital scalp sites. While we recorded decreasing differential activation over this component range as the SOA values between target and mask increased, the negative activation was significantly higher for the low attentional load (set-size two) condition.

The second negatively trending difference, recorded around the late VAN range over occipital and parieto-occipital scalp sites, indicated an interaction where the effect of attentional load on masking strength changed depending on the effectiveness of the SOA values. Specifically, for effective SOA conditions (30 and 60 ms), the low attentional load resulted in lowered masking strength compared to the ineffective SOA condition (150 ms) while high attentional demand resulted in larger negativity for masking-effective SOA values.

The analyses on the following positive component centered over centro-parietal sites around LP/P3 time range (350-500 ms), revealed that the attentional load (i.e., an increase in set-size) facilitated an overall activation in masking conditions

(Figure 2.7).

Furthermore, in the earliest and the latest components where we observed no interaction effects, the activation patterns with regards to the masking effect were in line with the behavioral masking results, such that the larger differential activation in these time ranges was higher in short SOA conditions and gradually decreased inversely to the SOA values. For the VAN range where we observed an interaction effect on mean differential activity on the other hand, the results lined up with the behavioral performance pertaining to the observed attentional modulation in each SOA separately. More specifically, mirroring the behavioral results, there was no significant difference in activation depending on set size in 30 ms condition, while for 60 ms a significantly larger negativity for high attentional load condition was observed. For 150 ms condition where we recorded the least masking effect behaviorally, the difference between the attentional conditions were still significantly different, however unlike behavioral results the direction of activation is switched in mean activation values with larger activity observed in low attentional load condition. The specific implications of these findings with comparisons to previous research are discussed in the following sub-sections.

2.4.2 Do masking and spatial attention interact?

Some theories on visual masking proposed that low-level visual processing may not provide a complete account of the mechanisms underlying masking. They further propose a complex interaction between high-level visual processes and masking [224, 225, 76]. Visual attention, in particular, is believed to play a role in the effectiveness of metacontrast masking and to have the ability either to decrease the visibility of the stimuli or to bring it into awareness. In the present study, the overall effectiveness of the attentional load was demonstrated through lowered performance along with the effect of the trailing mask, thus producing a modified masking function. These results diverge from the findings of Agaoglu et al. [78] where they report not interactive but additional effects of metacontrast

masking and attentional load on perceived visibility. This discrepancy in the results could be a result of the modifications we applied to the design (see Section 2.2.3) to be able to collect ERP data such as changing the task parameters or generalizing the mask/target luminance ratio for all participants. Both the change in task difficulty and the contrast level are expected to influence the criterion contents, hypothetically affecting which mechanisms, sustained or transient, will contribute to performance [4]. Since different criterion contents have been known to produce different masking functions [34, 4], and attention is also known to influence similar early mechanisms in different ways, the interaction effects that were recorded may be due to changes in criterion contents. On the other hand, these findings are consistent with a growing body of evidence demonstrating the effects of attention on masking, including similar studies using attentional load and exogenous cueing [226, 75, 210] as well as others where the voluntary direction of attention, in which target visibility ratings were increased with the valid allocation of attention [208, 227, 200] and with studies showing a modulatory effect of salient stimuli [209] on the metacontrast masking function. Tata [210] examined the allocation of attention across a circular visual array containing several distractors in a metacontrast masking paradigm. They reported a typical U-shaped function with a sharp and longer-lasting decrease in performance with higher set sizes, consistent with earlier reports by Spencer and Shuntich [226] who found that the masking function was extended under conditions of high attentional load compared to that of low load. These reports suggest that attentional load may interact with masking effects in such a way that high load elicits a greater masking effect [228, 229].

Notably, the attentional effect observed in the present study primarily occurs within the window of the non-optimal masking conditions, approaching closer to the end of the masking function. Other studies have also shown that the strength of the metacontrast effect depends on attention manipulations robustly at the rising side of the U-shaped metacontrast function but barely downward side over shorter SOAs [230, 200, 202, 231], suggesting that suppression of target visibility from a mask can occur before attention has a chance to effect target visibility at short onset asynchronies of 30-80 ms or under conditions of strong

masking. At longer SOAs of 100 or higher or with greater spatial separations, however, attention may enhance the processing and therefore individuation of the target, making it more resilient to the effects of the trailing mask [200]. In the case of common onset masking, Enns and Di Lollo [75] showed that even a mask with minimal contours, such as four dots surrounding the target, can exert strong backward masking when coupled with a complex display of distractors that create uncertainty about the target location. Their findings suggest the attentional modulations become robust in otherwise non-optimal masking conditions. Similar results using metacontrast masking were reported by Neumann and Scharlau [202] where the effect of changing the display duration of the mask was observed only in the initial low-visibility phase of masking function while they observed the effect of distractors presented with the target at the rising phase of the masking function. They suggested that the increase of metacontrast effect in the shorter SOAs of the masking function may be due to a mechanism of masking where the effectiveness increases monotonously with the interval, while the decrease of masking over the longer SOAs relies on a different mechanism which becomes more ineffective as the interval between the target and the mask becomes larger, overlapping to produce a U-shaped masking function [202]. They further argue that experimental parameters that typically influence the early phases of the function invoke peripheral mechanisms such as exposure duration of the stimulus [232, 233], spatial distance [234, 233], or monoptic vs dichoptic viewing conditions [235, 236] while variables that seem to primarily affect the later branch of the metacontrast function reflects ‘higher’ information processing such as distractor number [237] or cognitive categorization [233] suggesting a complementary but not alternative localization of metacontrast masking mechanisms [202]. While the evidence presented here and that of prior studies [227, 209, 210, 75] suggest that attention may have the ability to modulate a masking effect, indicating a complex interplay between visual processing and attention.

2.4.3 Neural correlates of visual awareness and attention

Our electrophysiological results are relatively similar to the typical spatiotemporal pattern reported by various masking studies (see [6, 238] for reviews) where the evoked activities of visually available (unmasked) and unavailable (masked) conditions were compared. Most ERP studies that used backward masking manipulated by SOA, typically reported enhanced visual awareness negativity (VAN) related to visual awareness which is manipulated by SOA, in posterior temporal and occipital recording sites peaking around 200–250 ms after the stimulus onset, often starting shortly after 100 ms. [63, 64, 65, 66, 67]. This negative activation is usually followed by a late positive differential activation (LP), typically in the P3 time range peaking at parietal and central sites. For instance, Railo and Koivisto [68] SOAs of varying lengths together with an effective mask and a pseudo-mask design where the pseudo mask was ineffective at reducing the stimulus visibility but produces similar activation as the effective mask when displayed alone. Their results showed that the pseudo-mask which was successfully perceived at each SOA produced ERPs that were more negative compared to the ERPs of the masked stimuli, which were not perceived at the intermediate SOAs. This negativity (VAN) was recorded at lateral posterior areas between 300-400 ms time range, followed by a positive activation (LP) after 400 ms. They attributed the late onset of the negativity (VAN) compared to the previous literature, to the fact that the small effect of the pseudo-mask they used on target visibility. Our results also indicated that baseline trials were associated with larger negativity than masked trials in the 240-310 time window and this difference wave (VAN) was followed by larger activation in the P300 range for baseline stimulus compared to the masked trials than to unaware trials, forming the LP component (350-580) for the SOA windows that produced strong masking effect (i.e., 30 ms and 60 ms).

Our results also displayed an earlier negative difference between masked and unmasked conditions which was in the P1/ N1 complex. Similar results for this time range was reported by previous research using pattern masking. These studies

indicated that both masked and unmasked targets may elicit a strong occipito-temporal activation before 110 ms (consistent with the visual P100), which was attributed to the feedforward processing of visual stimuli [215]. Moreover, the unmasked trials resulted in activity between 110–140 ms at posterior occipital sites, with no activity for masked trials seen at this time frame. These findings were interpreted as reflecting reentrant processing being interrupted by the presence of the mask. With a similar backward masking procedure, however, Van Loon et al. [239] found that masking had no effect on the earliest ERP components before 120 ms, corresponding to the P100 but effectively decreased later ERP components that appeared after 150 ms, (corresponding to the N100). Another study, using four letters surrounding a number as the target, found that early positive enhancement (P1), as well as negativity after 200 ms (VAN) and a later positivity (LP), correlated with SOA and with subjective visibility reports [240].

A series of ERP experiments aiming to understand the interaction between visual attention and awareness have combined the non-spatial selective attention procedures with metacontrast masking paradigms to manipulate visual availability [64, 65, 66, 241]. In these experimental designs, the observers were asked to attend to previously defined target stimuli or features and to ignore non-target stimuli. In one of these initial studies, Koivisto et al. [66] manipulated object-based selection where the stimuli displayed in the spatially cued area, were either masked with an effective SOA (33 ms) or with an ineffective SOA (133 ms) where the target recognition is easily achieved. They compared the elicited differential activation of the unattended non-targets with the attended targets. Their results displayed VAN activation between 130 and 260 ms post-stimulus onset for both target and non-target stimuli, indicating that the early part of VAN was independent of the attentional manipulation. However, the later part (200–260 ms) of VAN was found to be amplified by object-based attention at posterior and temporal sites. Moreover, this activity was followed by an LP activation in the P300 time range that was strongly manipulated by the attentional modulation. Based on these results, they suggested that while the early stages of visual awareness seem to be independent of the effect of attentional modulation, later stages of conscious processing could be affected by visual selection.

Another study investigating the ERP correlates of common-onset masking [213] reported that unmasked targets may elicit less posterior positivity/larger negativity than masked targets around 220 ms after the target onset (P2 time window). They also revealed an interaction between mask duration and set size where a larger P2 activation was observed when the mask was accompanied by a larger set size of distractors. These results were reflecting the behavioral results where a decrease in performance was observed in conditions where the set size is larger and the trailing mask is longer.

Furthermore, in a study where spatial and object-based attention was manipulated together with visual awareness, the observers were instructed to attend to previously specified target letters in either the right or the left visual field [64]. The results indicated no change in differential activation in the VAN range due to spatial manipulation, but the following LP was larger for stimuli in the attended field compared to the unattended. However, they later argued that the nature of the unilateral stimuli which required quick shifts of attention between stimuli in attended and unattended fields could be the reason for the lack of attentional manipulation observed in VAN activation. Indeed, when the study was repeated using bilateral stimulation with one stimulus in each visual field, the results displayed a larger VAN (200–300 ms) amplitude for target stimuli compared to non-targets in the attended field [241], comparable to the previous reports for stimuli presented in the center of the visual field [66, 65].

Even though we employed a different attentional manipulation method with the masking paradigm, our ERP results were similar to the previous reports of attentional manipulation on the late VAN and LP time ranges. Especially, we observed a similar pattern of an interaction effect where the effect of attentional load on masking strength changed depending on the effectiveness of the SOA values. Specifically, we also recorded the effect of attentional load in later VAN latency in effective SOA conditions, where high attentional demand resulted in larger negativity. Moreover, our analyses on the following positive component around LP/P3 time range, similarly revealed that the attentional load facilitated overall activation in masking conditions in line with the behavioral visibility reduction.

2.5 Conclusions

There is a close functional relationship between attention and awareness, which has been established in behavioral and neurophysiological studies [66, 65, 64, 241, 6]. Taken together, the present results highlight the significant roles of attention at specific stages of visual information processing, after the initial entry of information into the visual system and before complete processing of it. Attentional effects seem to be not uniform and additive to the effects of other factors and they are especially sensitive to the characteristics of target-mask timing.

Chapter 3

Behavioral and ERP Evidence that Object-based Attention Utilizes Fine-grained Spatial Mechanisms

This chapter is based on the publication by Catak, E. N., Özkan, M., Kafaligonul, H., Stoner, G. R. (2022). Behavioral and ERP evidence that object-based attention utilizes fine-grained spatial mechanisms. *Cortex*, 151, 89-104. <https://doi.org/10.1016/j.cortex.2022.02.013> Reproduced (or reproduced in part) based on the author rights provided by Elsevier Publications.

3.1 Introduction

Valdes-Sosa, Cobo, and Pinilla [185] introduced a transparent-motion design that provided evidence of object-based attention whereby attention embraces all features of an attentionally cued perceptual object including new unpredictable features such as a brief translation. Subsequent studies using variants of that

design appeared to provide further behavioral, electrophysiological, and brain imaging evidence of object-based attention. Stoner and Blanc [189] observed, however, that these previous results could potentially be explained by feature-based competition/normalization models of attention. To distinguish between the object-based and feature-based accounts, they introduced “feature swaps” into a delayed-onset variant of the transparent-motion design [181]. Whereas the object-based attention account predicted that the effect of cueing would survive these feature swaps, the motion-competition account predicted that the effect of cueing would be reversed by these feature swaps. The behavioral results by Stoner and Blanc [189] supported the object-based account, and in doing so, provided evidence that the attentional advantage in this design is spatially selective at the scale of the intermixed texture elements (i.e., dots) of the overlapping and moving dot fields. In the present chapter, we used the design of Stoner and Blanc [189] to investigate both psychophysical performances and evoked activities under different cueing and feature swapping conditions. We had several goals in the current study. First, as the Stoner and Blanc [189] study is the only study of the numerous studies cited above that provided evidence of object-based selection that cannot potentially be explained by previously identified competitive/normalization mechanisms, we wished to confirm their finding that the behavioral effect of cueing survives feature swaps. Second, since ERPs have not been previously collected with the delayed-onset design, it is conceivable that the ERP correlates observed using other variants of that paradigm are specific to the details of those designs (e.g., the presence of two translations per trial rather than one translation per trial as in the delayed-onset design). We hypothesized, however, that the N1 modulation found in previous studies was not specific to those designs and would also be found with the delayed-onset design. This would support the conclusion by Reynolds et al. [181] that the delayed-onset design captured the key features of the more complicated designs. Third, and most importantly, the ERP correlates observed in previous experiments are all subject to a motion-competition interpretation. Hence, it is unclear whether the previously identified ERPs associated with cueing are truly related to object-based attention. Thus, our goal was to identify ERPs associated with cueing that survived the feature-swaps and hence could be identified as supporting object-based attention rather than reflecting

competitive interactions between direction-selective neurons. Lastly, based on their findings, Stoner and Blanc [189] hypothesized that area V1 is involved in the object-based they identified. We were, therefore, interested in determining whether we might find further evidence of V1’s involvement, such as seen by Khoe et al. [176] and Ciaramitaro et al. [194]. Any such ERP modulation tentatively associated with V1 would need to survive feature swaps to be identified as supporting object-based cueing.

Our results confirmed that the behavioral effects of attentional cueing survived feature swaps and found event-related potential (ERP) correlates of those effects in the N1 component range over occipital and parieto-occipital scalp sites. These modulations of the neural activity were, moreover, significantly associated with variation in behavioral performance values across the different conditions. Our findings thus provide the first evidence of the role of the N1 component in object-based attention in this transparent-motion design under conditions that rule out feature-based mechanisms and that reveal selective processing at a fine spatial scale.

3.2 Methods

3.2.1 Participants

Fifteen adult human volunteers (8 females and 7 males, age range 18-27 years) out of 20 recruited subjects completed all the experimental procedures and EEG sessions. All participants had normal or corrected-to-normal visual acuity and no history of neurological disorders. Before their participation, they were informed about experimental procedures and signed a consent form. The data from five participants that failed to reach criterion performance (see section 3.2.3) or could not complete a full number of experimental sessions were not included. The final sample size was commensurate with previous reports [196]. The inclusion/exclusion criteria were established prior to data analyses. All procedures

were carried out under the Declaration of Helsinki (World Medical Association, 2013) and approved by the local Ethics Committee of Bilkent University.

3.2.2 Apparatus

Visual stimuli were generated with Matlab 7.12 (The MathWorks, Natick, MA) and presented by using the PsychToolbox 3.0 (Brainard, 1997; Pelli, 1997). A 20-inch CRT monitor (Mitsubishi Diamond Pro 2070sb, 1600×1200 -pixel resolution and 60 Hz refresh rate) was used to display the stimulus from a viewing distance of 57 cm with a chinrest to stabilize the head. All procedures were carried out in a dark room. A photometer (SpectroCAL, Cambridge Research Systems, Rochester, Kent, UK) was used for the calibration of the display. Using a digital oscilloscope (Rigol DS 10204B, GmbH, Puchheim, Germany) connected to a photodiode centered over the position of our stimuli, we continuously synchronized our EEG recordings with the stimulus/event onset times.

3.2.3 Training and performance testing

Before engaging in the main EEG experiment, potential participants first engaged in fixation training, the design of which also allowed identification of subjects that could not reliably fixate. We did this for several reasons. First, we wanted to ensure that subjects were not visually tracking a subset of dots (despite being instructed to neither track dots nor attend either dot field). Second, in preliminary experiments, we observed that the cueing effect was weak or absent in some subjects. We subsequently discovered that training subjects to fixate accurately, and only including subjects that could do so reliably, substantially increased the average cueing effect. The training session included central and peripheral conditions. The combination of a bull's eye and crosshair was used as a central fixation for both conditions as this fixation target has been shown to elicit reliable and stable fixation [242]. The bull's eye was constructed of outer and inner circles with diameters of 0.6° and 0.24° , respectively. In the central condition, across

the diameter of the inner circle, a small 0.06° wide bar changed orientation from horizontal to vertical for 133 ms at the center of the screen. For the peripheral condition, there was an additional target (i.e., bull's eye with crosshair) located 0.6° away from the central target. In this condition, the bar was located inside the peripheral target rather than the central one. The fixation training started with each participant determining their threshold luminance/contrast level by adjusting the brightness of the bar till the repetitive transition was barely detectable. This was done separately for central and peripheral target conditions. After 10 repeats of this adjustment procedure for each condition (central and peripheral) separately, the estimated mean gun values at threshold detection for the two conditions were then used in the main fixation task. Since the task was personalized for each participant, the effects of differential visual acuity were minimized. The main fixation task was to detect an orientation transition (from horizontal to vertical to horizontal) in the central or peripheral target conditions. While the participants were maintaining fixation on the central fixation target, a transition in the middle of a target (either central or peripheral) occurred for 133 ms with a random onset timing during half of the trials (i.e., 108 trials of a session). Participants reported, with a key-press, whether they saw a transition or not. Under these conditions, they would not be able to notice the transition in the central condition when there was an eye movement of more than 0.6° . Also, they would only notice the transitions on peripheral conditions if there were a fixation break. Therefore, a high difference in detecting the transition between central and peripheral conditions suggests that the fixation was sustained. To be eligible to continue with the rest of the experiment, participants were required to have a performance value at least 25% higher than the chance level for the central condition and to have the same difference between the central and peripheral conditions. This session (2 conditions x 108 trials per condition) allowed us to train participants to sustain fixation throughout the main experiment as well as to screen their fixation performance.

Each participant that was found eligible based on fixation performance engaged in a heterochromatic flicker fusion task [243] to establish equiluminance between the red and green guns of the monitor with a flicker rate of 60 Hz with the goal

being to have red and green dot fields of approximately equal salience. Using a $2 \times 2^\circ$ square stimulus, the red gun was held constant at maximum intensity (19.7 cd/m^2) and the green gun was adjusted until a minimal flicker was reported. This procedure was repeated 10 times. The averaged green value was then used for each participant in preliminary practice sessions as well as in the main EEG experiment. To ensure that participants understood the task completely and were able to achieve above-chance level performance, each participant first engaged in a practice session. The practice session consisted of the basic cued and uncued conditions without feature-swaps (no-swap conditions, see section 3.2.4). There were 240 trials per condition, leading to a total of 480 trials (2 cued/uncued conditions \times 240 trials). The observers were considered to have achieved criterion performance during the practice session if they correctly indicated the translation direction for more than 25% of the total trials (i.e., more than 120 trials). This criterion performance level corresponds to twice the chance level (12.5% chance level based on 8 different translation directions, see section 3.2.4).

3.2.4 Stimuli and procedure

Visual stimuli consisted of two superimposed circular fields (3.3° diameter) of randomly distributed dots rotating in opposite directions around a central fixation target on a black background (0.16 cd/m^2). As in fixation training, we used a fixation target that was a combination of a bull's eye and crosshair, which has been shown to elicit reliable and stable fixation [242]. The diameters of the inner and outer circles of the bull's eye were 0.24° and 0.6° , respectively. The average density of each dot field was 5 dots per square degree of visual angle. Each dot had a diameter of 0.05° . The two dot fields rotated (in opposite directions) with a speed of $81^\circ/\text{sec}$ around the fixation target. One dot field was red and the other was green, the luminance values were equiluminant based on the heterochromatic flicker fusion task (see above). Whether the red or green dot field appeared first was randomized across trials.

Subjects initiated a trial with a key-press. To ensure that subjects had time

to stabilize fixation, trials started with the fixation target (Figure 3.1A). After a variable duration of between 500 ms and 1 sec, one dot field appeared, which rotated (clockwise or counter-clockwise) continuously around the fixation target for 750 ms. Next, the second (“delayed-onset”) dot field appeared and rotated in the opposite direction (clockwise or counter-clockwise). After the onset of the second dot field, both dot fields continued to rotate for 300 ms. Following this 300 ms period, either the delayed (a “cued translation”) or the non-delayed (an “uncued translation”) dot field translated briefly (133 ms) in one of eight (cardinal and diagonal) directions. Participants reported the translation direction via the numeric keypad of the keyboard. They were instructed to think of the ‘5’ key as the center and map the eight directions to the remaining keys, similar to a compass. Our design also included motion or color swaps on some trials yielding six different conditions (2 cued/uncued x 3 feature swaps; Figure 3.1B). At the onset of the translation, the non-translating dot field either continued to rotate in its original direction (“no-swap” trials) or reversed rotation direction (“motion-swap” trials). After the translation, the translating dot field either resumed its original rotation direction (“no-swap” trials) or assumed the other dot field’s previous rotation direction (“motion-swap” trials). Similarly, the colors of the two dot fields were swapped at the onset of translation (“color-swap” trials). Motion and color swaps (when introduced) persisted until the end of the trial. The rotation duration after the translation offset was 500 ms (Figure 3.1C). The percentage of coherently moving dots was 60% and all dots translated at a speed of $2.26^\circ/\text{sec}$. The remaining dots were distributed equally to move in the other seven directions. The translation duration was kept constant at 133 ms. Different random-dot fields were used for each translation direction, color-order (i.e., red or green dot field was presented first in a trial), and experimental conditions. The demonstrations for the main experimental conditions (Figure 3.1B) are available at Open Science Framework (<https://osf.io/kpjgv/>).

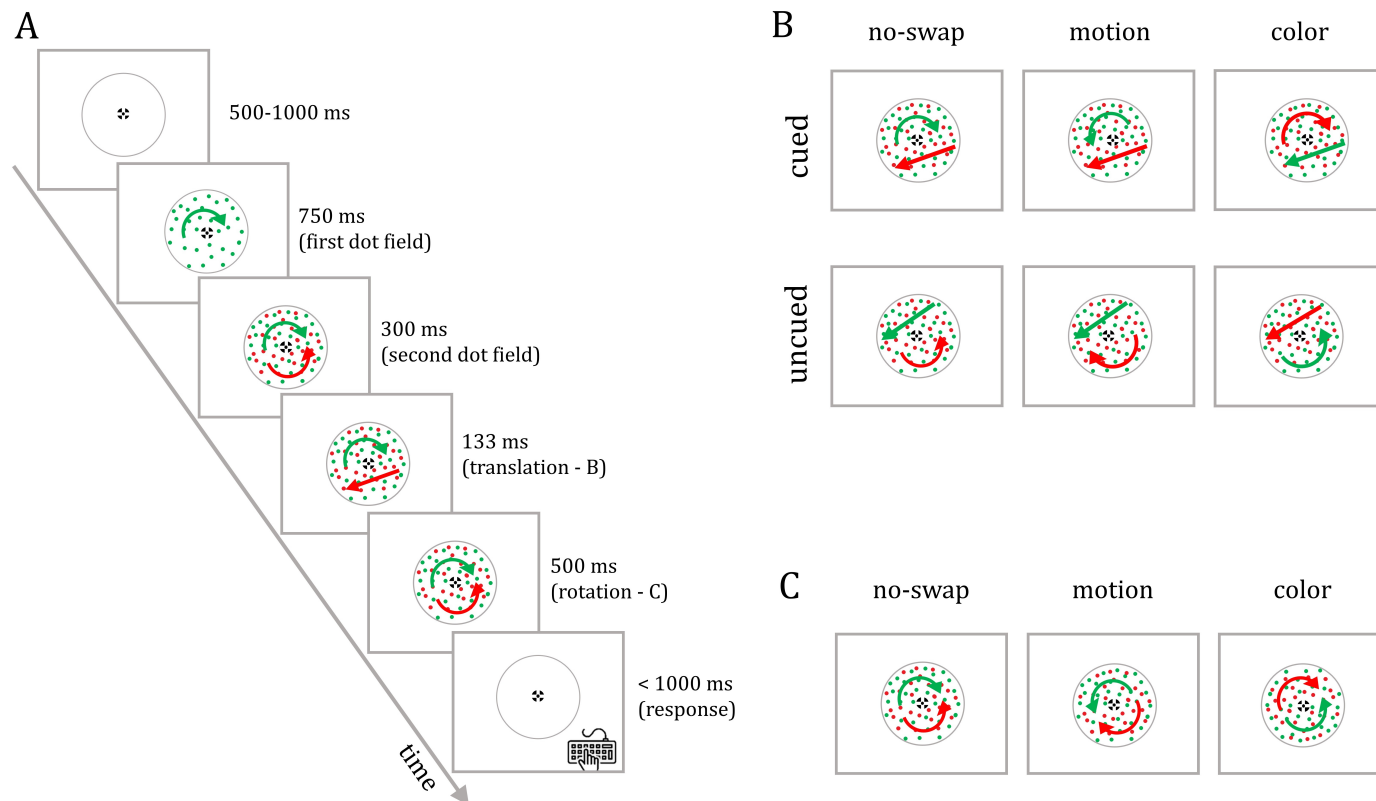


Figure 3.1: Schematic representation of stimuli. (A) Each trial started with a variable fixation period, followed by the appearance of the first dot field rotating around the fixation point for 750 ms. A second (delayed) dot field appeared and both fields rotated in opposite directions around the fixation point for 300 ms. (B) Following this period of dual rotation, one dot field translated in one of the eight directions for 133 ms. At the translation onset, the non-translating dot field either continued to rotate in its original direction (no-swap) or reversed rotation direction (motion-swap). The colors of the two dot fields were similarly swapped at the onset of translation on half of the trials (color-swap). The resulting six different conditions are illustrated separately. (C) After the translation, the translating dot field either resumed its original rotation direction or assumed the other dot field's previous rotation direction, and both surfaces kept rotating for 500 ms in their newly assigned directions. The subject's response window started 100 ms after the translation onset and ended 1 second after stimulus offset. The stimulus shown in (A) is an example of the cued no-swap condition.

Response registration and timing were based on the translation onset. If the participant responded earlier than 100 ms after the translation onset or failed to respond until 1 sec after the stimulus left the screen, the trial was repeated. The participants either reported the direction or skipped the trial in case of an interruption (e.g., fixation break). Skipped trials were also repeated. The response registration continued until the end of a trial or the participant passed forward to the next trial. Prior to each session, all participants were informed about the limited response time and told that the trials would be repeated if they failed to respond within this time range. The participants were informed that the translating dots could be of either field and that only a subset of one of the dot fields translated coherently. Accordingly, they were told to attend to the entirety of both dot fields to maximize their ability to discriminate the global direction of those translations. Hence, there was no incentive to selectively attend to one of the two dot fields or any subset of dots. As described above, each participant had been trained to fixate and screened based on their ability to do so. Subjects were instructed to fixate throughout each trial. Each participant completed a main experimental session including 96 trials per condition.

3.2.5 EEG data acquisition and preprocessing

EEG recording and preprocessing steps were similar to those described previously [244, 245]. A 64-channel MR-compatible system (Brain Products GmbH, Gilching, Germany) was used to record high-density EEG activities. Prior to each experimental session, we carefully placed the EEG cap on a participant’s head. The placement of scalp electrodes was based on the extended 10-20 system. Two electrodes were used as reference (FCz) and ground (AFz). We used q-tips and a syringe with a blunt tip to apply conductive paste (ABRALYT 2000 FMS, Herrsching-Breitbrunn, Germany) in order to reduce the impedance of each electrode below 10 k. The impedance levels were monitored during the sessions for reliable recording. EEG signals were sampled at 5 kHz and band-pass filtered between 0.016 and 250 Hz. We stored the EEG data, event markers, and behavioral responses using the Vision Recorder Software (Brain Products GmbH, Gilching,

Germany) for offline analyses.

EEG preprocessing steps were carried out offline with Brain Vision Analyzer 2.0 software (Brain Products GmbH, Germany). First, EEG signals were down-sampled to 500 Hz and filtered using a zero-phase Butterworth band-pass filter (0.5-100 Hz, 24 dB/octave) and a 50 Hz notch filter (50 Hz \pm 2.5 Hz, 16th order). Using the recorded signal from the electrocardiogram electrode, the cardioballistic artifacts were removed [221]. After these preprocessing steps, the data were next divided into epochs starting from 500 ms before the onset of the first dot field to 1 sec after the translation offset. Independent component analysis with the Infomax algorithm was used on the data to remove common EEG artifacts such as eye blinks. Lastly, we used a combination of manual and automated selection to find and remove trials contaminated with oscillations over 50 μ V/ms, voltage changes more than 200 μ V in 200 ms, or changes of less than 0.5 μ V in 100 ms window. Bad channels were restored using spherical spline interpolation [246]. After applying these preprocessing steps, on average 92% of trials (SEM = 1.11%) were preserved for further ERP analyses. The excluded trials during the EEG preprocessing stage were also not used in the analysis of the behavioral data.

3.2.6 ERP analyses

After preprocessing, we averaged the EEG signals from each electrode across all valid trials to compute ERPs time-locked to the onset of the first rotating dot field. For further smoothing, these averaged ERPs were filtered with a low-pass filter (6th order zero-phase Butterworth IIR filter with 40 Hz cut-off frequency). A baseline correction was also applied using the 100 ms time window before the onset of the first dot field. We adopted a two-step approach in our ERP analyses. The current study is the first EEG investigation using the delayed-onset design and the first to incorporate the feature-swaps that allow identification of object-based mechanisms. Given these key design differences between the current and previous studies, we could not assume that we would see the ERPs previously identified in those studies. For this reason, we used a data-driven approach at

the first stage of the analyses to comprehensively evaluate modulations in the spatiotemporal profile of neural activity. We performed the cluster-based permutation test integrated into the Fieldtrip toolbox to identify spatiotemporal clusters associated with the significant modulations of ERPs [247]. This is a data-driven non-parametric framework to overcome multiple statistical comparisons (Type I error) and to cluster selected samples objectively [248, 249]. Our experimental design included conditions with a sequence of visual events during each trial. It is possible to have overlapping components and leakage from the pre-translation period to the evoked activities after translation onset. On the other hand, the types of visual events were the same up to translation onset for the cued and uncued conditions. Therefore, we compared the cued trials with the uncued trials (i.e., baseline condition) to avoid any potential confounding factor. Our first goal was to identify spatiotemporal ERP clusters that reflected the effects of cueing across all of the swap conditions. Accordingly, we combined all the waveforms (i.e., averaged across swap conditions) for the cued and uncued conditions, separately. These two combined waveforms (cued vs. uncued) were compared at each electrode location and time point (2-ms bin) using a paired samples t-test. The samples with t-values exceeding an uncorrected alpha level of 0.05 were clustered together based on spatial (i.e., electrode location) and temporal (i.e., time point) proximity. At least three neighboring electrodes were required to form a cluster. The t-values within a cluster were summed up to have cluster-level statistics. To obtain a null hypothesis distribution of the cluster-level statistics, 10,000 random permutations of the original data were generated using the Monte Carlo method. A cluster in the experimental data was considered to be significant when it fell in the highest or the lowest 2.5th percentile of the generated distribution (corresponding to the significance level of a two-tailed test). That is to say, since the tests were two-sided, the significance threshold for testing the null hypothesis (alpha level) was 0.025 [249]. Previous EEG studies identified the evoked activities and components within the first 400-500 ms time window after the translation onset (e.g., [176, 196, 180]). By following the same approach and conventions, we restricted our analyses (i.e., cluster-based permutation test) to the first 400 ms time range and hence identified the modulations.

Following the cluster-based permutation test, we identified the time-range and electrode locations (i.e., exemplar sites) of spatiotemporal clusters associated with the significant effect of cueing. Using the exemplar sites, we displayed the time-courses of evoked brain activities to all six conditions (2 cued/uncued x 3 swap conditions) for illustrative purposes. At the second stage of ERP analyses, we averaged activities within the identified time-range of a cluster and carried out a regression analysis between these mean potentials and behavioral performance values across all six conditions to determine how these potentials related to performance. The correlation and association between the mean potentials and performance measures across the six experimental conditions were evaluated through linear regression fits having intercept and slope as coefficients. Next, to elucidate the nature of ERP modulations, we computed the peak amplitudes and latencies of ERP components over the exemplar sites. We performed a two-way repeated-measures ANOVA (with cueing and swapping as factors) on these ERP metrics. When Mauchly’s test indicated that the assumption of sphericity had been violated, the Greenhouse–Geisser correction was applied. The corresponding epsilon (ϵ) values (i.e., sphericity estimates) are supplied when the ANOVA results are presented. It is important to note that the cluster-level statistics were built upon t-values from selected samples and the permutation test outcome does not directly provide any additional metric for the effect sizes. These additional ANOVAs thus allow estimation of effect sizes for all experimental factors as well as any two-way interaction.

3.3 Results

3.3.1 Behavioral results

The average performance values of each participant and group-averaged data are shown in Figure 3.2. All participants performed above the chance level (12.5% based on 8 translation directions). A two-way repeated-measures ANOVA with

cueing (cued vs. uncued) and swapping (no-swap, motion, color) as factors indicated significant main effects for both cueing ($F_{1,14} = 49.545$, $p < 0.001$, $\eta_p^2 = 0.780$) and swapping ($F_{1.18,16.52} = 8.676$, $p = 0.007$, $\eta_p^2 = 0.383$, $\epsilon = 0.59$)¹. In agreement with Stoner and Blanc (2010), we found that observers were significantly better at judging translations of the cued (delayed) dot field (M = 51.34%, SEM = 3.46%) than of the uncued (non-delayed) dot field (M = 36.66%, SEM = 2.39%) in both the presence and absence of swaps. However, the overall accuracies of observers were reduced for the trials that included motion swaps (Table 3.1).

Table 3.1: The results of the post-hoc paired t-tests comparing swap conditions for each cueing condition. The descriptive statistics (mean, SEM) are based on the difference between the compared conditions. The values for each cueing condition are grouped in separate rows. Only the significant differences (Bonferroni-corrected $p < 0.05$) are listed in the table and highlighted in bold. The follow-up tests did not reveal any other significant comparisons across swap conditions.

	<i>t</i> ₁₄	<i>p</i>	Cohen's <i>d</i>	Mean (%)	SEM (%)
Cued					
no-swap vs. motion	3.186	0.020	0.823	17.08	5.361
color vs. motion	2.972	0.030	0.767	14.10	4.745
Uncued					
color vs. no-swap	2.884	0.036	0.745	3.825	1.326
color vs. motion	3.092	0.024	0.798	11.12	3.594

Moreover, a significant two-way interaction between cueing and swapping was revealed ($F_{2,28} = 4.971$, $p = 0.014$, $\eta_p^2 = 0.262$). In summary, while the cueing advantage survived motion swaps, the inclusion of motion swaps not only decreased the overall accuracy but also decreased the accuracy difference between cued and uncued conditions. To further understand the differential effects of cueing, we calculated the difference performance values between cued and uncued conditions

¹Mauchly's test indicated that the assumption of sphericity had been violated for main effect of swapping, therefore degrees of freedom were corrected using Greenhouse-Geisser estimates of sphericity.

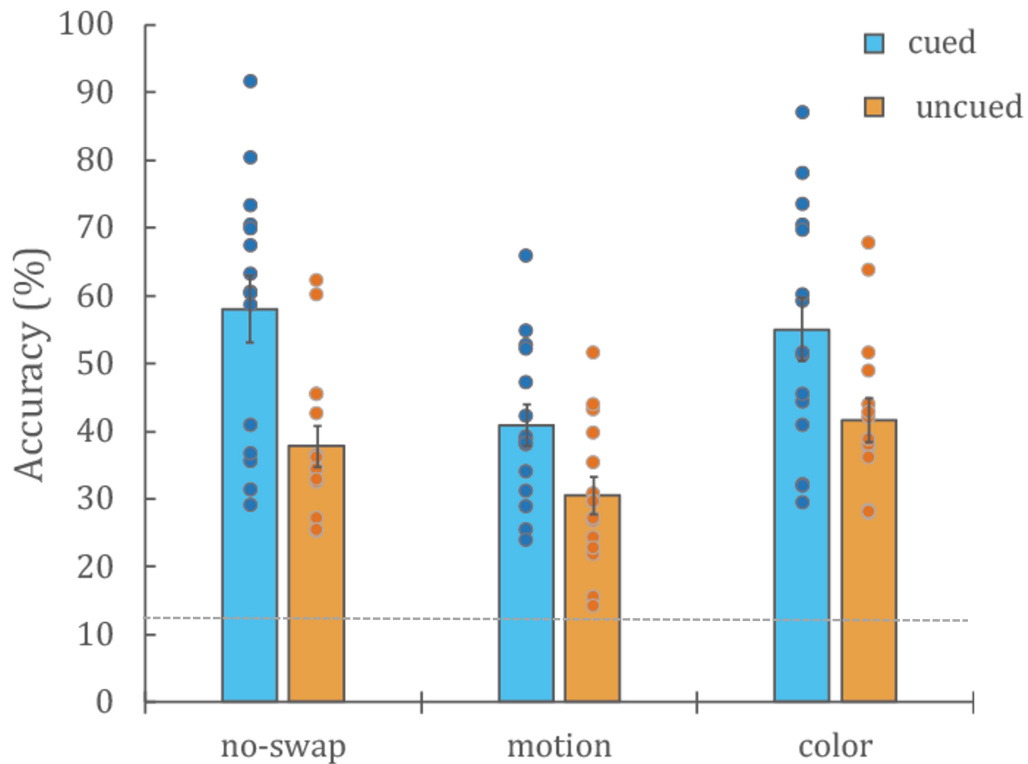


Figure 3.2: Behavioral results ($n=15$). The percentage of correct responses for each condition with blue and orange bars corresponding to cued and uncued conditions, respectively. Dots represent the data from individual participants. The dashed line indicates chance performance level (i.e., 12.5%). Error bars \pm SEM.

for all swap conditions (Table 3.2, two right-most columns for descriptive statistics) and performed paired t-tests on these difference values. Bonferroni-corrected pairwise comparisons indicated that the difference performance values of conditions with motion swaps were significantly different from that of the no-swap condition ($t_{14} = 3.225$, $p = 0.018$, Cohen's $d = 0.833$). Additionally, there was also a significant difference between the cueing effects of no-swap and color swap conditions ($t_{14} = 2.727$, $p = 0.049$, Cohen's $d = 0.704$). Despite the impact of feature swaps, the accuracy for the cued trials was significantly greater than for uncued trials for all conditions (Table 3.2).

Table 3.2: The results of post-hoc paired samples t-tests for the cueing effect (cued vs. uncued) for each swap condition. The descriptive statistics (mean, SEM) are based on the difference between cued and uncued conditions. Significant p values (Bonferroni-corrected $p < 0.05$) are highlighted in bold.

	t_{14}	p	Cohen's d	Mean (%)	SEM (%)
no-swap	6.626	<0.001	1.711	20.217	3.051
motion	5.096	<0.001	1.316	10.426	2.046
color	4.308	<0.001	1.112	13.415	3.114

3.3.2 EEG results

In line with behavioral results, we found a robust difference in the evoked activities elicited by the cued conditions compared to the uncued. A cluster-based permutation test on the averaged ERPs in the 400 ms time-range after translation revealed a spatiotemporal cluster associated with the significant effect of cueing (cued vs. uncued, cluster-level $t_{sum} = -7437$, $p = 0.002$). This cluster was mainly within the 238-326 ms time window. While the cluster spread over some centro-parietal electrodes, it was mainly over occipital and parieto-occipital scalp sites (Figure 3.3). Over these electrodes, the average activity for cued trials was larger in amplitude in a negative direction (i.e., more negativity) compared to the uncued trials.

The cluster-based permutation test also indicated an earlier (134-224 ms) and nonsignificant cluster (cued vs. uncued, cluster-level $t_{sum} = -2035$, $p = 0.042$). The average magnitude of cueing effect was smaller for this early time-range. In other words, the analyses reported some electrodes which were differentially activated for at least 20 ms such as medial parieto-occipital and parietal scalp sites (Figure 3.4). However, these observed cueing effects did not survive at the cluster level statistics which was based on the spatiotemporal domain. To elucidate the differential effects of swapping on the spatiotemporal profile of the neural activity, we subtracted the averaged ERPs of the cued trials from those of

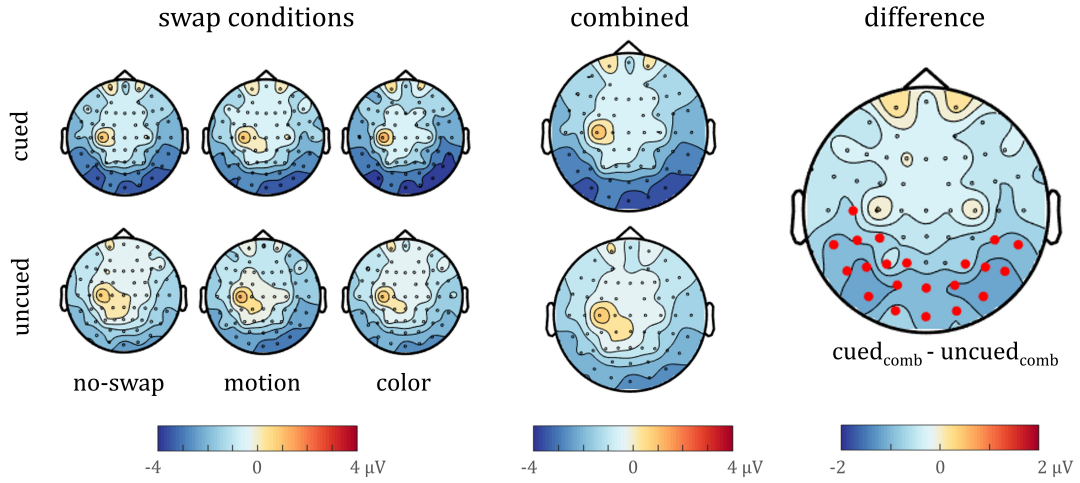


Figure 3.3: Voltage topographical maps of the averaged waveforms within the identified time window (238-326 ms). The voltage topographical maps of cued and uncued conditions are shown in separate rows. The averaged activities of each swap condition, combined waveforms across swap conditions, and the difference between them ($cued_{comb} - uncued_{comb}$) are displayed on the maps in separate columns. The result of the cluster-based base permutation test comparing the combined waveforms ($cued_{comb}$ vs. $uncued_{comb}$) is indicated in the last column. The electrodes that were part of the significant spatiotemporal cluster for at least 70 ms (i.e., more than 75% of the time-range) were chosen as exemplar electrodes and are marked by red-filled circles on the right-most topographical map (i.e., Oz, O1, O2, POz, PO3, PO4, PO7, PO8, P1, P3, P4, P5, P6, P7, P8, CP3, CP5, CP6, C5, TP8, TP7).

uncued trials for each swap condition. Based on the observed impact of motion and color swaps on behavioral performance, we were particularly interested in comparing the difference waveforms of these conditions with those of no-swap condition. These and other similar comparisons did not reveal any additional and meaningful spatiotemporal cluster.

Electrodes that were part of the identified significant cluster for more than 70 ms (i.e., more than 75% of the 238-326 ms time-range) were selected as exemplar sites (Figure 3.3). The averaged potentials over these electrodes are shown in Figure 3.5A. In these averages, there were robust evoked activities peaking around 300 ms (N1 component) post translation. The identified time window of the cluster corresponded to the range of this negative N1 component. In this

component range, the cued conditions elicited larger amplitudes compared to the uncued trials (Figure 3.5B). This was also reflected in the mean values within the identified time window (238-326 ms) for each swap condition (Figure 3.5C). We performed a linear regression fit using of these both mean potentials and performance values. The analyses revealed a significant association between these measures across different conditions ($R_{adj}^2 = 0.577$, $p < 0.05$; Figure 3.6).

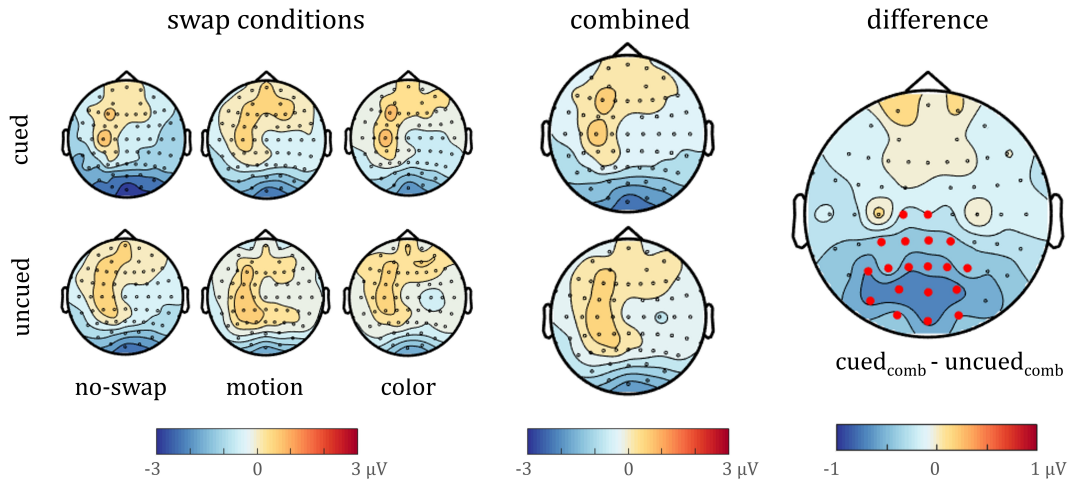


Figure 3.4: Voltage topographical maps of the averaged waveforms within the identified time window (134-224 ms). The voltage topographical maps of cued and uncued conditions are shown in separate rows. The averaged activities of each swap condition, combined waveforms across swap conditions, and the difference between them ($cued_{comb} - uncued_{comb}$) are displayed on the maps in separate columns. The result of the cluster-based base permutation test comparing the combined waveforms ($cued_{comb} - uncued_{comb}$) is indicated in the last column. The electrodes, which were part of the spatiotemporal cluster for at least 20 ms are marked by red-filled circles on the rightmost topographical map (i.e., Oz, O1, O2, POz, PO3, PO4, PO7, Pz, P1, P2, P4, P3, P5, CPz, CP1, CP2, CP3, Cz, C1).

To further understand the nature of these ERP modulations, we performed repeated-measures ANOVAs with cueing and swapping as factors on the peak amplitudes and latencies of the N1 component (Figure 3.5A, B). The peak amplitude was significantly dependent on cueing ($F_{1,14} = 20.549$, $p < 0.001$, $\eta_p^2 = 0.595$). Neither the main effect of swapping ($F_{2,28} = 0.179$, $p = 0.837$, $\eta_p^2 = 0.013$) nor the two-way interaction between cueing and swapping ($F_{2,28} = 0.176$, $p = 0.840$, $\eta_p^2 = 0.012$) were significant. Similarly, a secondary ANOVA on the mean potentials (Figure 3.5C) only revealed a significant main effect of cueing

and did not indicate a significant main effect of swapping or a two-way interaction. ANOVA applied to the peak latencies did not reveal significant main effects (cueing: $F_{1,14} = 0.084$, $p = 0.777$, $\eta_p^2 = 0.006$; swapping: $F_{1.33,18.65} = 2.438$, $p = 0.129$, $\eta_p^2 = 0.148$, $\epsilon = 0.67$)² or two-way interaction ($F_{2,28} = 1.862$, $p = 0.174$, $\eta_p^2 = 0.117$).

Although the above analysis revealed no significant impact of cueing on peak latencies, the time courses of an ERP component elicited by two different conditions can differ without having different peak latencies [250]. Indeed, an inspection of Figure 3.5B suggests that the evoked activities of the cued conditions might have had an earlier onset than those of the uncued conditions. To determine whether these onset latencies differed significantly, we computed the latency to the half-peak amplitude applying methods used in previous neurophysiological studies [251, 252]. This latency measure was defined as the time point when the response reached half the difference between the peak amplitude and baseline amplitude. We established this latency by first identifying the first 5 successive 2-ms bins within the N1 time-range that exceeded this midpoint estimate. The latency was taken to be the first of these bins. We computed this metric for all conditions of each participant. A two-way repeated-measures ANOVA did not reveal any main effect of cueing ($F_{1,14} = 0.011$, $p = 0.919$, $\eta_p^2 = 0.001$), swapping ($F_{2,28} = 2.809$, $p = 0.077$, $\eta_p^2 = 0.167$) or a significant two-way interaction ($F_{2,28} = 0.162$, $p = 0.851$, $\eta_p^2 = 0.011$). Thus, neither analysis of the peak latency nor the latency to the half-peak amplitude revealed a significant effect of cueing or swapping on the time course of the N1.

These analyses thus demonstrated that the N1 amplitude was impacted by cueing but revealed no significant effect of swapping thereby supporting an object-based account of our results and providing no support for feature-based effects (such as those proposed by the motion-competition explanations). To further investigate the possibility that swapping (and hence feature-based effects) might nevertheless have impacted the N1, we applied Bayesian statistics on all the N1

²Mauchly's test indicated that the assumption of sphericity had been violated for main effect of swapping, therefore degrees of freedom were corrected using Greenhouse-Geisser estimates of sphericity.

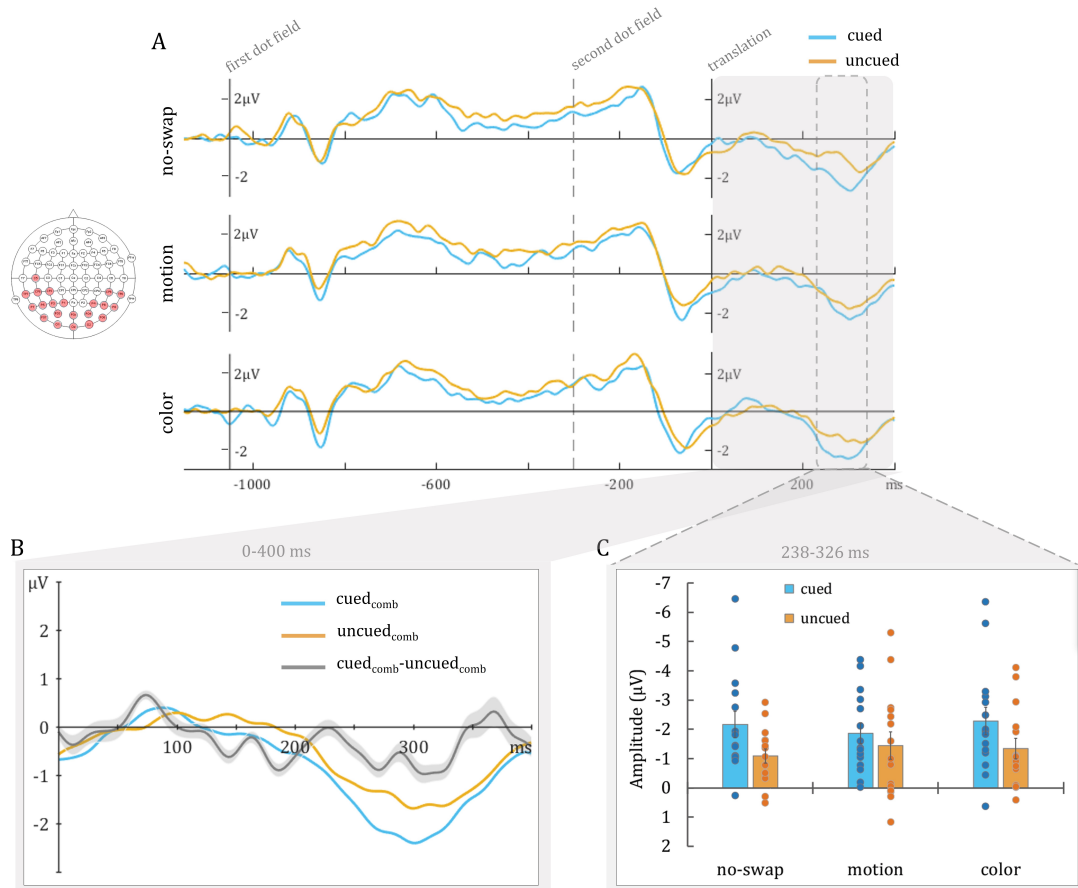


Figure 3.5: Averaged activities and derived waveforms from the exemplar scalp sites ($n=15$). The exemplar electrodes that were used in analyses are shown on a head model (i.e., Oz, O1, O2, POz, PO3, PO4, PO7, PO8, P1, P3, P4, P5, P6, P7, P8, CP3, CP5, CP6, C5, TP8, TP7). (A) The averaged ERPs for each swap condition are displayed in separate plots, the blue and orange curves correspond to evoked activities for cued and uncued conditions, respectively. The ERPs were time-locked to the onset of the translation and displayed in the range from the start of each trial to 400 ms after translation. The 100 ms time window before the onset of the first dot field was used as the baseline period. The identified time window based on the cluster-based permutation test is marked by a dashed rectangle. (B) The averaged combined waveform for the cued (blue) and uncued (orange) conditions after translation. The difference waveform ($cued_{comb} - uncued_{comb}$) is indicated by the gray curve, and the shaded area corresponds to the standard error (+SEM) across participants. (C) Bar plots displaying the averaged amplitudes within the identified time window (238-326 ms) for each condition. The blue and orange bars correspond to cued and uncued conditions, respectively. The dots represent the data from individual participants. Error bars \pm SEM.

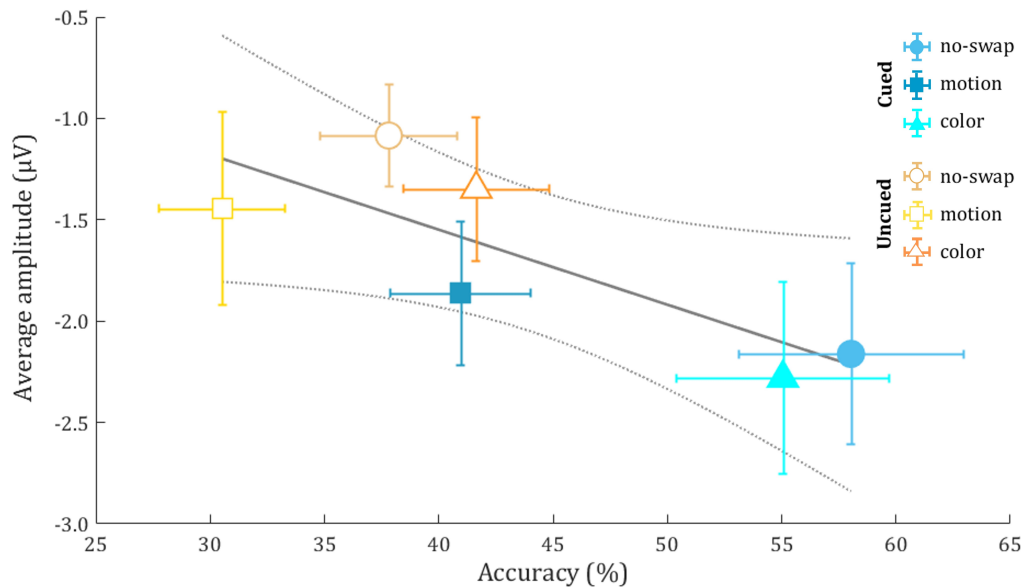


Figure 3.6: Averaged potentials in the time-range of the identified cluster (238-326 ms) with the performance values for each condition (2 cued/uncued x 3 feature swaps). The locations of exemplar electrodes used in our analyses are shown in Figure 3.5. Filled and open symbols correspond to the cued and uncued conditions, respectively. Each swap condition is represented by different symbols. Vertical and horizontal error bars correspond to the variance across observers (+SEM). The black solid line indicates the best linear fit and dotted lines denote the 95% confidence intervals on the linear fit.

component metrics (peak amplitude, latency, and half-peak latency). Consistent with our ANOVA results, a Bayesian repeated-measures ANOVA suggested that the changes in peak amplitudes were best represented by the model including only cueing as the main factor, compared to the null model ($BF_{10} = 132.3$). With regards to the peak and half-peak latency values, the outcome of Bayesian tests mainly supported the null hypotheses similar to the previously reported ANOVA results (Table 3.3).

In conclusion, the analyses on the N1 component revealed a robust cueing effect on amplitude, with N1 responses to translations being larger (i.e., more negative) for cued conditions than for uncued conditions. This trend held for all swap conditions. Since motion-competition and other feature-based mechanisms predict that feature swaps should reverse the cueing effect [189], our results rule

Table 3.3: The results of Bayesian repeated-measures ANOVA on the N1 amplitude, latency, and half-peak latency values. The Model Comparisons column displays the Null model, followed by the four alternative hypotheses models. The “Cueing” and “Swaps” rows displays the probabilities based on the alternative hypothesis that one of the main factors alone is responsible for the variability in the data. The “Cueing + Swaps” model is based on the alternative hypothesis that the changes the data depends on both Cueing and Swaps factors together, and the “Cueing + Swaps + Cueing * Swaps” model displays the probabilities for the alternative hypothesis that the change is due to both main factors and the interaction. $P(M)$ indicates the prior probabilities of each model which was set to be equal at the beginning. $P(M|data)$ shows the updated posterior probabilities after the data was provided as input. BF_M shows the change in prior model odds due to data. BF_{10} indicates the Bayes factors for each model. The percent error in the last column is based on the accuracy of the Bayes factor calculations.

Model Comparisons	P(M)	P(M data)	BF_M	BF₁₀	error %
Peak Amplitude					
Null model (incl. subject)	0.200	0.007	0.027	1.000	
Cueing	0.200	0.878	28.671	132.316	1.827
Swaps	0.200	0.0007	0.003	0.109	0.746
Cueing + Swaps	0.200	0.096	0.424	14.448	1.248
Cueing + Swaps + Cueing * Swaps	0.200	0.019	0.079	2.903	3.925
Peak Latency					
Null model (incl. subject)	0.200	0.337	2.034	1.000	
Cueing	0.200	0.080	0.348	0.237	2.183
Swaps	0.200	0.451	3.287	1.338	1.977
Cueing + Swaps	0.200	0.052	0.450	0.300	1.780
Cueing + Swaps + Cueing * Swaps	0.200	0.008	0.126	0.091	1.470
Half-Peak Latency					
Null model (incl. subject)	0.200	0.360	2.252	1.000	
Cueing	0.200	0.081	0.354	0.226	3.281
Swaps	0.200	0.445	3.205	1.235	0.566
Cueing + Swaps	0.200	0.096	0.424	0.266	1.163
Cueing + Swaps + Cueing * Swaps	0.200	0.018	0.073	0.049	2.202

out those explanations for the N1 effect observed in the current study. Conversely, we observed no significant impact on the time course of the N1 for either our cueing or feature-swapping manipulations. These follow-up tests further emphasize that the strength modulations (rather than pure latency shifts) mainly contributed to the observed cueing effect on the N1 component (Figure 3.5B) over the identified occipital and parieto-occipital scalp sites.

3.4 Discussion

3.4.1 Summary

The present study confirmed earlier findings [181, 189] that the delayed onset of one of two superimposed counter-rotating dot fields yields an advantage in judging the direction of subsequent brief translations of the delayed dot field relative to translations of the non-delayed dot field. By introducing motion-direction and color “feature swaps” simultaneously with the translation onset, we also confirmed Stoner and Blanc’s [189] finding that this performance advantage is indeed specific to the delayed dot field rather than to the overall color and/or motion direction configuration of these stimuli. Most importantly, we found ERP correlates of this processing advantage in the N1 component range. The spatial distribution of this ERP component was consistent with the involvement of mid- and perhaps low-level visual areas. Our findings rule out explanations based on feature-specific selection as well as those based on feature competition/normalization. They support an object-based interpretation of the cueing effects observed in the delayed-onset transparent-motion design used here, as well as in the studies that have used variations of the original Valdes-Sosa et al. [185] two-translation design [193, 176, 196, 177, 178, 188, 180, 181, 182, 187].

3.4.2 Object-based versus motion-competition explanations

As reviewed in section 1.3.4, Stoner and Blanc [189] offered a motion-competition account that parsimoniously accounted for previous findings without the need to invoke object-specific attentional enhancement. Critically, the motion-competition account asserts that the key determinant of behavioral and neuronal responses is whether the translation competes with a new or old rotation irrespective of which objects (i.e., dot fields) happen to undergo those motions. To test that prediction, Stoner and Blanc [189] introduced the motion-swap manipulations used in the current study. If the motion-competition account were valid, this manipulation should reverse the cueing effect: translations of the undelayed (“uncued”) dot field should yield better accuracy than translations of the delayed (“cued”) dot field. Contrary to that prediction, they found (and we confirmed in the current study) that the performance advantage conferred by delayed onset was not reversed by motion swaps. These results thus ruled out the motion-competition explanation and demonstrated that the advantage was indeed object-specific. Most importantly, these findings demonstrated that the link between rotations and translations are the spatially intermixed dots that undergo those motions. As the receptive fields of neurons in areas MT and MST (medial superior temporal area) are too large to distinguish the dots from different fields, Stoner and Blanc [189] suggested that earlier areas such as V1 (and/or V2) were likely involved and outlined a mechanism involving top-down feature-specific interactions between areas MT (and/or MST) and area V1 coupled with spatially local cooperative interactions between neurons tuned to different features within V1. The current study was motivated, in part, to look for further evidence of that mechanism.

3.4.3 Behavioral findings

Our behavioral findings confirmed the dot specificity of the cueing effect found by Stoner and Blanc [189] behavioral accuracy was greater for translations of

the cued (delayed) dot field than for translations of the uncued dot field even in the presence of motion and color swaps. Consistent with the results of Stoner and Blanc [189], we did, however, find a slight (but significant) decrease in the cueing effect when introducing color swaps (see section 3.4.4). Our results did diverge slightly from those of Stoner and Blanc [189]. Specifically, we found that motion swaps resulted in an overall decrease in performance (i.e., for both cued and uncued trials) as well as a decrease in the cueing effect. They found neither of these effects. The explanation for these discrepancies is unclear but may reflect small differences in the two designs. For example, in the current study, the translation duration (133 ms) was considerably longer than that (40 ms) used by Stoner and Blanc [189]. This longer duration was intended to yield more reliable behavioral responses but may have also resulted in the observed discrepancies: the dot-field specificity of the cueing effect may not survive the full 133 ms. In addition, the dot fields in Stoner and Blanc [189] were significantly brighter than those used in the current study and this difference might conceivably account for the differential impact of motion swaps and/or color swaps in the two studies. How these brightness differences might be related to the different findings is not immediately clear but might be related to the differential attentional salience accompanying swaps. Lastly, it should be emphasized that the differences in the findings of the two studies are relatively small and may simply be due to chance variations in the subject pool: different subjects likely have slightly different mechanisms or strategies underlying their performance in these tasks.

3.4.4 Role of color

The two dot fields differed in color in the original Valdes-Sosa et al. [185] design as well as in most subsequent studies using variants of that design and hence color could conceivably have mediated the cueing effects found in those studies. As previously noted, however, Mitchell et al. [178] found that the cueing effect survived the removal of color differences in the two-translation design. The results of the color swap experiments documented here, and by Stoner and Blanc [189], demonstrate that the cueing effect is mostly not color specific: swapping the colors

of the two dot fields did not reverse the cueing effect. It did, however, reduce the cueing effect very slightly. While these findings do not reveal a substantial role for color in the preferential processing of motion documented in those studies. They do not mean, however, that the color of the cued dot field is not itself granted a processing advantage when color differences are present. Indeed, Fallah et al. [193], using the delayed-onset design, found a color processing advantage in the responses of color-selective neurons in area V4. Those findings revealed that the color, as well as the motion direction of the delayed dot fields as revealed in other studies, enjoy a processing advantage as would be predicted from the object-based account. We predict that this processing advantage would also be dot-field specific (rather than color-specific) and hence extend to a “new” color as occurs in our color-swap conditions.

3.4.5 Spatial attention

The finding that the cueing effect is specific to the individual dots might suggest that, despite the spatial superimposition of the two dot fields, subjects in these experiments were attentively tracking a subset of these dots thus employing a type of spatial attention (i.e., with a moveable “spotlight”). We think this is unlikely for several reasons. First, there is no motivation for subjects to attend one set of dots or the other as the translations of the two dot fields occur with equal probability. Second, the subjects were firmly and explicitly instructed to diffusely attend and not attend to either dot field or a subset of the dots. Third, only a subset of the dots translated coherently so, as the subjects were informed, attending to the global motion is a better strategy than attending to a particular dot or set of dots. Finally, Intriligator and Cavanaugh [253] found that the spatial resolution of attentive tracking is much coarser than visual resolution. Thus, while the dots of the two dot fields in our study can be visually resolved, the close spatial proximity of the spatially intermixed rapidly moving dots would seemingly defeat any attempt to attentively track them.

3.4.6 ERP findings

Using a two-translation design in which the first translation serves as an exogenous cue, Khoe et al. [176] found evidence that exogenous cueing modulated the early C1 component (75-110 ms) as well as the N1 component (160-210 ms). The C1 effect is consistent with the involvement of early areas, including area V1, whereas the N1 component is generally thought to involve mid-level cortical areas. Earlier ERP studies using the two-translation design had included an endogenous cue (fixation point color) and did not find a C1 effect [177, 180]. Moreover, while those studies reported N1 effects, the N1 had a later time course (244-293) than that of Khoe et al. [176]. In the present study, the ERP modulations were similarly most prominent in the N1 component range (238-326 ms). More importantly, these modulations indicated dot-field specific cueing that survived feature swaps (i.e., of motion and/or color). Compared to the prior EEG findings using transparent-motion (e.g., [177, 180, 176, 196, 184, 197]), the peak of N1 component observed in this study was somewhat delayed and/or the overall component range was extended in time. One potential explanation for these differences lies in the differing rotation speeds used in the studies. It has been established that the amplitude and latency of the N1 component elicited by a motion-onset can be reduced and delayed by a previous period of motion stimulation [254, 180]. More to the point, using a transparent-motion design similar to the one here, Pinilla et al. [180] demonstrated that N1 peak latency to brief translations is dependent on the preceding rotation speeds of the two dot fields. They found that the peak latency of the N1 was shortest when the dot fields were stationary prior to the translation and increased as the speed of the background rotation was increased. Our rotation speed of $81^\circ/\text{s}$ was greater than those used in previous EEG studies and based on the findings of Pinilla et al. [180], this is consistent with a delay of several tens of milliseconds. Pinilla et al. [180] found, moreover, that the duration of this component increases as the rotation speed is increased. Consistent with their findings, the latency and duration of the N1 reported here was similar to that reported by Pinilla et al. [180] for the highest rotation speed (i.e., $80^\circ/\text{s}$). Lastly, our translation was of longer duration and this could plausibly contribute to both a delay in the peak of the N1 and longer

duration relative to the findings of Pinilla et al. [180].

3.5 Conclusions

Our findings provide the first evidence of the role of the N1 component in object-based attention under conditions that rule out the feature-based explanations admitted by previous studies [189]. Together with previous research, these findings reinforce the importance of the N1 component in object-based selective processing as well as other types of attentional phenomena. Both our behavioral and EEG results provide evidence of an attentional processing advantage that spreads from one feature to another based on the spatiotemporal continuity of local texture elements (dots in the case of dot fields) rather than relying on higher-order mechanisms. Although we have speculated that this fine-grained spatial selection may involve area V1, future research is needed to identify the mechanisms underlying the behavioral and neuronal effects documented in this study.

Chapter 4

General Discussion and Future Directions

The visual experience is elicited by full of complex and dynamic information; however, not all can be selected for further processing due to the limited capacity of the sensory system. Distinct processing mechanisms of attention are employed to prioritize the processing of relevant information filtering out the irrelevant stimulus. Even during the steady-state (e.g., fixation), visual experience relies on highly dynamic neural processes. Since attention is a matter of organizing neural processes at different stages, studying attentional modulations sheds light on the underlying principles of visual processing in daily life situations.

The current thesis focused on understanding the time course and different stages of visual information processing and selection mechanisms using paradigms such as visual masking, attentional load, and transparent motion design that operate in different attentional modes with a steady-state setting. To uncover the ever-changing neural activation processes, we also employed the EEG technique due to its high temporal resolution. Using metacontrast masking combined with the manipulation of attentional load in the visual field, we aimed to understand the role of spatial attention in information processing and its possible interactions

with masking mechanisms. This design allowed us to understand the role of attention in a simple scenario including only brief and rapidly changing static stimulations. Daily life situations also involve dynamic moving objects and the role of attention in these situations is still subject to debate. Moreover, by employing a novel variant of transparent motion design, we aimed to isolate the object-based effect from a possible feature-based explanation in both psychophysical measures and neural activities. In the following sections, the implications of these findings are discussed within the theoretical framework of visual attention.

4.1 Contributions to the models of attention

Although attention is known to enhance sensory processing, the mechanisms by which attention extracts relevant information from noise are not very well understood. Based on psychophysical, neurophysiological, and neuroimaging data, several explanatory models of attentional mechanisms have been proposed (see section 1.3.1). A common notion in the proposed mechanisms is the existence of a form of competition for limited brain resources [255, 85, 90]. For example, according to the biased-competition hypothesis this competition occurs between neurons whose receptive fields lay at the attended location and the surrounding neurons whose responses are suppressed [85]. Similarly, it has been reported that spatial attention improves spatial resolution, specifically acuity performance when targets appear at the attended location, in exchange for deteriorated temporal resolution [256, 257]. These findings illustrate that attention is an optimization process that prioritizes the most relevant information at the cost of the less relevant information due to limited resources.

In this context, an influential theoretical model initially proposed to explain the non-linear feedback and feedforward processes, the retino-cortical dynamics model (RECOD), can reveal the nature of the trade-off within the visual system for optimization due to attentional modulation. The RECOD model is based on the premise of inhibitory interactions within and between the cortical areas

that specialize in complementary visual functions, such as temporal (magnocellular pathway), and spatial (parvocellular pathway) aspects of visual processing [258, 257, 256, 259]. As mentioned before (Section 1.2.1), the RECOD model has been extensively studied in visual masking [260, 261]. In metacontrast masking paradigms, the target stimulus is presented first and generates a fast transient activity followed by a slower sustained activity in the afferent pathways. The visibility of the target is correlated with the activity in the post-retinal areas that receive their main input from the sustained (parvocellular) pathway. The mask is presented second to the target and generates similar activation with a delay equal to the stimulus onset asynchrony (SOA). From the nature of the temporal overlap between the target’s sustained and mask’s both transient and sustained activation, both the intra-channel and inter-channel inhibition leads to a suppression of the sustained channel activation of the target. As a result, the visibility of the target is predicted to decrease [5]. More recently, attentional modulation is introduced to the model as a direct effect on post-retinal activities [262]. Specifically, the authors provided computational evidence in support of a signal-enhancing mechanism where spatial attention facilitates the activation in the parvocellular system over the magnocellular system and the mutual inhibition between these two pathways, accounts for the effects of spatial attention on spatial and temporal resolution. Since the parvocellular and magnocellular systems possess different spatiotemporal sensitivities with the parvocellular system being more sensitive to high spatial frequencies and the magnocellular system to high temporal frequencies [263, 264], the offered attentional mechanism that favors the parvocellular system can explain the enhancement in spatial resolution [262]. A cortical competition between the parvocellular and magnocellular systems, in turn, can explain why an enhancement of parvocellular activity by attention can lead to a decrease in magnocellular activity, which in turn results in reduced temporal acuity [258, 257, 256, 259].

Even though the attention mechanism is introduced as an add-on effect to the masking process in the model update, our behavioral results may suggest a more intricate relationship between these mechanisms. The behavioral results from our first study (see Section 2) illustrate an inverse relationship where the

effect of attentional load (set-size) on masking increases as the effectiveness of SOA decreases. More specifically, when the metacontrast masking was effective in short SOA conditions, the attentional load had small to no influence on target visibility, on the other hand, in longer SOA conditions where the masking effect was very low, high attentional load (set-size six) reduced the target visibility more effectively compared to low attentional load condition (set-size two). Increasing the attentional load has been documented to cause a decrease in the overall performance due to limited capacity of attention [265]. The task we used requires the participant to distribute their attention to several stimuli (two or six) that had an equal probability of being a potential target or a distractor, thus reducing the overall resources directed to each possible target. In the computational modeling by Penaloza and Ogmen [262], they employed a peripheral cueing paradigm where the target appeared in the attended area before being affected by the mask. Contrarily, the design we used divided the attentional resources at the beginning through set-size modulation and the following mask acted as a cue to the target among distractors while also hindering the performance. Following the predictions of Penaloza and Ogmen [262], due to the divided attention, we would expect a reduced sustained activity in possible target stimuli in high attentional load conditions even before any inhibition from the following mask. Since the mask also acts a spatial cue, attending to both the mask and the cued target would result in an improved sustained activation for both, therefore in short SOA conditions the possible attentional modulation would be expected to emerge over the intra-channel inhibition part of metacontrast masking. Specifically, at short SOAs the overlap between the sustained activation from target and mask is larger, since the mask would have a stronger intra-channel inhibition due to the attentional improvement, the visibility could be already very low due to masking for any attentional load effects to be detected. However as the SOAs grow longer, the overlap of activation and therefore intra-channel inhibition, weakens. In this case, the effects of attention on the target's sustained activity would be more apparent since the suppression by masking would be weaker. Penaloza and Ogmen [262] further predicted that the attentional enhancement of the sustained signal of initial stimulus inhibits the transient response of the transient signal

produced by the following second stimulus and that this effect would be significantly stronger at shorter SOAs, continually decreasing as the interval between the stimuli increases. In our case, the mask following the possible targets as the second stimulus may be susceptible to an inhibition in transient channels' activation due to the sustained signal of the target. In a high attentional load condition, target's reduced sustained activity may produce a weak inhibition on mask's transient activation compared to low attentional load condition, therefore may account for the emerging set-size effect in the intermediate SOA conditions where the transient on sustained inhibition due to masking is more prominent. These predictions, however, need to be tested as a line to expand the model's scope to explain more of the attentional phenomena, with more complex stimuli.

Another model that could be reasonably fitting to explain the interaction between masking and attentional modulation is a signal detection/perceptual template model. In our first study (see Section 2), we investigated the effects of spatial attentional mechanisms combined with metacontrast masking. Our behavioral results suggest a role of attention at specific stages of visual information processing that have sensitivity to target-mask timing. Two mechanisms proposed in the perceptual template model that improve sensory processing through attention are signal amplification and noise filtering. The amplification mechanism is expected to boost all visual input, simultaneously increasing the sensory gain of both the relevant signal and any irrelevant noise at the attended stimuli. The noise-filtering mechanism, on the other hand, is assumed to selectively reduce the responses to the noise component of the visual input while preserving the relevant signal [266, 267]. These processes are not mutually exclusive and can work in parallel with different influences in different task conditions. There is physiological evidence in support of these mechanisms in the form of increased cellular response sensitivity [90, 91], smaller neuronal receptive fields to filter unwanted information [85]; as well as behavioral findings of enhancement of the attended stimuli [266, 268, 269], exclusion of external noise or distractors [267, 270, 271], and modulation of contrast-gain [272]. Lu and Doshier [273] found that endogenous attention works by external noise exclusion whereas exogenous attention

invokes both external noise exclusion and signal enhancement mechanisms. Similarly, in the metacontrast paradigm here, masking reduces the strength of the target signal and consequently, the signal-to-noise ratio, while attention enhances signal strength. According to the perceptual template model, signal enhancement is most effective when external noise is low. Therefore, our behavioral data supports the notion that the attentional effect should be strongest when masking is weak and vice versa, predicting interactions similar to one we observed between attention and masking.

One of the hallmarks of object-based attention is that observers are typically better at discriminating two features of the same attended object than features of two different spatially superimposed objects. In a similar vein to the signal enhancement mechanism, a key prediction of object-based theories of attention is that directing attention to a particular feature of an object, such as its shape or color, results in the whole object being selected, including both its task-relevant and irrelevant features regardless whether the features are of different dimensions, such as color and orientation [173, 174, 182], or are of the same dimension, such as translation [181, 186]. Additional support for this assumption is reported from an fMRI study [179] demonstrating that neural activity was increased both in the cortical area encoding an attended feature, as well as in the area encoding a task-irrelevant feature of the attended object. Similarly, ERPs and MEG recordings also revealed that task-irrelevant features of an attended object could be selected fast enough for the multiple features to be integrated perceptually [183].

Both our behavioral and EEG results observed in the second study (see Section 3) provide evidence of an attentional processing advantage that spreads from one feature to another based on the spatiotemporal continuity of local texture elements (i.e. dots). Accordingly, we consider the most plausible interpretation of the cueing effects should involve a mechanism of object selection where we ruled out explanations based on feature-specific selection as well as those based on feature competition or normalization models (e.g., [85, 97]).

Multiple stimuli compete for attention at an early stage of sensory processing

and attention biases this competition by enhancing the representation of behaviorally relevant stimuli. Thus, when attention is directed toward a particular location or object, it improves the quality of sensory data acquired at the focus of attention. Improved quality means that the neural representation has higher fidelity, stronger signal, and less noise. Better signal to noise should enhance the detectability of weak signals. The signal detection theory approach is a general framework that applies to a broad range of results including visual masking and attention that generates quantitative predictions consistent with experimental data.

4.2 Neural correlates of spatial and object-based attention

ERP data have been very informative about the time course of visual processing in humans and its modulation by different modes of attention. Directing attention to the location of a stimulus typically results in an amplitude enhancement of the P1 and multiple N1 components evoked by that stimulus with little or no change in component latencies or scalp distributions [137, 274]. This pattern of P1/N1 amplitude enhancement seems to be a general characteristic of attentional focus that has been associated with speeded reaction times and improved detectability of target signals [120, 275]. These observed changes in ERP amplitude, therefore, are hypothesized to reflect sensory information that is used for perceptual judgments.

Similarly, ERP studies of object-based attention indicated modulation of both P1 and N1 components under endogenous cueing [184, 196]. Whereas follow-up studies have consistently found only N1 modulation but not of earlier components [177, 180, 197]. More recently, however, Khoe et al. [176], using only an exogenous cue, found modulation of the even earlier C1 component, which is usually associated with striate cortex, even though the timing and scalp distribution of the observed C1 component may reflect an extrastriate origin.

This relatively early activation due to attention is in line with the observation recorded in the present thesis. In our first chapter, we observed early spatial attentional modulation of the metacontrast masking effect in the P1/N1 time range due to a change in attentional load with peripheral cueing. Likewise, we also reported ERP correlates of the exogenous object-based processing advantage in the N1 component range. The spatial distribution of this ERP component was consistent with the involvement of mid-and perhaps low-level visual areas. These results are also in line with ERP studies that have shown that exogenous attention modulates the P1 [276, 277] as well as N1 components [141].

4.3 Potential Implications for Applied Research

There is a growing literature regarding the functional and structural neuroimaging of cognitive processes in healthy populations. This considerable progress, leading to a better understanding of normal brain activity and neural networks, has been applied to various neurocognitive disorders including hemispatial neglect, attention-deficit/hyperactivity disorder (ADHD), schizophrenia and bipolar disorder [278, 279, 280, 281, 282, 283, 284]. Even though the present thesis consists of two neuroscience studies on normal groups, our results have potential to contribute to the understanding of sensory and perceptual processing in these neurological disorders. Visual processing impairments are fairly well established in schizophrenia research, including abnormalities in attentional impairments [285, 286], feedforward and feedback connections involved in forward and backward masking [287], and motion processing [288]. In particular, the sensory processing for dynamic vision and motion perception are also significantly different in schizophrenic individuals [289, 290]. Research into understanding these alterations extensively benefits from visual masking, especially metacontrast masking paradigms (see [291] for a review). Patients suffering from schizophrenia consistently demonstrate larger performance deficits in masking experiments compared to healthy controls [292, 293]. Metacontrast masking is also reported to be an endophenotype of schizophrenia, meaning these deficits have been observed in unaffected siblings of the patients [294, 295, 296], suggesting they may indicate

vulnerability to the disorder and therefore could be a potential trait marker of schizophrenia [297]. The interpretations of previous findings and the origin of these alterations in schizophrenia patients have been subject to debate. While a large portion of studies consistently reported impairments in early processing of visual information associated with changes in the magnocellular system and suggested an important role for transient signals [298, 299, 300, 301, 302], others have localized changes at higher cortical stages thought to depend on re-entrant activation [287, 303, 304, 305]. Although few studies have confirmed the role of attention in these deficits observed in masking studies, attentional modulations have been frequently described in patients with schizophrenia [285], especially concerning visual perception [306, 286]. Patients with schizophrenia are less efficient in detecting a target, especially when it is presented with several distractors [307, 308]. Recently, it was proposed that impairments in terms of precise control of attentional selection may account, at least in part, for these changes observed in these patients [309, 310]. Specifically, it has been suggested that patients either failed to allocate sufficient resources or that they incorrectly distributed them toward the mask instead of the target. In this context, understanding the relationship between masking and attention has important implications for theories of attention and visual masking, and is consequently crucial for the interpretation of previously reported findings on schizophrenia and similar neurological disorders. Our results highlight that attentional modulation is affected by target mask timing at a point during perceptual processing (see section 2). Further research using a similar paradigm by Agaoglu and colleagues [78] could bring more insight into the differences observed in patients compared to the healthy population.

Impairments in schizophrenia have been also observed as irregular object perception for integrating discontinuous object contours or recognizing object identities during backward masking [311, 287, 312, 313]. While object-based attention can be considered a novel topic of interest in psychosis research, a recent study found that the defining process of object-based attention which is the automatic spread of attention across object features does not occur reliably in patients with schizophrenia [314]. In this regard, understanding how attentional processing advantage that spreads from one feature to another is insightful for determining

the area of disturbance in schizophrenia. Our results indicate that the feature binding that leads to the attentional spread occurs based on the spatiotemporal continuity of local texture elements (dots in the case of dot fields) rather than relying on higher-order mechanisms (see section 3).

Another research area that can potentially benefit from the results of the current thesis is the development of computer vision algorithms to achieve better visual search and tracking. The ability to perceive edges clearly for both static and moving objects is essential for visual quality and also necessary to achieve effective computer vision algorithms. Under normal viewing conditions moving objects look more blurred in brief than in long exposures, suggesting the existence of an active mechanism that suppresses motion blur in dynamic vision [315, 316]. This reduction of the perceived blur for moving targets was named “motion deblurring” [315]. To offer a coherent explanation for the implied mechanism underlying motion deblurring and to interpret experimental findings for both moving and static targets, the RECOD model has been utilized [317, 318]. According to the RECOD model, the perception of extensive blur due to movement is proposed to be the result of the discrepancy between spatial and temporal offsets among transient and sustained signals transferred to post-retinal levels [206, 317, 318]. Thus, the reduction of perceived blur at long exposure durations is proposed to stem from the spatio-temporal overlap between the transient activity generated by the trailing stimuli in time and the sustained activity generated by the leading stimuli. This proposed mechanism is very similar to metacontrast masking in terms of its dependence on spatial and temporal separations of the targets. Therefore, our current findings may potentially contribute to elaboration of the RECOD model. Combined with the evidence we supplied for the mechanisms of object perception through attentional spreading, our results could be used to broaden the literature and produce effective algorithms that could be used in object detection and tracking.

4.4 Future Directions

4.4.1 How would paracontrast masking interact with attention?

In the first study of the current thesis, our focus was to investigate whether metacontrast masking and spatial attention interact by using an experimental design where we avoided the saturation and floor effects. Specifically, we wanted to see if the increased attentional load had any effect on perceived visibility disruption that was created by metacontrast masking and to record the ERP changes due to this possible interaction. Even though our data still suffered from small saturation effects, we observed a prominent interaction between attentional load and metacontrast masking in our behavioral data. However, EEG results point to variation in early and late stages of attentional processing that were largely dependent on set-size rather than a two-way interaction, consistent with an add-on effect. As established in previous sections, both masking and attention take a role in information processing at multiple stages of visual perception. Thus, observing these mechanisms work together leads to a better-integrated understanding of visual information processing. Although the masking theories predict the effects of both paracontrast and metacontrast masking, the main focus of literature has been mostly on the metacontrast masking paradigm due to its intrinsically interesting nature of the backward masking, compared to the paracontrast masking paradigm which has a temporally linear timeline. Metacontrast and paracontrast masking have been proposed to engage different neural mechanisms and the existing literature indicates a non-linear relationship between SOA and target visibility [260, 45]. Several components of paracontrast masking cannot be explained by the basic notions such as the temporal order of stimuli, in particular, the facilitation effect which is likely to be mediated by the sub-cortical structure and non-specific pathways, together with the prolonged and brief inhibition effects that may interact with the attentional manipulation distinctively [46, 5, 319]. Previous studies as well as the current data indicate significant interactions between different types of metacontrast masking and attention (e.g.,

[76, 208, 210]. Therefore, studying the underlying neural relationship between attention and paracontrast masking and characterizing the temporal dynamics of attention-induced modulations can further our understanding of how visual information is processed in the early stages. The possible alterations in the range of brief and prolonged inhibitions due to changing attentional load spatially can be informative to understand the differential effects of attention on the early and late inhibitory mechanisms.

4.4.2 What is the neuronal basis of object-based attention?

Stoner and Blanc [189] have argued that the dot-field specificity of the cueing effect appears to rule out mechanisms that solely rely on mid-level cortical areas (e.g., area MT), as receptive fields in those areas are too large to distinguish between the intermixed dots of the superimposed dot fields. Stoner and Blanc [189] noted that area V1 receptive fields, on the other hand, are small enough to contain mostly dots of one field or the other at any given moment in time. Based on these observations, they outlined a model involving “cooperative” (recursive excitatory) connections within direction-of-motion V1 hypercolumns [320, 321]. Stoner [322] implemented a simple neuronal network version of this model and demonstrated that it could replicate the dot-field specific cueing observed by Stoner and Blanc [189]. Stoner [322] also demonstrated that this model can be readily extended to include hypercolumns¹ tuned to additional feature dimensions (e.g., color) and could thus account for the spreading of attention across feature dimensions (e.g., [195, 183, 323, 187]). Because this model achieves object-specific spreading of an attentional bias by relying on the fine-grained locations of object parts (e.g. texture elements or edges) and occurs before the feature dimensions of color and motion are partially segregated in higher-order areas, it sidesteps the need to postulate a higher-order mechanism that would somehow identify which

¹Hypercolumns are defined here as a complete set of cortical columns (or just neurons) that encompass the whole range of a given variable (e.g., direction-of-motion) and which have approximately the same receptive field retinotopy.

features belong to which objects and then coordinate the activity in the separate cortical areas (such as MT and V4) specialized for different feature dimensions [324].

While this model has the appeal of offering a concrete and simple means to account for the object-based effects described in this and related studies, neither our EEG findings nor earlier studies have demonstrated ERP modulations that definitively arise from area V1 (though see [176]). To date, the best direct evidence of area V1's involvement in object-based attention appears to come from imaging studies [194, 195]. We think it is likely that EEG recordings have insufficient spatial resolution to test our proposal of area V1 and/or V2's involvement and that single-cell recording, such as used to examine area MT's involvement in surface-based attention [187], will be needed to resolve the roles of these lower-order cortical areas.

Lastly, we note that the terms object-based and surface-based attention has been used to refer to a variety of different effects in different paradigms. We think the mechanisms underlying the object-based effects used in the transparent-motion stimuli are likely different, at least in part, from that found in other paradigms. For instance, one (now classic) paradigm uses spatially separated stimuli and hence admits spatial selection based on the outline of the object in question (e.g., [325, 175, 326, 327]). Other studies have used superimposed objects but plausibly allow for object-class template mechanisms [328]. Further work is needed to determine the overlap in neuronal mechanisms that support these various attentional phenomena.

Bibliography

- [1] J. E. Dowling and B. B. Boycott, “Organization of the primate retina: electron microscopy.,” *Proceedings of the Royal Society of London. Series B. Biological sciences*, vol. 166, pp. 80–111, 11 1966.
- [2] D. C. Van Essen and J. L. Gallant, “Neural mechanisms of form and motion processing in the primate visual system,” *Neuron*, vol. 13, no. 1, pp. 1–10, 1994.
- [3] M. T. Schmolesky, Y. Wang, D. P. Hanes, K. G. Thompson, S. Leutgeb, J. D. Schall, and A. G. Leventhal, “Signal timing access the macaque visual system,” *Journal of Neurophysiology*, vol. 79, pp. 3272–3278, 1998.
- [4] B. Breitmeyer and H. Ogmen, “Visual masking: Time slices through conscious and unconscious vision,” *Visual Masking: Time Slices Through Conscious and Unconscious Vision*, pp. 1–384, 4 2010.
- [5] H. Ogmen, B. G. Breitmeyer, and R. Melvin, “The what and where in visual masking,” *Vision Research*, vol. 43, pp. 1337–1350, 2003.
- [6] M. Koivisto and A. Revonsuo, “Event-related brain potential correlates of visual awareness,” *Neuroscience & Biobehavioral Reviews*, vol. 34, no. 6, pp. 922–934, 2010.
- [7] J. T. Enns and V. D. Lollo, “What’s new in visual masking?,” *Trends in Cognitive Sciences*, vol. 4, pp. 345–352, 9 2000.
- [8] D. A. Baylor, “Photoreceptor signals and vision. proctor lecture,” *Investigative ophthalmology & visual science*, vol. 28, pp. 34–49, 1987.

- [9] K. W. Yau, “Phototransduction mechanism in retinal rods and cones. the friedenwald lecture.,” *Investigative Ophthalmology & Visual Science*, vol. 35, no. 1, pp. 9–32, 1994.
- [10] D. Purves, G. J. Augustine, D. Fitzpatrick, W. C. Hall, A.-S. LaMantia, J. O. McNamara, and S. M. Williams, eds., *Neuroscience, 3rd ed.* Sinauer Associates, 2004.
- [11] P. H. Schiller, J. H. Sandell, and J. H. Maunsell, “Functions of the on and off channels of the visual system,” *Nature 1986 322:6082*, vol. 322, pp. 824–825, 1986.
- [12] S. W. Kuffler, “Discharge patterns and functional organization of mammalian retina,” *Journal of neurophysiology*, vol. 16, no. 1, pp. 37–68, 1953.
- [13] G. von Békésy, “Mach band type lateral inhibition in different sense organs,” *The Journal of general physiology*, vol. 50, no. 3, pp. 519–532, 1967.
- [14] L. Squire, D. Berg, F. E. Bloom, S. Du Lac, A. Ghosh, and N. C. Spitzer, *Fundamental neuroscience*. Academic press, 2012.
- [15] D. H. Hubel and T. N. Wiesel, “Receptive fields, binocular interaction and functional architecture in the cat’s visual cortex,” *The Journal of physiology*, vol. 160, no. 1, p. 106, 1962.
- [16] D. H. Hubel and T. N. Wiesel, “Receptive fields and functional architecture of monkey striate cortex,” *J. Physiol*, vol. 195, pp. 215–243, 1968.
- [17] D. H. Hubel and T. N. Wiesel, “Early exploration of the visual cortex,” *Neuron*, vol. 20, pp. 401–412, 1998.
- [18] H. B. Barlow, C. Blakemore, and J. D. Pettigrew, “The neural mechanism of binocular depth discrimination,” *The Journal of Physiology*, vol. 193, p. 327, 11 1967.
- [19] B. G. Cumming, “An unexpected specialization for horizontal disparity in primate primary visual cortex,” *Nature*, vol. 418, pp. 633–636, 8 2002.

- [20] M. Mishkin and L. G. Ungerleider, “Contribution of striate inputs to the visuospatial functions of parieto-preoccipital cortex in monkeys,” *Behavioural Brain Research*, vol. 6, pp. 57–77, 9 1982.
- [21] S. M. Zeki, “Functional organization of a visual area in the posterior bank of the superior temporal sulcus of the rhesus monkey,” *The Journal of Physiology*, vol. 236, pp. 549–573, 2 1974.
- [22] T. D. Albright, “Direction and orientation selectivity of neurons in visual area mt of the macaque,” *Journal of neurophysiology*, vol. 52, no. 6, pp. 1106–1130, 1984.
- [23] T. D. Albright, “Form-cue invariant motion processing in primate visual cortex,” *Science (New York, N.Y.)*, vol. 255, pp. 1141–1143, 1992.
- [24] M. A. Goodale and G. K. Humphrey, “The objects of action and perception,” *Cognition*, vol. 67, pp. 181–207, 7 1998.
- [25] S. M. Zeki, “Colour coding in the superior temporal sulcus of rhesus monkey visual cortex,” *Proceedings of the Royal Society of London. Series B. Biological Sciences*, vol. 197, pp. 195–223, 5 1977.
- [26] A. Pasupathy and C. E. Connor, “Population coding of shape in area v4,” *Nature Neuroscience 2002 5:12*, vol. 5, pp. 1332–1338, 11 2002.
- [27] L. L. Cloutman, “Interaction between dorsal and ventral processing streams: Where, when and how?,” *Brain and Language*, vol. 127, pp. 251–263, 11 2013.
- [28] S. T. Grafton, “The cognitive neuroscience of prehension: recent developments,” *Experimental Brain Research 2010 204:4*, vol. 204, pp. 475–491, 6 2010.
- [29] H. Kafaligonul, B. G. Breitmeyer, and H. Öğmen, “Feedforward and feedback processes in vision,” *Frontiers in psychology*, vol. 6, p. 279, 2015.
- [30] E. D. Lumer and G. Rees, “Covariation of activity in visual and prefrontal cortex associated with subjective visual perception,” *Proceedings of the*

- National Academy of Sciences of the United States of America*, vol. 96, pp. 1669–1673, 2 1999.
- [31] V. Van Polanen and M. Davare, “Interactions between dorsal and ventral streams for controlling skilled grasp,” *Neuropsychologia*, vol. 79, pp. 186–191, 2015.
- [32] W. McDougall, “The sensations excited by a single momentary stimulation of the eye,” *British Journal of Psychology*, vol. 1, p. 78, 1904.
- [33] C. S. Sherrington, “On reciprocal action in the retina as studied by means of some rotating discs,” *The Journal of Physiology*, vol. 21, p. 33, 2 1897.
- [34] T. Bachmann, “Psychophysiology of visual masking : the fine structure of conscious experience,” p. 298, 1994.
- [35] E. Averbach and A. S. Coriell, “Short-term memory in vision,” *The Bell System Technical Journal*, vol. 40, no. 1, pp. 309–328, 1961.
- [36] S. Chen, H. E. Bedell, and H. Ögmen, “A target in real motion appears blurred in the absence of other proximal moving targets,” *Vision research*, vol. 35, no. 16, pp. 2315–2328, 1995.
- [37] B. Noory, M. H. Herzog, and H. Ogmen, “Retinotopy of visual masking and non-retinotopic perception during masking,” *Attention, Perception, and Psychophysics*, vol. 77, pp. 1263–1284, 5 2015.
- [38] R. C. Atkinson and R. M. Shiffrin, “The control of short-term memory,” *Scientific american*, vol. 225, no. 2, pp. 82–91, 1971.
- [39] K. R. Gegenfurtner and G. Sperling, “Information transfer in iconic memory experiments,” *Journal of Experimental Psychology: Human Perception and Performance*, vol. 19, pp. 845–866, 8 1993.
- [40] G. R. Loftus, J. Duncan, and P. Gehrig, “On the time course of perceptual information that results from a brief visual presentation,” *Journal of Experimental Psychology: Human Perception and Performance*, vol. 18, pp. 530–549, 5 1992.

- [41] K. Schill and C. Zetzsche, “A model of visual spatio-temporal memory: The icon revisited,” *Psychological Research* 1995 57:2, vol. 57, pp. 88–102, 1995.
- [42] B. H. Crawford, “Visual adaptation in relation to brief conditioning stimuli,” *Proceedings of the Royal Society of London. Series B - Biological Sciences*, vol. 134, pp. 283–302, 3 1947.
- [43] L. A. Riggs and B. R. Wooten, “Electrical measures and psychophysical data on human vision,” *Visual Psychophysics*, pp. 690–731, 1972.
- [44] G. Sperling, “Temporal and spatial visual masking. i. masking by impulse flashes,” *JOSA*, vol. 55, no. 5, pp. 541–559, 1965.
- [45] B. G. Breitmeyer and H. Ögmen, “Visual masking,” *Scholarpedia*, vol. 2, no. 7, p. 3330, 2007.
- [46] B. G. Breitmeyer, H. Kafaligönül, H. Ögmen, L. Mardon, S. Todd, and R. Ziegler, “Meta- and paracontrast reveal differences between contour- and brightness-processing mechanisms,” *Vision research*, vol. 46, no. 17, pp. 2645–2658, 2006.
- [47] H. Kafaligönül, B. G. Breitmeyer, and H. Ögmen, “Effects of contrast polarity in paracontrast masking,” *Attention, Perception, & Psychophysics*, vol. 71, no. 7, pp. 1576–1587, 2009.
- [48] B. G. Breitmeyer, E. Tapia, H. Kafaligönül, and H. Ögmen, “Metacontrast masking and stimulus contrast polarity,” *Vision research*, vol. 48, no. 23-24, pp. 2433–2438, 2008.
- [49] G. Felsten and G. S. Wasserman, “Visual masking: Mechanisms and theories,” *Psychological Bulletin*, vol. 88, pp. 329–353, 9 1980.
- [50] T. Bachmann, “Visibility of brief images: The dual-process approach,” *Consciousness and Cognition*, vol. 6, pp. 491–518, 12 1997.
- [51] D. C. Dennett, “Review of mcginn, the problem of consciousness,” 1991.

- [52] W. Klotz and O. Neumann, “Motor activation without conscious discrimination in metacontrast masking,” *Journal of Experimental Psychology: Human Perception and Performance*, vol. 25, pp. 976–992, 1999.
- [53] S. L. Macknik, “Visual masking approaches to visual awareness,” *Progress in brain research*, vol. 155, pp. 177–215, 2006.
- [54] T. Bachmann and G. Francis, *Visual masking: Studying perception, attention, and consciousness*. Academic Press, 2013.
- [55] B. G. Breitmeyer and L. Ganz, “Implications of sustained and transient channels for theories of visual pattern masking, saccadic suppression, and information processing.,” *Psychological review*, vol. 83, no. 1, p. 1, 1976.
- [56] B. G. Breitmeyer, W. S. Hoar, D. Randall, and F. P. Conte, *Visual masking: An integrative approach*. Clarendon Press, 1984.
- [57] B. G. Breitmeyer, “Predictions of u-shaped backward pattern masking from considerations of the spatio-temporal frequency response,” *Perception*, vol. 4, no. 3, pp. 297–304, 1975.
- [58] B. Breitmeyer, D. M. Levi, and R. S. Harwerth, “Flicker masking in spatial vision,” *Vision Research*, vol. 21, no. 9, pp. 1377–1385, 1981.
- [59] S. M. Sherman and R. Guillery, “Functional organization of thalamocortical relays,” *Journal of neurophysiology*, vol. 76, no. 3, pp. 1367–1395, 1996.
- [60] J. H. Maunsell and J. R. Gibson, “Visual response latencies in striate cortex of the macaque monkey,” *Journal of Neurophysiology*, vol. 68, no. 4, pp. 1332–1344, 1992.
- [61] J. L. Andreassi, J. J. D. Simone, and B. W. Mellers, “Amplitude changes in the visual evoked cortical potential with backward masking,” *Electroencephalography and Clinical Neurophysiology*, vol. 41, pp. 387–398, 10 1976.
- [62] D. A. Jeffreys and M. J. Musselwhite, “A visual evoked potential study of metacontrast masking,” *Vision Research*, vol. 26, pp. 631–642, 1 1986.

- [63] M. Genetti, A. Khateb, S. Heinzer, C. M. Michel, and A. J. Pegna, “Temporal dynamics of awareness for facial identity revealed with erp,” *Brain and cognition*, vol. 69, no. 2, pp. 296–305, 2009.
- [64] M. Koivisto and A. Revonsuo, “Electrophysiological correlates of visual consciousness and selective attention,” *NeuroReport*, vol. 18, pp. 753–756, 5 2007.
- [65] M. Koivisto and A. Revonsuo, “The role of selective attention in visual awareness of stimulus features: Electrophysiological studies,” *Cognitive, Affective and Behavioral Neuroscience*, vol. 8, pp. 195–210, 6 2008.
- [66] M. Koivisto, A. Revonsuo, and N. Salminen, “Independence of visual awareness from attention at early processing stages,” *Neuroreport*, vol. 16, no. 8, pp. 817–821, 2005.
- [67] M. Koivisto, A. Revonsuo, and M. Lehtonen, “Independence of visual awareness from the scope of attention: An electrophysiological study,” *Cerebral Cortex*, vol. 16, pp. 415–424, 3 2006.
- [68] H. Railo and M. Koivisto, “The electrophysiological correlates of stimulus visibility and metacontrast masking,” *Consciousness and Cognition*, vol. 18, pp. 794–803, 9 2009.
- [69] M. E. Wilenius and A. T. Revonsuo, “Timing of the earliest erp correlate of visual awareness,” *Psychophysiology*, vol. 44, pp. 703–710, 9 2007.
- [70] M. Niedeggen, P. Wichmann, and P. Stoerig, “Change blindness and time to consciousness,” *European Journal of Neuroscience*, vol. 14, pp. 1719–1726, 11 2001.
- [71] D. Lamy, M. Salti, and Y. Bar-Haim, “Neural correlates of subjective awareness and unconscious processing: An erp study,” *Journal of Cognitive Neuroscience*, vol. 21, pp. 1435–1446, 7 2009.
- [72] M. Turatto, A. Angrilli, V. Mazza, C. Umiltà, and J. Driver, “Looking without seeing the background change: electrophysiological correlates of

- change detection versus change blindness,” *Cognition*, vol. 84, pp. B1–B10, 5 2002.
- [73] G. Pourtois, M. D. Pretto, C. A. Hauert, and P. Vuilleumier, “Time course of brain activity during change blindness and change awareness: Performance is predicted by neural events before change onset,” *Journal of Cognitive Neuroscience*, vol. 18, pp. 2108–2129, 11 2006.
- [74] W. Zhang and S. J. Luck, “Feature-based attention modulates feedforward visual processing,” *Nature Neuroscience* 2008 12:1, vol. 12, pp. 24–25, 11 2008.
- [75] J. T. Enns and V. Di Lollo, “Object substitution: A new form of masking in unattended visual locations,” *Psychological science*, vol. 8, no. 2, pp. 135–139, 1997.
- [76] V. Di Lollo, J. T. Enns, and R. A. Rensink, “Competition for consciousness among visual events: the psychophysics of reentrant visual processes.,” *Journal of Experimental Psychology: General*, vol. 129, no. 4, p. 481, 2000.
- [77] I. Argyropoulos, A. Gellatly, M. Pilling, and W. Carter, “Set size and mask duration do not interact in object-substitution masking.,” *Journal of Experimental Psychology: Human Perception and Performance*, vol. 39, no. 3, p. 646, 2013.
- [78] S. Agaoglu, B. Breitmeyer, and H. Ogmen, “Metacontrast masking and attention do not interact,” *Attention, Perception, and Psychophysics*, vol. 78, pp. 1363–1380, 7 2016.
- [79] D. J. Prime, P. Pluchino, M. Eimer, R. Dell’acqua, and P. Jolicœur, “Object-substitution masking modulates spatial attention deployment and the encoding of information in visual short-term memory: Insights from occipito-parietal erp components,” *Psychophysiology*, vol. 48, pp. 687–696, 5 2011.
- [80] C. M. Salahub and S. M. Emrich, “Erp evidence for temporal independence of set size and object updating in object substitution masking,” *Attention, Perception, and Psychophysics*, vol. 80, pp. 387–401, 2 2018.

- [81] T. A. Carlson, R. Rauschenberger, and F. A. Verstraten, “No representation without awareness in the lateral occipital cortex,” *Psychological Science*, vol. 18, pp. 298–302, 4 2007.
- [82] G. F. Woodman, “Masked targets trigger event-related potentials indexing shifts of attention but not error detection,” *Psychophysiology*, vol. 47, pp. 410–414, 5 2010.
- [83] D. Broadbent, “Perception and communication.,” 1958.
- [84] J. Duncan and G. W. Humphreys, “Visual search and stimulus similarity,” *Psychological review*, vol. 96, no. 3, p. 433, 1989.
- [85] R. Desimone, J. Duncan, *et al.*, “Neural mechanisms of selective visual attention,” *Annual review of neuroscience*, vol. 18, no. 1, pp. 193–222, 1995.
- [86] J. Moran and R. Desimone, “Selective attention gates visual processing in the extrastriate cortex,” *Science*, vol. 229, pp. 782–784, 1985.
- [87] S. J. Luck, L. Chelazzi, S. A. Hillyard, and R. Desimone, “Neural mechanisms of spatial selective attention in areas v1, v2, and v4 of macaque visual cortex,” *Journal of Neurophysiology*, vol. 77, pp. 24–42, 1997.
- [88] J. H. Reynolds and R. Desimone, “The role of neural mechanisms of attention in solving the binding problem,” *Neuron*, vol. 24, pp. 19–29, 9 1999.
- [89] C. J. McAdams and J. H. Maunsell, “Effects of attention on orientation-tuning functions of single neurons in macaque cortical area v4,” *Journal of Neuroscience*, vol. 19, no. 1, pp. 431–441, 1999.
- [90] J. H. Reynolds, L. Chelazzi, *et al.*, “Attentional modulation of visual processing,” *Annual review of neuroscience*, vol. 27, no. 1, pp. 611–647, 2004.
- [91] J. H. Reynolds, T. Pasternak, and R. Desimone, “Attention increases sensitivity of v4 neurons,” *Neuron*, vol. 26, pp. 703–714, 6 2000.
- [92] J. H. Reynolds and R. Desimone, “Interacting roles of attention and visual salience in v4,” *Neuron*, vol. 37, pp. 853–863, 3 2003.

- [93] V. S. Störmer, J. J. McDonald, and S. A. Hillyard, “Cross-modal cueing of attention alters appearance and early cortical processing of visual stimuli,” *Proceedings of the National Academy of Sciences*, vol. 106, no. 52, pp. 22456–22461, 2009.
- [94] S. Treue, “Perceptual enhancement of contrast by attention,” *Trends in Cognitive Sciences*, vol. 8, pp. 435–437, 10 2004.
- [95] A. Thiele, A. Pooresmaeili, L. S. Delicato, J. L. Herrero, and P. R. Roelfsema, “Additive effects of attention and stimulus contrast in primary visual cortex,” *Cerebral Cortex*, vol. 19, pp. 2970–2981, 12 2009.
- [96] T. Williford and J. H. Maunsell, “Effects of spatial attention on contrast response functions in macaque area v4,” *Journal of Neurophysiology*, vol. 96, pp. 40–54, 2006.
- [97] J. H. Reynolds and D. J. Heeger, “The normalization model of attention,” *Neuron*, vol. 61, no. 2, pp. 168–185, 2009.
- [98] M. I. Posner, “Orienting of attention,” *Quarterly journal of experimental psychology*, vol. 32, no. 1, pp. 3–25, 1980.
- [99] C. W. Eriksen and Y.-y. Yeh, “Allocation of attention in the visual field.,” *Journal of Experimental Psychology: Human Perception and Performance*, vol. 11, no. 5, p. 583, 1985.
- [100] U. Castiello and C. Umiltà, “Size of the attentional focus and efficiency of processing,” *Acta Psychologica*, vol. 73, pp. 195–209, 4 1990.
- [101] J. M. Henderson and A. D. Macquistan, “The spatial distribution of attention following an exogenous cue,” *Perception & Psychophysics 1993 53:2*, vol. 53, pp. 221–230, 3 1993.
- [102] D. LaBerge, R. L. Carlson, J. K. Williams, and B. G. Bunney, “Shifting attention in visual space: Tests of moving-spotlight models versus an activity-distribution model.,” *Journal of Experimental Psychology: Human Perception and Performance*, vol. 23, no. 5, p. 1380, 1997.

- [103] G. R. Mangun and S. A. Hillyard, “Spatial gradients of visual attention: behavioral and electrophysiological evidence,” *Electroencephalography and Clinical Neurophysiology*, vol. 70, pp. 417–428, 11 1988.
- [104] M. Eimer, “An event-related potential (erp) study of transient and sustained visual attention to color and form,” *Biological Psychology*, vol. 44, pp. 143–160, 1 1997.
- [105] K. R. Cave and J. M. Zimmerman, “Flexibility in spatial attention before and after practice,” *Psychological Science*, vol. 8, no. 5, pp. 399–403, 1997.
- [106] D. O. Bahcall and E. Kowler, “Attentional interference at small spatial separations,” *Vision Research*, vol. 39, pp. 71–86, 1 1999.
- [107] J. H. Fecteau and J. T. Enns, “Visual letter matching: Hemispheric functioning or scanning biases?,” *Neuropsychologia*, vol. 43, pp. 1412–1428, 1 2005.
- [108] J. S. McCarley and J. R. Mounts, “Localized attentional interference affects object individuation, not feature detection,” *Perception*, vol. 36, pp. 17–32, 6 2007.
- [109] N. G. Müller, M. Mollenhauer, A. Rösler, and A. Kleinschmidt, “The attentional field has a mexican hat distribution,” *Vision research*, vol. 45, no. 9, pp. 1129–1137, 2005.
- [110] J. R. Mounts, “Attentional capture by abrupt onsets and feature singletons produces inhibitory surrounds,” *Perception & Psychophysics 2000 62:7*, vol. 62, pp. 1485–1493, 2000.
- [111] G. Caputo and S. Guerra, “Attentional selection by distractor suppression,” *Vision Research*, vol. 38, pp. 669–689, 3 1998.
- [112] L. Heinemann, A. Kleinschmidt, and N. G. Müller, “Exploring bold changes during spatial attention in non-stimulated visual cortex,” *PLOS ONE*, vol. 4, p. e5560, 5 2009.

- [113] J. M. Hopf, C. N. Boehler, M. A. Schoenfeld, H. J. Heinze, and J. K. Tsotsos, “The spatial profile of the focus of attention in visual search: Insights from meg recordings,” *Vision Research*, vol. 50, pp. 1312–1320, 6 2010.
- [114] N. G. Müller and A. Kleinschmidt, “The attentional ‘spotlight’s’ penumbra: center-surround modulation in striate cortex,” *Neuroreport*, vol. 15, no. 6, pp. 977–980, 2004.
- [115] C. N. Boehler, T. F. Münte, R. M. Krebs, H. J. Heinze, M. A. Schoenfeld, and J. M. Hopf, “Sensory meg responses predict successful and failed inhibition in a stop-signal task,” *Cerebral Cortex*, vol. 19, pp. 134–145, 1 2009.
- [116] C. N. Boehler, J. K. Tsotsos, M. A. Schoenfeld, H. J. Heinze, and J. M. Hopf, “Neural mechanisms of surround attenuation and distractor competition in visual search,” *Journal of Neuroscience*, vol. 31, pp. 5213–5224, 4 2011.
- [117] J. M. Hopf, C. N. Boehler, S. J. Luck, J. K. Tsotsos, H. J. Heinze, and M. A. Schoenfeld, “Direct neurophysiological evidence for spatial suppression surrounding the focus of attention in vision,” *Proceedings of the National Academy of Sciences*, vol. 103, pp. 1053–1058, 1 2006.
- [118] J. K. Tsotsos, A. J. Rodríguez-Sánchez, A. L. Rothenstein, and E. Simine, “The different stages of visual recognition need different attentional binding strategies,” *Brain Research*, vol. 1225, pp. 119–132, 8 2008.
- [119] G. R. Mangun, S. A. Hillyard, and S. J. Luck, “Electrocortical substrates of visual selective attention.,” 1993.
- [120] G. R. Mangun, “Neural mechanisms of visual selective attention,” *Psychophysiology*, vol. 32, no. 1, pp. 4–18, 1995.
- [121] S. A. Hillyard and L. Anllo-Vento, “Event-related brain potentials in the study of visual selective attention,” *Proceedings of the National Academy of Sciences*, vol. 95, no. 3, pp. 781–787, 1998.

- [122] M. I. Posner and S. Dehaene, “Attentional networks,” *Trends in Neurosciences*, vol. 17, pp. 75–79, 1 1994.
- [123] G. Mangun and S. Hillyard, “The spatial allocation of visual attention as indexed by event-related brain potentials,” *Human factors*, vol. 29, no. 2, pp. 195–211, 1987.
- [124] G. R. Mangun and S. A. Hillyard, “Modulations of sensory-evoked brain potentials indicate changes in perceptual processing during visual-spatial priming.,” *Journal of Experimental Psychology: Human perception and performance*, vol. 17, no. 4, p. 1057, 1991.
- [125] L. Anllo-Vento, “Shifting attention in visual space: the effects of peripheral cueing on brain cortical potentials,” *International Journal of Neuroscience*, vol. 80, no. 1-4, pp. 353–370, 1995.
- [126] S. J. Luck, S. Fan, and S. A. Hillyard, “Attention-related modulation of sensory-evoked brain activity in a visual search task,” *Journal of cognitive neuroscience*, vol. 5, no. 2, pp. 188–195, 1993.
- [127] S. D. Slotnick, “The experimental parameters that affect attentional modulation of the erp c1 component,” *Cognitive neuroscience*, vol. 9, no. 1-2, pp. 53–62, 2018.
- [128] H. M. Baumgartner, C. J. Grauly, S. A. Hillyard, and M. A. Pitts, “Does spatial attention modulate the earliest component of the visual evoked potential?,” *Cognitive neuroscience*, vol. 9, no. 1-2, pp. 4–19, 2018.
- [129] L. Anllo-Vento and S. A. Hillyard, “Selective attention to the color and direction of moving stimuli: electrophysiological correlates of hierarchical feature selection,” *Perception & psychophysics*, vol. 58, no. 2, pp. 191–206, 1996.
- [130] V. P. Clark and S. A. Hillyard, “Spatial selective attention affects early extrastriate but not striate components of the visual evoked potential,” *Journal of cognitive neuroscience*, vol. 8, no. 5, pp. 387–402, 1996.

- [131] S. P. Kelly, M. Gomez-Ramirez, and J. J. Foxe, “Spatial attention modulates initial afferent activity in human primary visual cortex,” *Cerebral cortex*, vol. 18, no. 11, pp. 2629–2636, 2008.
- [132] D. Acunzo, G. MacKenzie, and M. C. van Rossum, “Spatial attention affects the early processing of neutral versus fearful faces when they are task-irrelevant: a classifier study of the eeg c1 component,” *Cognitive, Affective, & Behavioral Neuroscience*, vol. 19, no. 1, pp. 123–137, 2019.
- [133] H. Heinze, G. R. Mangun, W. Burchert, H. Hinrichs, M. Scholz, T. Münte, A. Gös, M. Scherg, S. Johannes, H. Hundeshagen, *et al.*, “Combined spatial and temporal imaging of brain activity during visual selective attention in humans,” *Nature*, vol. 372, no. 6506, pp. 543–546, 1994.
- [134] G. R. Mangun, J. B. Hopfinger, C. L. Kussmaul, E. M. Fletcher, and H.-J. Heinze, “Covariations in erp and pet measures of spatial selective attention in human extrastriate visual cortex,” *Human brain mapping*, vol. 5, no. 4, pp. 273–279, 1997.
- [135] M. G. Woldorff, P. Fox, M. Matzke, J. Lancaster, S. Veeraswamy, F. Zamarripa, M. Seabolt, T. Glass, J. Gao, C. Martin, *et al.*, “Retinotopic organization of early visual spatial attention effects as revealed by pet and erps,” *Human brain mapping*, vol. 5, no. 4, pp. 280–286, 1997.
- [136] G. R. Mangun, H. Hinrichs, M. Scholz, H. Mueller-Gaertner, H. Herzog, B. Krause, L. Tellman, L. Kemna, and H. Heinze, “Integrating electrophysiology and neuroimaging of spatial selective attention to simple isolated visual stimuli,” *Vision research*, vol. 41, no. 10-11, pp. 1423–1435, 2001.
- [137] G. R. Mangun, M. H. Buonocore, M. Girelli, and A. P. Jha, “Erp and fmri measures of visual spatial selective attention,” *Human brain mapping*, vol. 6, no. 5-6, pp. 383–389, 1998.
- [138] A. Martinez, L. Anllo-Vento, M. I. Sereno, L. R. Frank, R. B. Buxton, D. Dubowitz, E. C. Wong, H. Hinrichs, H. J. Heinze, and S. A. Hillyard, “Involvement of striate and extrastriate visual cortical areas in spatial attention,” *Nature neuroscience*, vol. 2, no. 4, pp. 364–369, 1999.

- [139] A. Martínez, F. DiRusso, L. Anllo-Vento, M. I. Sereno, R. B. Buxton, and S. A. Hillyard, “Putting spatial attention on the map: timing and localization of stimulus selection processes in striate and extrastriate visual areas,” *Vision research*, vol. 41, no. 10-11, pp. 1437–1457, 2001.
- [140] T. Noesselt, S. A. Hillyard, M. G. Woldorff, A. Schoenfeld, T. Hagner, L. Jäncke, C. Tempelmann, H. Hinrichs, and H.-J. Heinze, “Delayed striate cortical activation during spatial attention,” *Neuron*, vol. 35, no. 3, pp. 575–587, 2002.
- [141] E. Natale, C. Marzi, M. Girelli, E. Pavone, and S. Pollmann, “Erp and fmri correlates of endogenous and exogenous focusing of visual-spatial attention,” *European Journal of Neuroscience*, vol. 23, no. 9, pp. 2511–2521, 2006.
- [142] S. Kastner, M. A. Pinsk, P. De Weerd, R. Desimone, and L. G. Ungerleider, “Increased activity in human visual cortex during directed attention in the absence of visual stimulation,” *Neuron*, vol. 22, no. 4, pp. 751–761, 1999.
- [143] H. Heinze, S. J. Luck, G. R. Mangun, and S. A. Hillyard, “Visual event-related potentials index focused attention within bilateral stimulus arrays. i. evidence for early selection,” *Electroencephalography and clinical neurophysiology*, vol. 75, no. 6, pp. 511–527, 1990.
- [144] S. J. Luck, H. Heinze, G. R. Mangun, and S. A. Hillyard, “Visual event-related potentials index focused attention within bilateral stimulus arrays. ii. functional dissociation of p1 and n1 components,” *Electroencephalography and clinical neurophysiology*, vol. 75, no. 6, pp. 528–542, 1990.
- [145] S. J. Luck, “Multiple mechanisms of visual-spatial attention: recent evidence from human electrophysiology,” *Behavioural brain research*, vol. 71, no. 1-2, pp. 113–123, 1995.
- [146] H. Heinze and G. R. Mangun, “Electrophysiological signs of sustained and transient attention to spatial locations,” *Neuropsychologia*, vol. 33, no. 7, pp. 889–908, 1995.

- [147] S. Yamaguchi, H. Tsuchiya, and S. Kobayashi, “Electrophysiologic correlates of age effects on visuospatial attention shift,” *Cognitive Brain Research*, vol. 3, no. 1, pp. 41–49, 1995.
- [148] G. M. Boynton, “A framework for describing the effects of attention on visual responses,” *Vision research*, vol. 49, no. 10, pp. 1129–1143, 2009.
- [149] J. C. Martinez-Trujillo and S. Treue, “Feature-based attention increases the selectivity of population responses in primate visual cortex,” *Current biology*, vol. 14, no. 9, pp. 744–751, 2004.
- [150] J. H. Maunsell and S. Treue, “Feature-based attention in visual cortex,” *Trends in neurosciences*, vol. 29, no. 6, pp. 317–322, 2006.
- [151] S. Treue and J. C. M. Trujillo, “Feature-based attention influences motion processing gain in macaque visual cortex,” *Nature*, vol. 399, no. 6736, pp. 575–579, 1999.
- [152] S. Yantis *et al.*, “Goal-directed and stimulus-driven determinants of attentional control,” *Attention and performance*, vol. 18, no. Chapter 3, pp. 73–103, 2000.
- [153] S. Ling, T. Liu, and M. Carrasco, “How spatial and feature-based attention affect the gain and tuning of population responses,” *Vision research*, vol. 49, no. 10, pp. 1194–1204, 2009.
- [154] T. Liu, J. Larsson, and M. Carrasco, “Feature-based attention modulates orientation-selective responses in human visual cortex,” *Neuron*, vol. 55, no. 2, pp. 313–323, 2007.
- [155] G. M. Boynton, V. M. Ciaramitaro, and A. C. Arman, “Effects of feature-based attention on the motion aftereffect at remote locations,” *Vision research*, vol. 46, no. 18, pp. 2968–2976, 2006.
- [156] F. M. Felisberti and J. M. Zanker, “Attention modulates perception of transparent motion,” *Vision Research*, vol. 45, no. 19, pp. 2587–2599, 2005.
- [157] T. Liu and I. Mance, “Constant spread of feature-based attention across the visual field,” *Vision research*, vol. 51, no. 1, pp. 26–33, 2011.

- [158] A. F. Rossi and M. A. Paradiso, “Feature-specific effects of selective visual attention,” *Vision research*, vol. 35, no. 5, pp. 621–634, 1995.
- [159] M. Saenz, G. T. Buraças, and G. M. Boynton, “Global feature-based attention for motion and color,” *Vision research*, vol. 43, no. 6, pp. 629–637, 2003.
- [160] B. Y. Hayden and J. L. Gallant, “Time course of attention reveals different mechanisms for spatial and feature-based attention in area v4,” *Neuron*, vol. 47, no. 5, pp. 637–643, 2005.
- [161] C. J. McAdams and J. H. Maunsell, “Attention to both space and feature modulates neuronal responses in macaque area v4,” *Journal of neurophysiology*, vol. 83, no. 3, pp. 1751–1755, 2000.
- [162] S. Treue, “Neural correlates of attention in primate visual cortex,” *Trends in neurosciences*, vol. 24, no. 5, pp. 295–300, 2001.
- [163] H. E. Egeth, R. A. Virzi, and H. Garbart, “Searching for conjunctively defined targets.,” *Journal of Experimental Psychology: Human Perception and Performance*, vol. 10, no. 1, p. 32, 1984.
- [164] B. McElree and M. Carrasco, “The temporal dynamics of visual search: evidence for parallel processing in feature and conjunction searches.,” *Journal of Experimental Psychology: Human Perception and Performance*, vol. 25, no. 6, p. 1517, 1999.
- [165] J. M. Wolfe and T. S. Horowitz, “What attributes guide the deployment of visual attention and how do they do it?,” *Nature reviews neuroscience*, vol. 5, no. 6, pp. 495–501, 2004.
- [166] C. M. Moore and H. Egeth, “How does feature-based attention affect visual processing?,” *Journal of Experimental Psychology: Human Perception and Performance*, vol. 24, no. 4, p. 1296, 1998.
- [167] S.-I. Shih and G. Sperling, “Is there feature-based attentional selection in visual search?,” *Journal of Experimental Psychology: Human Perception and Performance*, vol. 22, no. 3, p. 758, 1996.

- [168] M. R. Harter, C. J. Aine, and C. Schroeder, “Hemispheric differences in event-related potential measures of selective attention.,” *Annals of the New York Academy of Sciences*, 1984.
- [169] J. M. Baas, J. L. Kenemans, and G. R. Mangun, “Selective attention to spatial frequency: an erp and source localization analysis,” *Clinical neurophysiology*, vol. 113, no. 11, pp. 1840–1854, 2002.
- [170] K. R. Cave and N. P. Bichot, “Visuospatial attention: Beyond a spotlight model,” *Psychonomic bulletin & review*, vol. 6, no. 2, pp. 204–223, 1999.
- [171] A. Treisman and S. Sato, “Conjunction search revisited.,” *Journal of experimental psychology: human perception and performance*, vol. 16, no. 3, p. 459, 1990.
- [172] J.-M. Hopf, K. Boelmans, M. A. Schoenfeld, S. J. Luck, and H.-J. Heinze, “Attention to features precedes attention to locations in visual search: evidence from electromagnetic brain responses in humans,” *Journal of Neuroscience*, vol. 24, no. 8, pp. 1822–1832, 2004.
- [173] E. Blaser, Z. W. Pylyshyn, and A. O. Holcombe, “Tracking an object through feature space,” *Nature*, vol. 408, no. 6809, pp. 196–199, 2000.
- [174] J. Duncan, “Selective attention and the organization of visual information.,” *Journal of experimental psychology: General*, vol. 113, no. 4, p. 501, 1984.
- [175] R. Egly, J. Driver, and R. D. Rafal, “Shifting visual attention between objects and locations: evidence from normal and parietal lesion subjects.,” *Journal of Experimental Psychology: General*, vol. 123, no. 2, p. 161, 1994.
- [176] W. Khoe, J. Mitchell, J. Reynolds, and S. Hillyard, “Exogenous attentional selection of transparent superimposed surfaces modulates early event-related potentials,” *Vision research*, vol. 45, no. 24, pp. 3004–3014, 2005.
- [177] M. López, V. Rodríguez, and M. Valdés-Sosa, “Two-object attentional interference depends on attentional set,” *International Journal of Psychophysiology*, vol. 53, no. 2, pp. 127–134, 2004.

- [178] J. F. Mitchell, G. R. Stoner, M. Fallah, and J. H. Reynolds, “Attentional selection of superimposed surfaces cannot be explained by modulation of the gain of color channels,” *Vision research*, vol. 43, no. 12, pp. 1323–1328, 2003.
- [179] K. M. O’Craven, P. E. Downing, and N. Kanwisher, “fmri evidence for objects as the units of attentional selection,” *Nature*, vol. 401, no. 6753, pp. 584–587, 1999.
- [180] T. Pinilla, A. Cobo, K. Torres, and M. Valdes-Sosa, “Attentional shifts between surfaces: effects on detection and early brain potentials,” *Vision Research*, vol. 41, no. 13, pp. 1619–1630, 2001.
- [181] J. H. Reynolds, S. Alborzian, and G. R. Stoner, “Exogenously cued attention triggers competitive selection of surfaces,” *Vision research*, vol. 43, no. 1, pp. 59–66, 2003.
- [182] V. Rodriguez, M. Valdes-Sosa, and W. Freiwald, “Dividing attention between form and motion during transparent surface perception,” *Cognitive Brain Research*, vol. 13, no. 2, pp. 187–193, 2002.
- [183] M. A. Schoenfeld, C. Tempelmann, A. Martinez, J.-M. Hopf, C. Sattler, H.-J. Heinze, and S. Hillyard, “Dynamics of feature binding during object-selective attention,” *Proceedings of the National Academy of Sciences*, vol. 100, no. 20, pp. 11806–11811, 2003.
- [184] M. Valdes-Sosa, M. A. Bobes, V. Rodriguez, and T. Pinilla, “Switching attention without shifting the spotlight: Object-based attentional modulation of brain potentials,” *Journal of Cognitive Neuroscience*, vol. 10, no. 1, pp. 137–151, 1998.
- [185] M. Valdes-Sosa, A. Cobo, and T. Pinilla, “Transparent motion and object-based attention,” *Cognition*, vol. 66, no. 2, pp. B13–B23, 1998.
- [186] M. Valdes-Sosa, A. Cobo, and T. Pinilla, “Attention to object files defined by transparent motion,” *Journal of Experimental Psychology: Human Perception and Performance*, vol. 26, no. 2, p. 488, 2000.

- [187] A. Wannig, V. Rodríguez, and W. A. Freiwald, “Attention to surfaces modulates motion processing in extrastriate area mt,” *Neuron*, vol. 54, no. 4, pp. 639–651, 2007.
- [188] J. F. Mitchell, G. R. Stoner, and J. H. Reynolds, “Object-based attention determines dominance in binocular rivalry,” *Nature*, vol. 429, no. 6990, pp. 410–413, 2004.
- [189] G. R. Stoner and G. Blanc, “Exploring the mechanisms underlying surface-based stimulus selection,” *Vision research*, vol. 50, no. 2, pp. 229–241, 2010.
- [190] S. Yantis and J. Jonides, “Abrupt visual onsets and selective attention: evidence from visual search.,” *Journal of Experimental Psychology: Human perception and performance*, vol. 10, no. 5, p. 601, 1984.
- [191] S. Yantis and J. Jonides, “Abrupt visual onsets and selective attention: voluntary versus automatic allocation.,” *Journal of Experimental Psychology: Human perception and performance*, vol. 16, no. 1, p. 121, 1990.
- [192] J. Lee and J. H. Maunsell, “A normalization model of attentional modulation of single unit responses,” *PLoS one*, vol. 4, no. 2, p. e4651, 2009.
- [193] M. Fallah, G. R. Stoner, and J. H. Reynolds, “Stimulus-specific competitive selection in macaque extrastriate visual area v4,” *Proceedings of the National Academy of Sciences*, vol. 104, no. 10, pp. 4165–4169, 2007.
- [194] V. M. Ciaramitaro, J. F. Mitchell, G. R. Stoner, J. H. Reynolds, and G. M. Boynton, “Object-based attention to one of two superimposed surfaces alters responses in human early visual cortex,” *Journal of neurophysiology*, vol. 105, pp. 1258–1265, 3 2011.
- [195] Z. R. Ernst, G. M. Boynton, and M. Jazayeri, “The spread of attention across features of a surface,” *Journal of Neurophysiology*, vol. 110, no. 10, pp. 2426–2439, 2013.
- [196] W. Khoe, J. F. Mitchell, J. H. Reynolds, and S. A. Hillyard, “Erp evidence that surface-based attention biases interocular competition during rivalry,” *Journal of Vision*, vol. 8, no. 3, pp. 18–18, 2008.

- [197] M. Valdes-Sosa, M. A. Bobes, V. Rodríguez, Y. Acosta, A. Pérez, J. Iglesias, and M. Borrego, “The influence of scene organization on attention: Psychophysics and electrophysiology,” *Functional neuroimaging of visual cognition*, pp. 321–344, 2003.
- [198] V. P. Clark, S. Fan, and S. A. Hillyard, “Identification of early visual evoked potential generators by retinotopic and topographic analyses,” *Human brain mapping*, vol. 2, no. 3, pp. 170–187, 1994.
- [199] F. Di Russo, A. Martínez, and S. A. Hillyard, “Source analysis of event-related cortical activity during visuo-spatial attention,” *Cerebral cortex*, vol. 13, no. 5, pp. 486–499, 2003.
- [200] J. Boyer and T. Ro, “Attention attenuates metacontrast masking,” *Cognition*, vol. 104, no. 1, pp. 135–149, 2007.
- [201] M. Bruchmann, P. Hintze, and S. Mota, “The effects of spatial and temporal cueing on metacontrast masking,” *Advances in Cognitive Psychology*, vol. 7, p. 132, 2011.
- [202] O. Neumann and I. Scharlau, “Visual attention and the mechanism of metacontrast,” *Psychological Research*, vol. 71, no. 6, pp. 626–633, 2007.
- [203] P. L. Smith, R. Ratcliff, and B. J. Wolfgang, “Attention orienting and the time course of perceptual decisions: Response time distributions with masked and unmasked displays,” *Vision research*, vol. 44, no. 12, pp. 1297–1320, 2004.
- [204] T. Bachmann, “The process of perceptual retouch: Nonspecific afferent activation dynamics in explaining visual masking,” *Perception & Psychophysics*, vol. 35, no. 1, pp. 69–84, 1984.
- [205] G. Francis, “Quantitative theories of metacontrast masking.,” *Psychological review*, vol. 107, no. 4, p. 768, 2000.
- [206] H. Öğmen, “A neural theory of retino-cortical dynamics,” *Neural networks*, vol. 6, no. 2, pp. 245–273, 1993.

- [207] N. Weisstein, G. Ozog, and R. Szoc, “A comparison and elaboration of two models of metacontrast.,” *Psychological Review*, vol. 82, no. 5, p. 325, 1975.
- [208] V. S. Ramachandran and S. Cobb, “Visual attention modulates metacontrast masking,” *Nature*, vol. 373, no. 6509, pp. 66–68, 1995.
- [209] J. Shelley-Tremblay and A. Mack, “Metacontrast masking and attention,” *Psychological Science*, vol. 10, no. 6, pp. 508–515, 1999.
- [210] M. S. Tata, “Attend to it now or lose it forever: Selective attention, metacontrast masking, and object substitution,” *Perception & psychophysics*, vol. 64, no. 7, pp. 1028–1038, 2002.
- [211] H. L. Filmer, J. B. Mattingley, and P. E. Dux, “Size (mostly) doesn’t matter: The role of set size in object substitution masking,” *Attention, Perception, & Psychophysics*, vol. 76, no. 6, pp. 1620–1629, 2014.
- [212] M. Pilling, A. Gellatly, Y. Argyropoulos, and P. Skarratt, “Exogenous spatial precuing reliably modulates object processing but not object substitution masking,” *Attention, Perception, & Psychophysics*, vol. 76, no. 6, pp. 1560–1576, 2014.
- [213] E. Kotsoni, G. Csibra, D. Mareschal, and M. H. Johnson, “Electrophysiological correlates of common-onset visual masking,” *Neuropsychologia*, vol. 45, no. 10, pp. 2285–2293, 2007.
- [214] T. Bachmann, “Finding erp-signatures of target awareness: puzzle persists because of experimental co-variation of the objective and subjective variables,” *Consciousness and cognition*, vol. 18, no. 3, pp. 804–808, 2009.
- [215] J. J. Fahrenfort, H. S. Scholte, and V. A. Lamme, “Masking disrupts reentrant processing in human visual cortex,” *Journal of cognitive neuroscience*, vol. 19, no. 9, pp. 1488–1497, 2007.
- [216] J. J. Fahrenfort, H. Scholte, and V. Lamme, “The spatiotemporal profile of cortical processing leading up to visual perception,” *Journal of Vision*, vol. 8, no. 1, pp. 12–12, 2008.

- [217] M. Koivisto, G. Kastrati, and A. Revonsuo, “Recurrent processing enhances visual awareness but is not necessary for fast categorization of natural scenes,” *Journal of cognitive neuroscience*, vol. 26, no. 2, pp. 223–231, 2014.
- [218] J. A. Harris, S. Ku, and M. G. Woldorff, “Neural processing stages during object-substitution masking and their relationship to perceptual awareness,” *Neuropsychologia*, vol. 51, no. 10, pp. 1907–1917, 2013.
- [219] D. H. Brainard, “The psychophysics toolbox,” *Spatial vision*, vol. 10, no. 4, pp. 433–436, 1997.
- [220] D. G. Pelli, “The videotoolbox software for visual psychophysics: Transforming numbers into movies,” *Spatial vision*, vol. 10, no. 4, pp. 437–442, 1997.
- [221] P. J. Allen, G. Polizzi, K. Krakow, D. R. Fish, and L. Lemieux, “Identification of eeg events in the mr scanner: the problem of pulse artifact and a method for its subtraction,” *Neuroimage*, vol. 8, no. 3, pp. 229–239, 1998.
- [222] A. Revonsuo, *Inner presence: Consciousness as a biological phenomenon*. Mit Press, 2006.
- [223] A. Aydin, H. Ogmen, and H. Kafaligonul, “Neural correlates of meta-contrast masking across different contrast polarities,” *Brain Structure and Function*, vol. 226, no. 9, pp. 3067–3081, 2021.
- [224] T. Ro, B. Breitmeyer, P. Burton, N. S. Singhal, and D. Lane, “Feedback contributions to visual awareness in human occipital cortex,” *Current biology*, vol. 13, no. 12, pp. 1038–1041, 2003.
- [225] V. A. Lamme, K. Zipser, and H. Spekreijse, “Masking interrupts figure-ground signals in v1,” *Journal of cognitive neuroscience*, vol. 14, no. 7, pp. 1044–1053, 2002.
- [226] T. J. Spencer and R. Shuntich, “Evidence for an interruption theory of backward masking,” *Journal of Experimental Psychology*, vol. 85, no. 2, p. 198, 1970.

- [227] P. Havig, B. Breitmeyer, and V. Brown, “The effects of pre-cueing attention on metacontrast masking,” in *annual meeting of the Association for Research in Vision and Ophthalmology, Ft. Lauderdale, FL*, 1998.
- [228] N. Lavie, “Perceptual load as a necessary condition for selective attention.,” *Journal of Experimental Psychology: Human perception and performance*, vol. 21, no. 3, p. 451, 1995.
- [229] N. Lavie and S. Cox, “On the efficiency of visual selective attention: Efficient visual search leads to inefficient distractor rejection,” *Psychological science*, vol. 8, no. 5, pp. 395–396, 1997.
- [230] C. F. Michaels and M. Turvey, “Central sources of visual masking: Indexing structures supporting seeing at a single, brief glance,” *Psychological Research*, vol. 41, no. 1, pp. 1–61, 1979.
- [231] N. Ojasoo, C. Murd, M. Aru, and T. Bachmann, “Manipulation of arousal by caffeine reduces metacontrast masking mostly when target and mask shapes are incongruent.,” *Swiss Journal of Psychology*, vol. 72, no. 2, p. 111, 2013.
- [232] M. Alpern, “Metacontrast,” *JOSA*, vol. 43, no. 8, pp. 648–657, 1953.
- [233] P. M. Merikle, “On the nature of metacontrast with complex targets and masks.,” *Journal of Experimental Psychology: Human Perception and Performance*, vol. 3, no. 4, p. 607, 1977.
- [234] R. Growney, “The function of contour in metacontrast,” *Vision Research*, vol. 16, no. 3, pp. 253–261, 1976.
- [235] R. Growney and N. Weisstein, “Spatial characteristics of metacontrast,” *JOSA*, vol. 62, no. 5, pp. 690–696, 1972.
- [236] P. H. Schiller and M. C. Smith, “Monoptic and dichoptic metacontrast,” *Perception & Psychophysics*, vol. 3, no. 3, pp. 237–239, 1968.
- [237] N. Weisstein, “Backward masking and models of perceptual processing.,” *Journal of Experimental Psychology*, vol. 72, no. 2, p. 232, 1966.

- [238] H. Railo, M. Koivisto, and A. Revonsuo, “Tracking the processes behind conscious perception: a review of event-related potential correlates of visual consciousness,” *Consciousness and cognition*, vol. 20, no. 3, pp. 972–983, 2011.
- [239] A. M. van Loon, H. S. Scholte, S. van Gaal, B. J. van der Hoort, and V. A. Lamme, “Gaba_A agonist reduces visual awareness: a masking–eeg experiment,” *Journal of Cognitive Neuroscience*, vol. 24, no. 4, pp. 965–974, 2012.
- [240] A. Del Cul, S. Baillet, and S. Dehaene, “Brain dynamics underlying the nonlinear threshold for access to consciousness,” *PLoS biology*, vol. 5, no. 10, p. e260, 2007.
- [241] M. Koivisto, P. Kainulainen, and A. Revonsuo, “The relationship between awareness and attention: evidence from erp responses,” *Neuropsychologia*, vol. 47, no. 13, pp. 2891–2899, 2009.
- [242] L. Thaler, A. C. Schütz, M. A. Goodale, and K. R. Gegenfurtner, “What is the best fixation target? the effect of target shape on stability of fixational eye movements,” *Vision research*, vol. 76, pp. 31–42, 2013.
- [243] H. E. Ives, “Xii. studies in the photometry of lights of different colours,” *The London, Edinburgh, and Dublin Philosophical Magazine and Journal of Science*, vol. 24, no. 139, pp. 149–188, 1912.
- [244] S. Akyuz, A. Pavan, U. Kaya, and H. Kafaligonul, “Short-and long-term forms of neural adaptation: An erp investigation of dynamic motion after-effects,” *Cortex*, vol. 125, pp. 122–134, 2020.
- [245] U. Kaya and H. Kafaligonul, “Cortical processes underlying the effects of static sound timing on perceived visual speed,” *NeuroImage*, vol. 199, pp. 194–205, 2019.
- [246] F. Perrin, J. Pernier, O. Bertrand, and J. F. Echallier, “Spherical splines for scalp potential and current density mapping,” *Electroencephalography and clinical neurophysiology*, vol. 72, no. 2, pp. 184–187, 1989.

- [247] R. Oostenveld, P. Fries, E. Maris, and J.-M. Schoffelen, “Fieldtrip: open source software for advanced analysis of meg, eeg, and invasive electrophysiological data,” *Computational intelligence and neuroscience*, vol. 2011, 2011.
- [248] D. M. Groppe, T. P. Urbach, and M. Kutas, “Mass univariate analysis of event-related brain potentials/fields i: A critical tutorial review,” *Psychophysiology*, vol. 48, no. 12, pp. 1711–1725, 2011.
- [249] E. Maris and R. Oostenveld, “Nonparametric statistical testing of eeg-and meg-data,” *Journal of neuroscience methods*, vol. 164, no. 1, pp. 177–190, 2007.
- [250] S. J. Luck, “Ten simple rules for designing and interpreting erp experiments,” *Event-related potentials: A methods handbook*, vol. 4, 2005.
- [251] H. Kafaligonul, T. D. Albright, and G. R. Stoner, “Auditory modulation of spiking activity and local field potentials in area mt does not appear to underlie an audiovisual temporal illusion,” *Journal of Neurophysiology*, vol. 120, no. 3, pp. 1340–1355, 2018.
- [252] K. A. Sundberg, J. F. Mitchell, T. J. Gawne, and J. H. Reynolds, “Attention influences single unit and local field potential response latencies in visual cortical area v4,” *Journal of Neuroscience*, vol. 32, no. 45, pp. 16040–16050, 2012.
- [253] J. Intriligator and P. Cavanagh, “The spatial resolution of visual attention,” *Cognitive psychology*, vol. 43, no. 3, pp. 171–216, 2001.
- [254] R. Müller, E. Göpfert, D. Breuer, and M. W. Greenlee, “Motion veps with simultaneous measurement of perceived velocity,” *Documenta Ophthalmologica*, vol. 97, no. 2, pp. 121–134, 1998.
- [255] M. Carrasco, “Visual attention: The past 25 years,” *Vision research*, vol. 51, no. 13, pp. 1484–1525, 2011.

- [256] Y. Yeshurun, “Isoluminant stimuli and red background attenuate the effects of transient spatial attention on temporal resolution,” *Vision research*, vol. 44, no. 12, pp. 1375–1387, 2004.
- [257] Y. Yeshurun and L. Levy, “Transient spatial attention degrades temporal resolution,” *Psychological Science*, vol. 14, no. 3, pp. 225–231, 2003.
- [258] H. Ögmen, “Spatiotemporal dynamics of visual perception across neural maps and pathways,” in *Handbook of Geometric Computing*, pp. 1–29, Springer, 2005.
- [259] Y. Yeshurun and G. Sabo, “Differential effects of transient attention on inferred parvocellular and magnocellular processing,” *Vision research*, vol. 74, pp. 21–29, 2012.
- [260] B. Breitmeyer, H. Ogmen, H. Ögmen, *et al.*, *Visual masking: Time slices through conscious and unconscious vision*. Oxford University Press, 2006.
- [261] B. G. Breitmeyer and H. Ogmen, “Recent models and findings in visual backward masking: A comparison, review, and update,” *Perception & psychophysics*, vol. 62, no. 8, pp. 1572–1595, 2000.
- [262] B. Peñaloza and H. Ogmen, “Effects of spatial attention on spatial and temporal acuity: A computational account,” *Attention, Perception, & Psychophysics*, pp. 1–15, 2022.
- [263] B. G. Breitmeyer and L. Ganz, “Temporal studies with flashed gratings: Inferences about human transient and sustained channels,” *Vision Research*, vol. 17, no. 7, pp. 861–865, 1977.
- [264] J. Kulikowski and D. Tolhurst, “Psychophysical evidence for sustained and transient detectors in human vision,” *The Journal of Physiology*, vol. 232, no. 1, pp. 149–162, 1973.
- [265] J. Palmer, “Set-size effects in visual search: The effect of attention is independent of the stimulus for simple tasks,” *Vision research*, vol. 34, no. 13, pp. 1703–1721, 1994.

- [266] Z.-L. Lu and B. A. Doshier, “External noise distinguishes attention mechanisms,” *Vision research*, vol. 38, no. 9, pp. 1183–1198, 1998.
- [267] B. A. Doshier and Z.-L. Lu, “Noise exclusion in spatial attention,” *Psychological Science*, vol. 11, no. 2, pp. 139–146, 2000.
- [268] Z.-L. Lu, C. Q. Liu, and B. A. Doshier, “Attention mechanisms for multi-location first-and second-order motion perception,” *Vision Research*, vol. 40, no. 2, pp. 173–186, 2000.
- [269] M. I. Posner, M. J. Nissen, and W. C. Ogden, “Attended and unattended processing modes: The role of set for spatial location,” *Modes of perceiving and processing information*, vol. 137, no. 158, p. 2, 1978.
- [270] Z.-L. Lu, L. A. Lesmes, and B. A. Doshier, “Spatial attention excludes external noise at the target location,” *Journal of vision*, vol. 2, no. 4, pp. 4–4, 2002.
- [271] L.-p. Shiu and H. Pashler, “Negligible effect of spatial precuing on identification of single digits,” *Journal of Experimental Psychology: Human Perception and Performance*, vol. 20, no. 5, p. 1037, 1994.
- [272] D. K. Lee, L. Itti, C. Koch, and J. Braun, “Attention activates winner-take-all competition among visual filters,” *Nature neuroscience*, vol. 2, no. 4, pp. 375–381, 1999.
- [273] Z.-L. Lu and B. A. Doshier, “Spatial attention: Different mechanisms for central and peripheral temporal precues?,” *Journal of Experimental Psychology: Human Perception and Performance*, vol. 26, no. 5, p. 1534, 2000.
- [274] S. A. Hillyard, G. R. Mangun, M. G. Woldorff, and S. J. Luck, “Neural systems mediating selective attention.” 1995.
- [275] S. J. Luck, S. A. Hillyard, M. Mouloua, M. G. Woldorff, V. P. Clark, and H. L. Hawkins, “Effects of spatial cuing on luminance detectability: psychophysical and electrophysiological evidence for early selection,” *Journal of experimental psychology: human perception and performance*, vol. 20, no. 4, p. 887, 1994.

- [276] A. B. Chica and J. Lupiáñez, “Effects of endogenous and exogenous attention on visual processing: an inhibition of return study,” *Brain research*, vol. 1278, pp. 75–85, 2009.
- [277] J. B. Hopfinger and V. M. West, “Interactions between endogenous and exogenous attention on cortical visual processing,” *NeuroImage*, vol. 31, no. 2, pp. 774–789, 2006.
- [278] J. C. Adair and A. M. Barrett, “Spatial neglect: clinical and neuroscience review: a wealth of information on the poverty of spatial attention,” *Annals of the New York Academy of Sciences*, vol. 1142, no. 1, pp. 21–43, 2008.
- [279] M. Corbetta and G. L. Shulman, “Spatial neglect and attention networks,” *Annual review of neuroscience*, vol. 34, p. 569, 2011.
- [280] D. E. Hollingsworth, S. P. McAuliffe, and B. J. Knowlton, “Temporal allocation of visual attention in adult attention deficit hyperactivity disorder.,” *Journal of Cognitive Neuroscience*, vol. 13, no. 3, pp. 298–305, 2001.
- [281] J. L. Sunshine, J. S. Lewin, D. H. Wu, D. A. Miller, R. L. Findling, M. J. Manos, and M. A. Schwartz, “Functional mr to localize sustained visual attention activation in patients with attention deficit hyperactivity disorder: a pilot study.,” *American journal of neuroradiology*, vol. 18, no. 4, pp. 633–637, 1997.
- [282] F. Cross-Villasana, K. Finke, K. Hennig-Fast, B. Kilian, I. Wiegand, H. J. Müller, H.-J. Möller, and T. Töllner, “The speed of visual attention and motor-response decisions in adult attention-deficit/hyperactivity disorder,” *Biological Psychiatry*, vol. 78, no. 2, pp. 107–115, 2015.
- [283] M. F. Green and P. D. Harvey, “Cognition in schizophrenia: Past, present, and future,” *Schizophrenia Research: Cognition*, vol. 1, no. 1, pp. e1–e9, 2014.
- [284] C. Jahshan, J. K. Wynn, A. McCleery, D. C. Glahn, L. L. Altshuler, and M. F. Green, “Cross-diagnostic comparison of visual processing in bipolar disorder and schizophrenia,” *Journal of psychiatric research*, vol. 51, pp. 42–48, 2014.

- [285] C. S. Carter, L. C. Robertson, M. R. Chaderjian, L. J. Celaya, and T. E. Nordahl, “Attentional asymmetry in schizophrenia: controlled and automatic processes,” *Biological Psychiatry*, vol. 31, no. 9, pp. 909–918, 1992.
- [286] M. Van Assche and A. Giersch, “Visual organization processes in schizophrenia,” *Schizophrenia Bulletin*, vol. 37, no. 2, pp. 394–404, 2011.
- [287] M. Green, J. Wynn, B. Breitmeyer, K. Mathis, and K. Nuechterlein, “Visual masking by object substitution in schizophrenia,” *Psychological medicine*, vol. 41, no. 7, pp. 1489–1496, 2011.
- [288] Y. Chen, “Abnormal visual motion processing in schizophrenia: a review of research progress,” *Schizophrenia bulletin*, vol. 37, no. 4, pp. 709–715, 2011.
- [289] Y. Chen, G. P. Palafox, K. Nakayama, D. L. Levy, S. Matthyse, and P. S. Holzman, “Motion perception in schizophrenia,” *Archives of general psychiatry*, vol. 56, no. 2, pp. 149–154, 1999.
- [290] E. Yang, D. Tadin, D. M. Glasser, S. Wook Hong, R. Blake, and S. Park, “Visual context processing in bipolar disorder: a comparison with schizophrenia,” *Frontiers in psychology*, vol. 4, p. 569, 2013.
- [291] M. H. Herzog and A. Brand, “Visual masking & schizophrenia,” *Schizophrenia Research: Cognition*, vol. 2, no. 2, pp. 64–71, 2015.
- [292] B. R. Rund, “Backward-masking performance in chronic and nonchronic schizophrenics, affectively disturbed patients, and normal control subjects.,” *Journal of Abnormal Psychology*, vol. 102, no. 1, p. 74, 1993.
- [293] K. S. Cadenhead, Y. Serper, and D. L. Braff, “Transient versus sustained visual channels in the visual backward masking deficits of schizophrenia patients,” *Biological Psychiatry*, vol. 43, no. 2, pp. 132–138, 1998.
- [294] M. F. Green, K. H. Nuechterlein, and B. Breitmeyer, “Backward masking performance in unaffected siblings of schizophrenic patients: evidence for a vulnerability indicator,” *Archives of General Psychiatry*, vol. 54, no. 5, pp. 465–472, 1997.

- [295] M. F. Green, K. H. Nuechterlein, B. Breitmeyer, and J. Mintz, “Forward and backward visual masking in unaffected siblings of schizophrenic patients,” *Biological psychiatry*, vol. 59, no. 5, pp. 446–451, 2006.
- [296] S. Kéri, O. Kelemen, G. Benedek, and Z. Janka, “Different trait markers for schizophrenia and bipolar disorder: a neurocognitive approach,” *Psychological medicine*, vol. 31, no. 5, pp. 915–922, 2001.
- [297] D. W. Balogh and R. D. Merritt, “Susceptibility to type a backward pattern masking among hypothetically psychosis-prone college students.,” *Journal of Abnormal Psychology*, vol. 94, no. 3, p. 377, 1985.
- [298] P. D. Butler and D. C. Javitt, “Early-stage visual processing deficits in schizophrenia,” *Current opinion in psychiatry*, vol. 18, no. 2, p. 151, 2005.
- [299] P. D. Butler, I. Schechter, V. Zemon, S. G. Schwartz, V. C. Greenstein, J. Gordon, C. E. Schroeder, and D. C. Javitt, “Dysfunction of early-stage visual processing in schizophrenia,” *American Journal of Psychiatry*, vol. 158, no. 7, pp. 1126–1133, 2001.
- [300] I. Schechter, P. D. Butler, G. Silipo, V. Zemon, and D. C. Javitt, “Magnocellular and parvocellular contributions to backward masking dysfunction in schizophrenia,” *Schizophrenia research*, vol. 64, no. 2-3, pp. 91–101, 2003.
- [301] M. F. Green, K. H. Nuechterlein, and J. Mintz, “Backward masking in schizophrenia and mania: I. specifying a mechanism,” *Archives of General Psychiatry*, vol. 51, no. 12, pp. 939–944, 1994.
- [302] M. H. Herzog, M. Roinishvili, E. Chkonia, and A. Brand, “Schizophrenia and visual backward masking: a general deficit of target enhancement,” *Frontiers in Psychology*, vol. 4, p. 254, 2013.
- [303] A. Del Cul, S. Dehaene, and M. Leboyer, “Preserved subliminal processing and impaired conscious access in schizophrenia,” *Archives of general psychiatry*, vol. 63, no. 12, pp. 1313–1323, 2006.
- [304] S. Kéri, A. Antal, G. Szekeres, G. Benedek, and Z. Janka, “Visual information processing in patients with schizophrenia: evidence for the impairment

- of central mechanisms,” *Neuroscience Letters*, vol. 293, no. 1, pp. 69–71, 2000.
- [305] E. C. Lalor, P. De Sanctis, M. I. Krakowski, and J. J. Foxe, “Visual sensory processing deficits in schizophrenia: is there anything to the magnocellular account?,” *Schizophrenia research*, vol. 139, no. 1-3, pp. 246–252, 2012.
- [306] A. Giersch and V. Rhein, “Lack of flexibility in visual grouping in patients with schizophrenia.,” *Journal of Abnormal Psychology*, vol. 117, no. 1, p. 132, 2008.
- [307] A. Elahipanah, B. K. Christensen, and E. M. Reingold, “Visual search performance among persons with schizophrenia as a function of target eccentricity.,” *Neuropsychology*, vol. 24, no. 2, p. 192, 2010.
- [308] R. L. Fuller, S. J. Luck, E. L. Braun, B. M. Robinson, R. P. McMahon, and J. M. Gold, “Impaired control of visual attention in schizophrenia.,” *Journal of abnormal psychology*, vol. 115, no. 2, p. 266, 2006.
- [309] E. Granholm, S. C. Fish, and S. P. Verney, “Pupillometric measures of attentional allocation to target and mask processing on the backward masking task in schizophrenia,” *Psychophysiology*, vol. 46, no. 3, pp. 510–520, 2009.
- [310] L. Lalanne, A. Dufour, O. Després, and A. Giersch, “Attention and masking in schizophrenia,” *Biological Psychiatry*, vol. 71, no. 2, pp. 162–168, 2012.
- [311] P. D. Butler, S. M. Silverstein, and S. C. Dakin, “Visual perception and its impairment in schizophrenia,” *Biological psychiatry*, vol. 64, no. 1, pp. 40–47, 2008.
- [312] S. M. Silverstein and B. P. Keane, “Perceptual organization impairment in schizophrenia and associated brain mechanisms: review of research from 2005 to 2010,” *Schizophrenia bulletin*, vol. 37, no. 4, pp. 690–699, 2011.
- [313] S. M. Silverstein, “Visual perception disturbances in schizophrenia: a unified model,” *The neuropsychopathology of schizophrenia*, pp. 77–132, 2016.

- [314] E. A. Reavis, J. K. Wynn, and M. F. Green, “The flickering spotlight of visual attention: Characterizing abnormal object-based attention in schizophrenia,” *Schizophrenia Research*, vol. 248, pp. 151–157, 2022.
- [315] D. Burr, “Motion smear,” *Nature*, vol. 284, no. 5752, pp. 164–165, 1980.
- [316] V. Di Lollo and J. H. Hogben, “Suppression of visible persistence.,” *Journal of Experimental Psychology: Human Perception and Performance*, vol. 11, no. 3, p. 304, 1985.
- [317] G. Purushothaman, H. Ögmen, S. Chen, and H. E. Bedell, “Motion deblurring in a neural network model of retino-cortical dynamics,” *Vision Research*, vol. 38, no. 12, pp. 1827–1842, 1998.
- [318] G. Purushothaman, D. Lacassagne, H. E. Bedell, and H. Ogmen, “Effect of exposure duration, contrast and base blur on coding and discrimination of edges,” *Spatial Vision*, vol. 15, no. 3, pp. 341–376, 2002.
- [319] A. Konyalı, *Spatial Attention and Paracontrast Masking*. PhD thesis, Bilkent Universitesi (Turkey), 2021.
- [320] D. H. Hubel and T. N. Wiesel, “Sequence regularity and geometry of orientation columns in the monkey striate cortex,” *Journal of Comparative Neurology*, vol. 158, no. 3, pp. 267–293, 1974.
- [321] D. Y. Ts’o, M. Zarella, and G. Burkitt, “Whither the hypercolumn?,” *The Journal of physiology*, vol. 587, no. 12, pp. 2791–2805, 2009.
- [322] G. Stoner, “Area v1 “point-set” as the unit of “object-based” selection,” Program No. 172.13. 2018 Neuroscience Meeting Planner, 2010.
- [323] M. A. Schoenfeld, J.-M. Hopf, C. Merkel, H.-J. Heinze, and S. A. Hillyard, “Object-based attention involves the sequential activation of feature-specific cortical modules,” *Nature neuroscience*, vol. 17, no. 4, pp. 619–624, 2014.
- [324] J. Duncan, “Cooperating brain systems in selective perception and action.,” 1996.

- [325] Z. Chen, “Switching attention within and between objects: The role of subjective organization.,” *Canadian Journal of Experimental Psychology/Revue canadienne de psychologie expérimentale*, vol. 52, no. 1, p. 7, 1998.
- [326] N. Lavie and J. Driver, “On the spatial extent of attention in object-based visual selection,” *Perception & psychophysics*, vol. 58, no. 8, pp. 1238–1251, 1996.
- [327] A. D. Macquistan, “Object-based allocation of visual attention in response to exogenous, but not endogenous, spatial precues,” *Psychonomic Bulletin & Review*, vol. 4, no. 4, pp. 512–515, 1997.
- [328] E. H. Cohen and F. Tong, “Neural mechanisms of object-based attention,” *Cerebral Cortex*, vol. 25, no. 4, pp. 1080–1092, 2015.